AN ABSTRACT OF THE THESIS OF

John C. Gulick for the degree of Master of Science in Nuclear Engineering presented on January 19, 2001.

Title:

A "Mildly Inconsistent" Method for Accelerating Upstream Corner Balance Transport.

Abstract approved: _Redacted for Privacy_____

Todd S. Palmer

A new method for accelerating the Upstream Corner Balance (UCB) discretization of the equation of transfer is introduced. The inconsistent acceleration equations for the UCB discretization are derived by applying the "Modified 4-Step" diffusion synthetic acceleration technique *not* to the UCB discretization, but instead to the simple corner balance (SCB) transport discretization. The 1D and 2D convergence properties of the new method have been determined by Fourier analysis and this data agrees well with observed results. These results indicate that this inconsistent acceleration scheme will greatly increase the rate of iterative convergence of UCB compared to that of source iteration alone.

A "Mildly Inconsistent" Method for Accelerating Upstream Corner Balance
Transport

by

John C. Gulick

A THESIS

submitted to

Oregon State University

in partial fulfillment of
the requirements for the
degree of

Master of Science

Presented January 19, 2001
Commencement June 2001

Master of Science thesis of <u>John C. Gulick</u> presented on <u>January 19, 2001</u>.

APPROVED:

Redacted for Privacy

Major Professor, representing Nuclear Engineering

Redacted for Privacy

Chair of Department of Nuclear Engineering

Redacted for Privacy

Dean of Graduate School

I understand that my thesis will become part of the permanent collection of Oregon State University libraries. My signature below authorizes release of my thesis to any reader upon request.

Redacted for Privacy

John C. Gulick, Author

ACKNOWLEDGEMENT

I would like to thank my family for the support they have given me during this time. I greatly appreciate my parents Jim and Marsha for giving me the opportunity to attain an education and my brother David for continuously reminding me of what was really important in life. My wife, Nicole, has been a continuous support even though I do not know how she let me put so much time into this thesis. She is my source of inspiration and I really appreciate her for encouraging me during these final years of graduate school. Without her I would be lost.

TABLE OF CONTENTS

TABLE OF CONTENTS (Continued)

LIST OF FIGURES

LIST OF TABLES

A "MILDLY INCONSISTENT" METHOD FOR ACCELERATING UPSTREAM CORNER BALANCE TRANSPORT

1 INTRODUCTION

1.1 Motivation

Over the last five decades an area of intense research has been the development of numerical techniques used to simulate the propagation of thermal radiation as it flows through and interacts with a fluid. Characterizing the flow of thermal radiation allows researchers to accurately determine how the fluid responds and reacts to the thermal radiation field. Fluid motion, or hydrodynamics is very important in many systems of interest. In certain hydrodynamic systems the pressure or momentum forces exerted by the thermal radiation field on the fluid may actually dominate and dictate the dynamics of the system. The study of these types of systems is called *radiation hydrodynamics*, where the hydrodynamics of the system are driven, at least in part, by a thermal radiation field. Areas of research where radiation hydrodynamics is very important are astrophysics, inertially and magnetically confined fusion, and climate/atmospheric modeling.

Radiation hydrodynamics is described mathematically by the radiative transfer equations, and constitutive models (equations of state). Thermal radiation, photons, exist in densities high enough to drive the dynamics of the system. The underlying substrate that the photons are flowing through and exerting pressure on affects the photons and the photon distribution both in energy and in space. Because of the complexity of the coupled system, researchers often decouple the radiation and hydrodynamics components to computationally simulate these systems.

The radiation component of radiation hydrodynamics can be described by a kinetic or transport equation, traditionally referred to as the equation of transfer [Pom73]. The equation of transfer describes radiation flowing through and interacting with matter within a domain. Solution strategies for the equation of transfer have mainly involved numerical techniques. Analytic solutions do exist but only for very special idealized problems. The numerical techniques used to solve the equation of transfer fall into two classes: *deterministic* techniques, in which various discretizations are used to arrive at a solution, and *stochastic* techniques, in which statistical probabilities describing the system are used to directly simulate the movement of photons. Deterministic techniques involve the discretization of the space, angle, energy and time variables. Deterministic techniques automatically provide global information across the entire system [Lar99]. Stochastic techniques, sometimes known as *Monte Carlo* techniques, arrive at a solution by statistically sampling from a distribution that describes the transport process. Stochastic techniques are often very good at handling extremely complicated geometries and are better suited for determining the solution when a small amount of information is needed. Stochastic techniques are least efficient when global information is needed [Lar99]. A third emerging class of techniques, known as *hybrid* techniques, combines deterministic and stochastic ideologies. This thesis will concentrate on issues associated with deterministic solutions to the equation of transfer.

1.2 Literature Review

In 1999, Larsen [Lar99] related that there are three primary technical issues confronting deterministic transport researchers today.

- Limited geometric modeling

- Truncation errors

- Slow iterative convergence

In this thesis we will restrict ourselves to looking at two of these issues, "limited geometric modeling," and "slow iterative convergence."

1.2.1 Limited Geometric Modeling

"Limited geometric modeling" refers to the difficulty associated with deterministically solving the equation of transfer on non-orthogonal surfaces and/or curved surfaces. A substantial amount of research has been done studying new advanced spatial discretizations that enable solutions on *arbitrary* or unstructured grids. The reason for this is two-fold. First, the geometric error associated with applying discretizations that do not properly handle specific shapes can be reduced. Second, coupling the radiation solution to the fluid hydrodynamics becomes easier when the spatial grids are similar. Generally, there are two approaches for determining the grid in coupled radiation/hydrodynamics physics packages. One is to use a common mesh for both packages, the second is to let the radiation and the hydrodynamics packages generate their own meshes and provide some sort of functionality that translates results between the two meshes [Pal01].

In 1991 Adams [Ada91] introduced a new finite-volume (FV) transport discretization based in part on a hydrodynamic concept of Burton [Bur91]. Burton had previously employed a sub-cell concept known as *corners* in his hydrodynamics methods. Adams' corner balance (CB) finite-volume concept is based on imposing particle conservation over corner volumes. Corner balance, designed for arbitrary connected polygons, allows the radiation package to use a similar or even identical mesh as the hydrodynamics package. Adams initially derived simple-corner-balance (SCB) which represents the interior corner edge intensities as a simple average of the corner intensities. Adams [Ada91] found that in slab geometry SCB was equivalent to

the finite-element (FE) method known as the lumped linear-discontinuous (LLD). In x-y geometry Adams found SCB to be equivalent to the fully-lumped bilinear-discontinuous (FLBLD) FE method.

An initial analysis of SCB showed it was strictly positive, and very good in thick, diffusive regions. Radiative transfer problems of interest are often characterized as being *optically thick* and highly *diffusive*. SCB was found to have a leading-order solution that satisfies a discretized diffusion equation regardless of grid spacing.

While SCB has many desirable properties there are problems with this new discretization. The first is that as the cells become distorted the accuracy of the scheme degrades in optically thick, diffusive regions. Second, the boundary condition satisfied by the leading-order solution inside thick diffusive regions can become inaccurate [Ada91]. Another problem is the *simple* closure of SCB effectively couples all of the corners in a given cell. For each cell this requires the solution of a 2 × 2 linear system in slab geometry and a 4 × 4 linear system on orthogonal grids in x-y geometry. When SCB is used on arbitrarily connected polygons, where there are N corners in each cell, SCB requires the inversion of an $N \times N$ matrix for each cell. This can quickly become prohibitively expensive as the number of corners increases.

Adams designed a modification to SCB to alleviate the requirement to invert this within-cell matrix. He replaced the simple closure with an *upstream* closure which allows the transport sweeps to proceed corner by corner, instead of coupling all corners together. Adams designed upstream-corner-balance (UCB) to perform better than SCB for intermediate and thin optical thicknesses. Adams also designed UCB so that the leading-order solution in thick diffusive problems was identical to that of SCB [Ada97].

1.2.2 Slow Iterative Convergence

"Slow iterative convergence" refers to a problematic decrease in iterative convergence rate when the system of interest becomes *diffusive*. The reason for this is that photons undergo many interactions over the cell length and few if any these interactions remove photons from the system. In highly scattering problems the only removal mechanism that exists is sometimes leakage. If the problem is also very optically thick, few photons are eliminated. This means that source iteration (SI), the simplest and most common iterative technique for numerical transport, will require a very large number of iterations to converge to the correct solution. Source iteration degrades in this way for analytic and discretized transport equations, independent of the choice of discretization.

To increase the iterative rate of convergence of source iteration, acceleration techniques such as Chebyschev [LM84], rebalance [LM84], diffusion synthetic acceleration (DSA) [Kop63], transport synthetic acceleration (TSA) [RAN97], quasi-diffusion [Gol64], and multigrid [ABDP81], have been developed. Chebyschev becomes unstable for problems in which the scattering ratio is close to unity, or optically thick and diffusive. Rebalance is effective in one-dimension, but in higher dimensions it fails to effectively accelerate the rate of convergence. Active research is now being performed on DSA,TSA, multi-grid and quasi-diffusion.

Transport synthetic acceleration (TSA) [RAN97] was recently developed to deal with arbitrary spatial grids. TSA works by applying a correction based on the solution to a synthetic, low-order, transport equation. TSA is less efficient than DSA but can been implemented on any arbitrary transport discretization since it uses the same discretization as the high-order problem. TSA, however, loses effectiveness in systems where the scattering ratio is close to or equal to unity.

Multigrid, a very popular technique, uses a low-order operator to remove error

from source iteration. The low-order operator and hence the name multi-grid come from the changing of the mesh spacing. By changing the mesh spacing the slowest converging error modes in an iterative scheme, such as source iteration, can be removed. Multi-grid is a very successful method for certain types of problems, but, its effectiveness decreases as the fine mesh becomes coarser. [Kim00]

Quasi-diffusion, an established technique receiving more attention lately, works by using a low-order operator which has transport and diffusion characteristics. This might be a very promising technique in the future and active research is on going to better understand it.

Diffusion synthetic acceleration(DSA) [Kop63] is one of the most popular acceleration techniques today. It uses a low-order operator derived from the diffusion equation to accelerate the iterative rate of convergence of the transport operator. DSA was originally developed by Kopp in 1963 to solve simple slab geometry problems. Until 1977 when Alcouffe [Alc77] realized the importance in consistency between the transport discretization and the diffusion equations, DSA schemes were often unstable and only accelerated very specific problems. Alcouffe solved the stability problem by realizing that the differencing of the diffusion acceleration equations must be consistent with the transport operator. Alcouffe's method was unconditionally stable for all mesh sizes; however, Alcouffe had difficulty implementing it with the diamond-difference (DD) discretization. Diamond-difference was susceptible to non-physical negative fluxes. To treat negative fluxes, "fix-ups" were used which altered the transport operator enough to eliminate the consistency between the transport and diffusion operators.

Larsen built on Alcouffe's work and introduced a form of DSA along with a *four-step procedure* [Lar82b] that was unconditionally effective and stable for several slab geometry discretizations. Using the P_1 [GO99] approximation his four-step scheme produced consistently differenced diffusion acceleration equations directly from the

differenced transport equation. Larsen extended this work to a variety of families of discretizations including weighted diamond (WD), linear characteristics (LC), linear moments (LM), and finite element (FE). Larsen analyzed the stability of his acceleration techniques with a tool known as Fourier analysis. Fourier analysis has allowed researchers to effectively determine the convergence rate of iterative schemes. In slab geometries Larsen's four-step DSA has been very effective; however, Larsen [Lar84] postulated that for multi-dimensional problems the four-step technique might produce equations that would be difficult to reduce to diffusion equations. Khalil [Kha85] introduced an acceleration technique for nodal methods which was revolutionary in that the diffusion equations were not consistent with the transport operator. This led to the understanding that strict consistency was *not* a requirement.

Other break throughs have occurred but the most significant to the work being performed in this thesis was that of Adams and Martin [AM92]. They introduced a *Modified* four-step DSA, a new procedure that is very similar to Larsen's four-step DSA but was designed primarily for FE discretizations. It is applicable in slab, spherical, x-y and r-z geometries and is simpler then the traditional four-step method. The technique actually yields equations that are *inconsistent* with the transport operator but are unconditionally stable.

Wareing [War93] started pursuing the acceleration of corner balance discretizations using advanced DSA methods for slab and x-y geometry transport. When Adams [Ada97] introduced the upstream corner balance (UCB) discretization he made some key connections between SCB and finite element techniques. In fact he showed that SCB and LLD are exactly equivalent in slab geometry and SCB and FLBLD are exactly equivalent in x-y geometry. This meant that Modified Four-step (M4S) DSA could be applied to accelerate SCB. Palmer [Pal93], working on advanced curvilinear discretizations such as SCB, UCB, LD, LLD, and fully lumped bilinear discontinuous (FLBLD) noticed that UCB transport appeared to be effectively accelerated by dif-

fusion equations derived from SCB transport differencings. Palmer's motivation for applying inconsistent acceleration equations was based on results he obtained from an *asymptotic analysis* [LMM89]. Asymptotic analysis allows researchers to determine the behavior of a discretization in some limit. Palmer studied the thick diffusion limit and found that in curvilinear geometries SCB and UCB had *identical* thick diffusion limits. Palmer noticed that UCB could be accelerated by diffusion equations derived from applying M4S to SCB. His reasoning was that SCB and UCB were similar because they have identical thick diffusion limits. Palmer [Pal93] noticed effective acceleration but did not rigorously analyze applying this inconsistently derived SCB DSA equation to UCB.

Furthering the idea of inconsistently derived acceleration equations Adams and Wareing [MLA98] used inconsistent diffusion equations to accelerate linear bilinear characteristics transport. The equations they used came from Morel, Dendy and Wareing [MDW93]. They were developing a multi-level solution method for the diffusion acceleration equations of the M4S procedure for bilinear discontinuous (BLD) in x-y geometry. Morel, Dendy and Wareing showed that the bilinear continuous (BLC) FE diffusion equations could be used to accelerate the iterative solution of the BLD diffusion equations and that these BLC equations can be efficiently solved using multigrid techniques. Wareing [TWM94] then showed that he could accelerate the linear-bilinear nodal transport discretization using bilinear discontinuous diffusion. It was these *inconsistent* diffusion equations that Adams and Wareing used to accelerate bilinear characteristics transport.

1.3 Outline of the Thesis

This thesis focuses on the validation of the application of inconsistently derived diffusion acceleration equations for the UCB transport discretization in slab and x-y

geometries. Building on the initial results obtained by Palmer [Pal93] in curvilinear geometries we show that SCB derived M4S diffusion acceleration equations effectively accelerate the iterative convergence of UCB source iteration. This inconsistent method has been determined to be highly effective by Fourier analysis in slab and x-y geometries. We have shown that the Fourier analysis data agrees well with the observed effectiveness of the method. Our results indicate that this *mildly inconsistent* acceleration scheme will greatly increase the rate of iterative convergence of UCB compared to that of source iteration alone. We call our acceleration scheme *mildly inconsistent* because of the similarities shared between the SCB and UCB discretizations in the thick diffusion limit.

We begin by performing Fourier analyses of the proposed scheme in slab geometry. We then implement the method in a code to verify the convergence rates obtained by the Fourier analysis. We then repeat the same procedure in x-y geometry for orthogonal meshes. By performing both a rigorous Fourier analysis and then implementing the method we are able to verify the behavior of the acceleration scheme. The theoretical and computational results indicate that UCB can be effectively accelerated with inconsistently derived SCB diffusion equations.

The remainder of this thesis is organized as follows. We will begin by reviewing key concepts of the equation of transfer in Section 2. The information in this section will lay the foundation for the work in subsequent sections sections of the thesis. Section 2 also includes a discussion of iterative techniques and methods used to accelerate iterative techniques. We will then discuss our slab geometry analysis and results in Section 3. In Section 4 we discuss the x-y geometry analysis and results. We finally submit our conclusions and suggestions for future work in Section 5.

2   ANALYTIC TRANSPORT

2.1   Introduction

In this chapter we develop some of the concepts that are fundamental to the work being performed within this thesis. We motivate this chapter by discussing the characteristics of the physical system of interest, and the equation, known as the equation of transfer which describes the flow of radiation in this system. This discussion will begin with the continuous, general geometry, radiative transfer equation.

Next, we will discuss solution strategies for the equation of transfer. We begin by looking at iterative methods in general and then focus on source iteration, the simplest, and, perhaps most obvious method for solving the equation of transfer. We will introduce a tool known as Fourier analysis that will allow us to analyze the convergence characteristics of source iteration, and will guide us in our search for valid acceleration techniques.

2.2   Radiation Transport: The Equation of Transfer

Suppose we wanted to describe the propagation of thermal radiation through some material. In order to accomplish this we would use the equation of transfer, also known as the transport equation, to describe the conservation of the thermal radiation or photons within some domain, D, with surface δD, and outward surface normal n (see Figure (1)).

The equation of transfer describes the time rate of change of the specific intensity as the photons participate in five processes:

1. Photons streaming out of and into the domain through surface δD.

2. Photons absorbed within the domain.
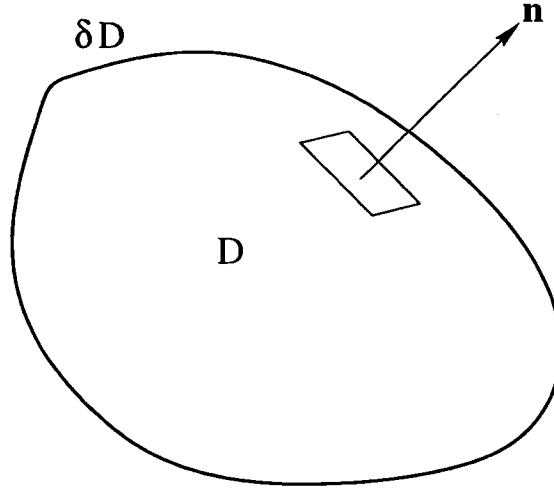
Fig. 1: Arbitrary domain D, with surface δD, and outward normal, **n**.

3. Photons scattering from frequency ν, and direction Ω to all other frequencies and directions (outscattering) within the domain.

4. Photons scattering into frequency ν, and direction Ω from all other frequencies and directions (inscattering) within the domain.

5. Photon (energy) emission within the domain.

The conventional form of the equation of transfer [Pom73],

$$\frac{1}{c}\frac{\partial}{\partial t}\psi\left(\mathbf{r},\nu,\mathbf{\Omega},t\right) + \mathbf{\Omega}\cdot\mathbf{\nabla}\psi\left(\mathbf{r},\nu,\mathbf{\Omega},t\right) = S\left(\mathbf{r},\nu,t\right) - \sigma_a\left(\mathbf{r},\nu,t\right)\psi\left(\mathbf{r},\nu,\mathbf{\Omega},t\right)$$

$$+ \int_0^\infty d\nu' \int_{4\pi} d\Omega' \left[\frac{\nu}{\nu'}\sigma_s\left(\mathbf{r},\nu'\to\nu,\mathbf{\Omega}'\cdot\mathbf{\Omega},t\right)\psi\left(\mathbf{r},\nu',\mathbf{\Omega}',t\right)\right.$$

$$\left. - \sigma_s\left(\mathbf{r},\nu\to\nu',\mathbf{\Omega}\cdot\mathbf{\Omega}',t\right)\psi\left(\mathbf{r},\nu,\mathbf{\Omega},t\right)\right] . \tag{1}$$

Here,

r	$= (length)$	spatial position vector,
Ω	$= (steradian)$	angular vector,
ν	$= (\frac{1}{time})$	frequency variable,
t	$= (time)$	time variable,

c	$= (\frac{length}{time})$	speed of light,
h	$= (energy - time)$	Planck's constant,
$\sigma_a(\mathbf{r}, \nu)$	$= (\frac{1}{length})$	macroscopic absorption cross-section,
$\sigma_s(\mathbf{r}, \nu)$	$= (\frac{1}{length})$	macroscopic scattering cross-section,
$\psi(\mathbf{r}, \nu, \mathbf{\Omega}, t)$	$= (\frac{energy}{area-time-frequency-steradian})$	specific intensity $(ch\nu f)$,
$q(\mathbf{r}, \nu, t)$	$= (\frac{photons}{volume-time-frequency})$	photon source.

The first term in Eq. (1),

$$\frac{1}{c}\frac{\partial}{\partial t}\psi(\mathbf{r}, \nu, \mathbf{\Omega}, t) \ , \tag{2}$$

represents the time rate of change of the specific intensity within our domain. The second term in this expression,

$$\mathbf{\Omega} \cdot \mathbf{\nabla}\psi(\mathbf{r}, \nu, \mathbf{\Omega}, t) \ , \tag{3}$$

represents the process by which energy (photons) stream through the domain. We have defined the function,

$$S(\mathbf{r}, \nu, t) = h\nu q(\mathbf{r}, \nu, t) \ , \tag{4}$$

which is equivalent to the rate of spontaneous thermal energy (photon) emission from the material or fluid. The next term,

$$\sigma_a(\mathbf{r}, \nu, t)\psi(\mathbf{r}, \nu, \mathbf{\Omega}, t) \ , \tag{5}$$

represents the rate at which energy (photons) are absorbed by the material within the domain. The final term,

$$\int_0^\infty d\nu' \int_{4\pi} d\Omega' \left[\frac{\nu}{\nu'}\sigma_s(\mathbf{r}, \nu' \to \nu, \mathbf{\Omega}' \cdot \mathbf{\Omega}, t)\psi(\mathbf{r}, \nu', \mathbf{\Omega}', t) \right.$$

$$\left. - \sigma_s(\mathbf{r}, \nu \to \nu', \mathbf{\Omega} \cdot \mathbf{\Omega}', t)\psi(\mathbf{r}, \nu, \mathbf{\Omega}, t) \right] \ , \tag{6}$$

represents the sum, over all frequencies and directions (ν, Ω), of the rate of outscattering and inscattering within the domain.

The equation of transfer mathematically describes the physical process by which photons are gained and lost from the domain, D. We can see that the various terms within the transport equation translate into corresponding physical gain and loss processes for photon conservation.

The scattering integral is often evaluated by defining, σ_s in Eq. (1) to be,

$$\sigma_s\left(\nu, \Omega' \cdot \Omega, t\right) = \int_0^\infty d\nu' \int_{4\pi} d\Omega' \sigma_s\left(\nu \to \nu', \Omega' \cdot \Omega, t\right),\qquad(7)$$

which results in,

$$\frac{1}{c}\frac{\partial}{\partial t}\psi\left(\mathbf{r}, \nu, \Omega, t\right) + \Omega \cdot \nabla\psi\left(\mathbf{r}, \nu, \Omega, t\right) = S\left(\mathbf{r}, \nu, t\right) - \sigma_t\left(\mathbf{r}, \nu, t\right)\psi\left(\mathbf{r}, \nu, \Omega, t\right)$$

$$+ \int_0^\infty d\nu' \int_{4\pi} d\Omega' \frac{\nu}{\nu'}\sigma_s\left(\mathbf{r}, \nu' \to \nu, \Omega' \cdot \Omega, t\right)\psi\left(\mathbf{r}, \nu', \Omega', t\right),\qquad(8)$$

where, the total interaction coefficient is defined by

$$\sigma_t(\mathbf{r}, \nu, t) = \sigma_s(\mathbf{r}, \nu, t) + \sigma_a(\mathbf{r}, \nu, t).\qquad(9)$$

In order to solve the equation of transfer we often make several assumptions about the physical system that we are interested in approximating. One assumption often invoked is the concept of local thermodynamic equilibrium or LTE. LTE assumes that matter at any given spatial location is in thermodynamic equilibrium, meaning that the the matter is governed by atomic collisions which establish local equilibrium. This, therefore, allows the radiation field to be described by a Planck distribution, and leads to a relationship between the source S and σ_a [Pom73]. Approximations are also often made to the scattering kernel. Several different methods exist to simplify this term. Most often we assume that the scattering kernel is coherent. This means that while scattering is frequency dependent, scattering events do not lead to a change in

photon frequency. Instead we assume that frequency change is due to the absorption-remission process and is thus properly handled by the assumption of LTE. Along with the assumption of LTE it is often appropriate to approximate the scattering kernel as isotropic or independent of direction. These two assumptions lead us to the following form of the equation of transfer,

$$\frac{1}{c}\frac{\partial}{\partial t}\psi\left(\mathbf{r},\nu,\mathbf{\Omega},t\right) + \mathbf{\Omega}\cdot\nabla\psi\left(\mathbf{r},\nu,\mathbf{\Omega},t\right) + \sigma_t\left(\mathbf{r},\nu,t\right)\psi\left(\mathbf{r},\nu,\mathbf{\Omega},t\right)$$

$$= \frac{1}{4\pi}\sigma_s\left(\mathbf{r},\nu,t\right)\phi\left(\mathbf{r},\nu,t\right) + \sigma_a\left(\mathbf{r},\nu,t\right)B(\nu,T)\,, \qquad (10)$$

where,

$$T(\mathbf{r},t) \quad = (temperature) \qquad\qquad \text{Material temperature,}$$

$$B(\nu,T) \quad = (\tfrac{energy}{area-time-frequency-steradian}) \text{ Plank function,}$$

$$\phi(\mathbf{r},\nu,t) \quad = (\tfrac{energy}{area-time-frequency}) \qquad\qquad \text{Direction-integrated intensity.}$$

We define the direction-integrated intensity as,

$$\phi\left(\mathbf{r},\nu,t\right) = \int_{4\pi} d\mathbf{\Omega}\,\psi\left(\mathbf{r},\nu,\mathbf{\Omega},t\right)\,, \qquad (11)$$

and the Planck function as,

$$B(\nu,T) = \frac{2h\nu^3}{c^2}\left[e^{\left[\frac{h\nu}{kT}\right]} - 1\right]^{-1}\,, \qquad (12)$$

where the Boltzmann constant k has units of $(\frac{energy}{temperature})$. The material temperature equation is defined as,

$$C_v\frac{\partial T}{\partial t} = \int_0^\infty d\nu\,\sigma_a\left(\phi - 4\pi B\left(\nu,T\right)\right) + Q\,, \qquad (13)$$

where,

$$C_v \quad = (\tfrac{energy}{volume-temperature}) \qquad\qquad \text{Heat capacity,}$$

$$Q \quad = (\tfrac{energy}{volume-time}) \qquad\qquad \text{Material energy source.}$$

The equation of transfer is a first-order integro-differential equation, and in order to close the system we must specify both initial conditions and boundary conditions. The initial condition specifies the specific intensity distribution within our domain at time $t = 0$,

$$\psi\left(\mathbf{r}, \nu, \mathbf{\Omega}, 0\right) = \psi_i\left(\mathbf{r}, \nu, \mathbf{\Omega}\right) . \tag{14}$$

In coupled problems, where our source is driven by the material temperature, the initial material temperature is defined as,

$$T\left(\mathbf{r}, 0\right) = T_i\left(\mathbf{r}\right) . \tag{15}$$

The spatial boundary condition specifies the incident radiation at the boundary δD of our domain. It should be noted that we require that the surface be non-reentrant. By non-reentrant we mean that any particle leaving the domain D through surface δD is not able to reenter the domain. We define this as,

$$\psi\left(\mathbf{r}, \nu, \mathbf{\Omega}, t\right) = \psi_b\left(\mathbf{r}, \nu, \mathbf{\Omega}, t\right) , \quad \mathbf{n} \cdot \mathbf{\Omega} < 0, \quad \mathbf{r} \in \delta D . \tag{16}$$

The general equation of transfer, Eq. (1), can be cast in various coordinate systems. The primary difference is the treatment of $\mathbf{\Omega} \cdot \mathbf{\nabla}$. We interpret $\mathbf{\Omega} \cdot \mathbf{\nabla}$ in Eq. (1) as being a directional derivative in the direction $\mathbf{\Omega}$. This is equivalent to saying,

$$\mathbf{\Omega} \cdot \mathbf{\nabla} = \frac{\partial}{\partial s}\psi , \tag{17}$$

where s is a length along direction $\mathbf{\Omega}$. It is important to note that the directional derivative is taken with time and frequency held constant [Pom73]. For this thesis we will concentrate on the equation of transfer in Cartesian geometry. In Cartesian geometry, the directional derivative can be expressed as,

$$\mathbf{\Omega} \cdot \mathbf{\nabla} = \mu\frac{\partial}{\partial x} + \eta\frac{\partial}{\partial y} + \xi\frac{\partial}{\partial z} . \tag{18}$$

Figure (2), illustrates the definition of the direction cosines, (μ, η, ξ), as the dot product of the direction vector, $\boldsymbol{\Omega}$, with each of the unit vectors of the characteristic directions (x, y, z).

$$\mu = \boldsymbol{\Omega} \cdot \boldsymbol{e}_x\,, \qquad\qquad \eta = \boldsymbol{\Omega} \cdot \boldsymbol{e}_y\,, \qquad\qquad \xi = \boldsymbol{\Omega} \cdot \boldsymbol{e}_z\,. \qquad (19)$$
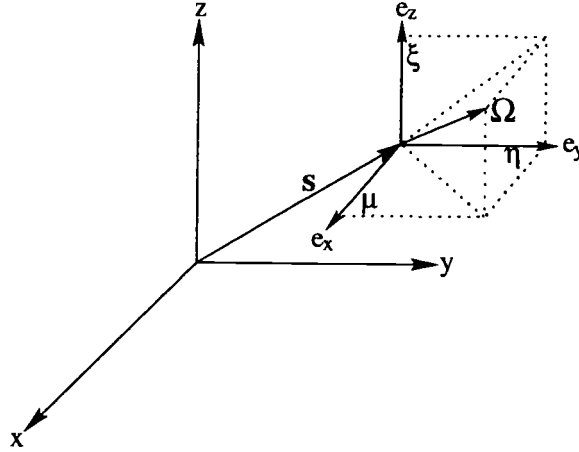
Fig. 2: Cartesian geometry coordinate system.

Three-Dimensional Cartesian Geometry   With the above definitions, we can rewrite the equation of transfer, in three-dimensional, Cartesian geometry,

$$\frac{1}{c}\frac{\partial}{\partial t}\psi\left(x, y, z, \nu, \boldsymbol{\Omega}, t\right)$$

$$+\Omega_x \frac{\partial}{\partial x}\psi\left(x, y, z, \nu, \boldsymbol{\Omega}, t\right) + \Omega_y \frac{\partial}{\partial y}\psi\left(x, y, z, \nu, \boldsymbol{\Omega}, t\right) + \Omega_z \frac{\partial}{\partial z}\psi\left(x, y, z, \nu, \boldsymbol{\Omega}, t\right)$$

$$= \frac{1}{4\pi}\sigma_s\left(x, y, z, \nu, t\right)\phi\left(x, y, z, \nu, t\right) + \sigma_a\left(x, y, z, \nu, t\right)B(\nu, T)\,, \qquad (20)$$

which can be rewritten was,

$$\frac{1}{c}\frac{\partial}{\partial t}\psi\left(x,y,z,\nu,\mu,\eta,\xi,t\right)$$

$$+\mu\frac{\partial}{\partial x}\psi\left(x,y,z,\nu,\mu,\eta,\xi,t\right)+\eta\frac{\partial}{\partial y}\psi\left(x,y,z,\nu,\mu,\eta,\xi,t\right)+\xi\frac{\partial}{\partial z}\psi\left(x,y,z,\nu,\mu,\eta,\xi,t\right)$$

$$=\frac{1}{4\pi}\sigma_s\left(x,y,z,\nu,t\right)\phi\left(x,y,z,\nu,t\right)+\sigma_a\left(x,y,z,\nu,t\right)B(\nu,T)\,, \tag{21}$$

with an initial condition,

$$\psi\left(x,y,z,\nu,\mu,\eta,\xi,0\right)=\psi_i\left(x,y,z,\nu,\mu,\eta,\xi\right)\,, \tag{22}$$

and boundary conditions,

$$\psi\left(\mathbf{r},\nu,\mu,\eta,\xi,t\right)=\psi_b\left(\mathbf{r},\nu,\mathbf{\Omega},t\right)\,,\quad \mathbf{n}\cdot\mathbf{\Omega}<0,\quad \mathbf{r}\in\delta D\,. \tag{23a}$$

Two-Dimensional Cartesian Geometry   We can obtain the Cartesian geometry equations in two dimensions by assuming that the quantities of interest, notably the specific intensity, are invariant with respect to one of the spatial dimensions. This causes the directional derivative in that direction to vanish. The resulting equation of transfer, often called the *x-y geometry* equation of transfer is,

$$\frac{1}{c}\frac{\partial}{\partial t}\psi\left(x,y,\nu,\mathbf{\Omega},t\right)+\Omega_x\frac{\partial}{\partial x}\psi\left(x,y,\nu,\mathbf{\Omega},t\right)+\Omega_y\frac{\partial}{\partial y}\psi\left(x,y,\nu,\mathbf{\Omega},t\right)$$

$$=\frac{1}{4\pi}\sigma_s\left(x,y,\nu,t\right)\phi\left(x,y,\nu,t\right)+\sigma_a\left(x,y,\nu,t\right)B(\nu,T)\,, \tag{24}$$

which can be rewritten as,

$$\frac{1}{c}\frac{\partial}{\partial t}\psi\left(x,y,\nu,\mu,\eta,t\right)+\mu\frac{\partial}{\partial x}\psi\left(x,y,\nu,\mu,\eta,t\right)+\eta\frac{\partial}{\partial y}\psi\left(x,y,\nu,\mu,\eta,t\right)$$

$$=\frac{1}{4\pi}\sigma_s\left(x,y,\nu,t\right)\phi\left(x,y,\nu,t\right)+\sigma_a\left(x,y,\nu,t\right)B(\nu,T)\,, \tag{25}$$

with an initial condition,

$$\psi\left(x, y, \nu, \mu, \eta, 0\right) = \psi_i\left(x, y, \nu, \mu, \eta\right), \tag{26}$$

and boundary conditions,

$$\psi\left(\mathbf{r}, \nu, \mu, \eta, t\right) = \psi_b\left(\mathbf{r}, \nu, \boldsymbol{\Omega}, t\right), \quad \mathbf{n} \cdot \boldsymbol{\Omega} < 0, \quad \mathbf{r} \in \delta D. \tag{27a}$$

One-Dimensional Cartesian Geometry   We can obtain the Cartesian geometry equations in one dimensions in a fashion similar to the one used to generate the two-dimensional form: assuming that the quantities of interest, notably the specific intensity, are invariant with respect to two dimensions. This causes the directional derivative in those specific directions to vanish. The resulting equation of transfer, often called the *slab geometry* form of the equation of transfer is,

$$\frac{1}{c}\frac{\partial}{\partial t}\psi\left(x, \nu, \boldsymbol{\Omega}, t\right) + \Omega_x \frac{\partial}{\partial x}\psi\left(x, \nu, \boldsymbol{\Omega}, t\right)$$

$$= \frac{1}{4\pi}\sigma_s\left(x, \nu, t\right)\phi\left(x, \nu, t\right) + \sigma_a\left(x, \nu, t\right)B\left(\nu, T\right), \tag{28}$$

which can be rewritten as,

$$\frac{1}{c}\frac{\partial}{\partial t}\psi\left(x, \nu, \mu, t\right) + \mu\frac{\partial}{\partial x}\psi\left(x, \nu, \mu, t\right)$$

$$= \frac{1}{4\pi}\sigma_s\left(x, \nu, t\right)\phi\left(x, \nu, t\right) + \sigma_a\left(x, \nu, t\right)B\left(\nu, T\right), \tag{29}$$

with an initial condition,

$$\psi\left(x, \nu, \mu, 0\right) = \psi_t\left(x, \nu, \mu\right), \tag{30}$$

and boundary conditions,

$$\psi\left(\mathbf{r}, \nu, \mu, t\right) = \psi_b\left(\mathbf{r}, \nu, \boldsymbol{\Omega}, t\right), \quad \mathbf{n} \cdot \boldsymbol{\Omega} < 0, \quad \mathbf{r} \in \delta D. \tag{31}$$

2.3   Solution Strategies for General Geometry Transport

To solve the general geometry equation of transfer, the transport community most often uses iterative methods. Direct solution methods do exist, but for most problems of interest these methods are prohibitively slow. The two most common forms of iteration are Cell Block Inversion (CI), and Source Iteration (SI). For this thesis we will restrict our analysis to source iteration.

2.3.1   General Iterative Methods

We will start our discussion of source iteration by reviewing some of the concepts of general iterative methods. This discussion will follow one presented by Morel [Mor82]. Consider the system,

$$\mathbf{H}f = s\,,\tag{32}$$

where $\mathbf{H}$ is some *high-order* (possibly matrix) operator, f is the unknown function (or vector) and s is some *source* function (or vector). For the systems of interest $\mathbf{H}$ is often very difficult to directly invert. Instead of directly inverting $\mathbf{H}$ it is often possible to *split* $\mathbf{H}$ into two operators where one of the operators is chosen so that it is easily invertible.

$$\mathbf{H} = \mathbf{A} - \mathbf{B}\,.\tag{33}$$

This allows us to define the following iterative scheme,

$$\mathbf{A}f^{(l+1)} = \mathbf{B}f^{(l)} + s\,,\tag{34}$$

where l is the iteration index and $f^{(0)}$ is some initial guess to the system solution. Inverting $\mathbf{A}$ yields,

$$f^{(l+1)} = \mathbf{A}^{-1}\mathbf{B}f^{(l)} + A^{-1}s\,,\tag{35}$$

or,

$$f^{(l+1)} = \mathbf{Z}f^{(l)} + \mathbf{A}^{-1}s. \tag{36}$$

Operator $\mathbf{Z} = \mathbf{A}^{-1}\mathbf{B}$ is known as the *iteration operator*. If we write Eq. (35) in terms of the converged solution the result is,

$$f^{(converged)} = \left[\mathbf{A}^{-1}\mathbf{B}\right] f^{(converged)} + \mathbf{A}^{-1}s. \tag{37}$$

If we subtract Equation [35] from Equation [37] the result is,

$$e^{(l+1)} = \left[\mathbf{A}^{-1}\mathbf{B}\right] e^{(l)}, \tag{38}$$

where,

$$e^{(l)} = f^{(converged)} - f^{(l)}, \tag{39}$$

is the error at iteration l. To determine the convergence characteristics of this general iterative scheme, we consider the characteristics of the iteration operator $[\mathbf{A}^{-1}\mathbf{B}]$. If we consider the set of $\{eigenvalue, eigenfunction\}$ pairs of this operator,

$$\left[\mathbf{A}^{-1}\mathbf{B}\right] v_n = \omega_n v_n, \quad n = 1, 2, 3..., \tag{40}$$

these eigenfunctions form a complete set or *basis*. This allows us to express the initial iterative error, $e^{(0)}$, in terms of this set. The initial error is,

$$e^{(0)} = \sum_n \alpha_n v_n. \tag{41}$$

Knowing $e^{(0)}$ allows us to determine $e^{(1)}$ using the eigenfunctions for the iteration operator $\mathbf{A}^{-1}\mathbf{B}$,

$$e^{(1)} = \left[\mathbf{A}^{-1}\mathbf{B}\right] e^{(0)} = \sum_n \alpha_n \left[\mathbf{A}^{-1}\mathbf{B}\right] v_n = \sum_n \alpha_n \omega_n v_n, \tag{42}$$

or in general,

$$e^{(l)} = \left[\mathbf{A}^{-1}\mathbf{B}\right] e^{(l-1)} = \left[\mathbf{A}^{-1}\mathbf{B}\right]^{l} = \sum_{n} \alpha_n \omega_n^l v_n \,. \tag{43}$$

The eigenvalues and associated eigenvectors of the iteration operator dictate the behavior of the scheme. In order for an iterative scheme to be useful it must converge to the correct answer. If every eigenvalue $\omega_n < 1$, then as l increases the error $e^{(l)}$ decreases. We define the eigenvalue largest in magnitude, to be the *spectral radius, ρ*. The spectral radius is a metric for whether or not a iteration scheme converges, but it also represents the *rate* at which an iterative scheme converges. In the asymptotic limit as the number of iterations becomes large, the rate of convergence will be the slowest converging error mode. This means that the spectral radius,

$$\rho \equiv max_n \left\{ |\omega_n| \right\} \,, \tag{44}$$

when l is large, becomes equivalent to the factor by which the error is reduced on each iteration. If the spectral radius, ρ, is close to or equal to unity the iterative method will converge prohibitively slowly. Another concern, besides the problem of extremely slow or no convergence, is that the iteration scheme could appear to converge when in fact little or no reduction in error has occurred. This is known as *false convergence*. To demonstrate false convergence we return to Eq. (38). If we apply this equation recursively, we get

$$e^{(l)} = \left[\mathbf{A}^{-1}\mathbf{B}\right] e^{(l-1)} = \left[\mathbf{A}^{-1}\mathbf{B}\right]^{2} e^{(l-2)} = \left[\mathbf{A}^{-1}\mathbf{B}\right]^{3} e^{(l-3)} = \cdots \left[\mathbf{A}^{-1}\mathbf{B}\right]^{l} e^{(0)} \,. \tag{45}$$

Taking the norm of Eq. (45) we obtain the estimate,

$$||e^{(l)}|| \leq || \left[\mathbf{A}^{-1}\mathbf{B}\right]^{(l)} || \ \ ||e^{(0)}|| \approx \omega_{max}||e^{(0)}|| \,, \tag{46}$$

where ω_{max} is the largest eigenvalue of iteration operator $\mathbf{A}^{-1}\mathbf{B}$ and $\omega_{max} < 1.0$ for convergence. Eq. (38) can also be written as,

$$e^{(l)} = \left[\mathbf{A}^{-1}\mathbf{B}\right] e^{(l-1)} = \left[\mathbf{A}^{-1}\mathbf{B}\right] e^{(l)} + \left[\mathbf{A}^{-1}\mathbf{B}\right] \left(f^{(l)} - f^{(l-1)} \right) \,, \tag{47}$$

which can be rewritten as,

$$e^{(l)} = \left(\mathbf{I} - [\mathbf{A}^{-1}\mathbf{B}]\right)^{-1} \left[\mathbf{A}^{-1}\mathbf{B}\right] \left(f^{(l)} - f^{(l-1)}\right) . \tag{48}$$

Using a Taylor series expansion we arrive at a second estimate for the error,

$$||e^{(l)}|| \leq || \left(I - [\mathbf{A}^{-1}\mathbf{B}]^{(1)}\right)^{-1} [\mathbf{A}^{-1}\mathbf{B}]^{(1)} || \ \ || \left(f^{(l)} - f^{(l-1)}\right) ||, \tag{49}$$

or,

$$||e^{(l)}|| \approx \frac{\omega_{max}^{(l)}}{1 - \omega_{max}^{(l)}} || \left(f^{(l)} - f^{(l-1)}\right) || . \tag{50}$$

If $\omega_{max} < 1.0$, then the method should be unconditionally convergent as $l \to \infty$. The rate at which convergence occurs will depend on the maximum eigenvalue ω_{max}. If $\omega_{max} \approx 1.0$ then the rate of error reduction on each successive iteration will be prohibitively small. Usually a convergence criterion, ϵ, is selected to determine if an iterative scheme has converged. Convergence is normally measured by comparing the norm of successive solutions to ϵ:

$$||f^{(l)} - f^{(l-1)}|| < \epsilon \quad \{ \text{ Converged } , \tag{51}$$

$$||f^{(l)} - f^{(l-1)}|| > \epsilon \quad \{ \text{ Not Converged } . \tag{52}$$

When Eq. (51) is satisfied, after some number of l iterations, Eq. (50) implies,

$$||e^{(l)}|| \leq \frac{\omega_{max}\epsilon}{1 - \omega_{max}} . \tag{53}$$

If the maximum eigenvalue is near unity, $\omega_{max}^{(l)} \approx 1.0$, Eq. (53) implies that the error $e^{(l)}$ in the final solution $f^{(converged)}$ would be significantly larger than that specified by ϵ. This is what is known as *false convergence*. As an example say that our maximum eigenvalue, $\omega_{max} = 0.999$, then Eq. (43) implies that,

$$l = \frac{\ln 0.1}{\ln 0.999} \approx 2303 , \tag{54}$$

iterations are needed to reduce the iterative error by one order of magnitude. From Eq. (53) we observe that upon convergence to the tolerance ϵ that the iteration error may be three orders of magnitude larger then the convergence tolerance, ϵ.

We gather from this discussion two principle ideas to keep in mind about iterative schemes. The first is that we must be aware of the possibility of incorrect results due to false convergence in slowly converging systems. To guard against false convergence requires that we are diligent in our implementation of these iterative schemes. The second is that these schemes may converge at a prohibitively slow rate.

2.3.2 Acceleration Techniques

In order to decrease the computational expense of these calculations and effectively increase the *rate* of convergence we need to reduce the spectral radius of the iterative scheme. Recalling Eqs. (33)-(39), an *exact* expression for the error can be formulated,

$$\mathbf{H}e^{(l+1)} = \mathbf{B}r^{(l+1)}, \tag{55}$$

where,

$$r^{(l+1)} = f^{(l+1)} - f^{(l)} \equiv \text{Residual}. \tag{56}$$

Using Eq. (55), given the exact residual, $r^{(l+1)}$, a solution could be found after a single iteration. However, Eq. (55) is just as hard to solve as Eq. (32), our original system. The difficulty arises that in both the original problem, Eq. (32), and the expression incorporating the error, Eq. (55), the matrix $\mathbf{H}$ must be inverted. If, however, we could *approximate*, in an efficient and timely manner, the expression for the error, Eq. (55), we could add the *approximated* error $e^{(l+1)}$ to any given iterative solution to the original problem $f^{(l+1)}$. This leads to a better iterative approximation on each iteration of the original problem leading to an increase in the rate of convergence. To demonstrate this acceleration technique we again follow the

description given by Morel [Mor82]. In our error expression, Eq. (55), we replace the exact operator $\mathbf{H}$ with an approximation,

$$\mathbf{L}\tilde{e}^{(l+1)} = \mathbf{B}r^{(l+1)}, \tag{57}$$

where $\mathbf{L}$ is a *low-order* approximation to $\mathbf{H}$. This suggests the following modified iterative scheme,

$$f^{(l+\frac{1}{2})} = \mathbf{Z}f^{(l)} + \mathbf{A}^{-1}s, \tag{58}$$

$$r^{(l+\frac{1}{2})} = f^{(l+\frac{1}{2})} - f^{(l)}, \tag{59}$$

$$\tilde{e}^{(l+\frac{1}{2})} = \mathbf{L}^{-1}\mathbf{B}r^{(l+\frac{1}{2})}, \tag{60}$$

$$f^{(l+1)} = f^{(l+\frac{1}{2})} + \tilde{e}^{(l+\frac{1}{2})}, \tag{61}$$

which can be rewritten as,

$$f^{(l+1)} = \left(\mathbf{I} - \mathbf{L}^{-1}\mathbf{H}\right)\mathbf{Z}f^{(l)} + \left(\mathbf{I} - \mathbf{L}^{-1}\mathbf{B}\right)\mathbf{A}^{-1}s. \tag{62}$$

If $\mathbf{L}$ is a good approximation to $\mathbf{H}$ then the spectral radius of the iteration operator $\mathbf{Z}' = \left(\mathbf{I} - \mathbf{L}^{-1}\mathbf{H}\right)\mathbf{Z}$ will be very small and the iterative scheme will converge rapidly. This modification to the original iterative scheme is called an *acceleration technique* and $\mathbf{L}$ is a *preconditioner* of the system since it changes the eigenvalues and thus the condition number of the iteration operator. [Pau98]

Devising an effective acceleration technique for an iterative scheme requires that the low-order operator, $\mathbf{L}$, be carefully selected. Various choices for $\mathbf{L}$ exist but the most important property of $\mathbf{L}$ is that it should be far less costly to invert than $\mathbf{H}$. Although we wish $\mathbf{L}$ to be similar to $\mathbf{H}$ we do not want it to be *too* similar as it

will cost the same amount to invert and thus not yield the solution in less time. We also require that the accelerated scheme yield the same result as the unaccelerated iterative scheme. The acceleration scheme should only change the rate of convergence, not the solution.

The low-order operator $\mathbf{L}$ must also be *effective*. In order to determine whether or not a preconditioner will be effective we need to express the error, e^l as a linear combination of the eigenvectors of the iteration operator. This allows us to determine the rates at which the various error modes are removed during the iterative scheme. The technique to do this is known as Fourier analysis. By analyzing the error modes of the iterative technique and determining which ones dominate, acceleration operators $\mathbf{L}$ can be evaluated.

2.3.3 Source Iteration

To solve the transport equation an iterative method called Source iteration is most commonly used. Source iteration gets its name because the technique iterates on the *scattering source*. In slab geometry source iteration (SI) is described by,

$$\mu \frac{\partial}{\partial x} \psi^{(l+\frac{1}{2})}(x,\mu) + \sigma_t(x) \psi^{(l+\frac{1}{2})}(x,\mu) = \frac{1}{2}\sigma_s(x) \phi^{(l)}(x) + \frac{Q(x)}{2}, \qquad (63)$$

$$\phi^{(l+1)}(x) = \int_{-1}^{1} d\mu' \psi^{(l+\frac{1}{2})}(x,\mu') , \qquad (64)$$

where l is the iteration index and,

$$\sigma_s(x) \phi^{(l)}(x) , \qquad (65)$$

is the scattering source. An initial guess at $l = 0$ for the scalar intensity, ϕ, is required. Solving for the approximation of the specific intensity, ψ, at $l + \frac{1}{2}$, Eq. (64) is used to calculate the new scalar intensity. This procedure is repeated until the difference between successive iterates is less then some tolerance, ϵ.

Source iteration has the same problem as the iterative methods described in Section (2.3.1). When the iteration operator has maximum eigenvalues close to unity the convergence rate of the iteration scheme will be very slow. The source iteration operator has eigenvalues close to unity when material regions are optically thick and highly scattering. The scalar intensity, ϕ, at the lth iterate is the scalar intensity due to photons which have experienced $l - 1$ collisions after emission. If the problem is optically thick and the photons undergo a large number of scattering events before absorption or leakage, a large number of iterations will be required before the iterative method converges.

2.3.4 Fourier Analysis

Often we represent the response of a system as a linear function of time. The function that measures the frequency, ω, that comprises this response is called the *spectral function* of the original function. These two functions, the original function and the spectral function, are mathematically related through what is known as the Fourier transform [LP97]. The mapping of a function $f(t)$ to a function $Y(\omega)$ in ω space is done using the Fourier transform. For example,

$$y(t) = \frac{1}{\sqrt{2\pi}} \int_{-\infty}^{\infty} d\omega Y(\omega) e^{i\omega t}, \tag{66}$$

is actually called the *inverse transform* because it relates $Y(\omega)$ to $y(t)$. The related Fourier transform is,

$$Y(\omega) = \frac{1}{\sqrt{2\pi}} \int_{-\infty}^{\infty} d\omega e^{i\omega t} y(t). \tag{67}$$

Here we apply the Fourier transform to the equation of transfer where the coordinate space is symbolized by $\mathbf{r}$ and the frequency space is the complex domain symbolized by $\boldsymbol{\lambda}$. Applying the Fourier transform to the angular intensity in the spatial domain, $\psi(\mathbf{r}, \boldsymbol{\Omega})$ results in a mapping to the frequency domain, $A(\boldsymbol{\lambda}, \boldsymbol{\Omega})$ [Kim00].

The Fourier transforms which we call *ansatz* in general Cartesian geometry are,

$$A\left(\boldsymbol{\lambda}, \boldsymbol{\Omega}\right) = \frac{1}{\sqrt{\left(2\pi\right)^3}} \int_{-\infty}^{\infty} d^3r \psi\left(\boldsymbol{\lambda}, \boldsymbol{\Omega}\right) e^{i\sigma_t \left(\boldsymbol{\lambda} \cdot \mathbf{r}\right)}, \tag{68}$$

$$\psi\left(\boldsymbol{\lambda}, \boldsymbol{\Omega}\right) = \frac{1}{\sqrt{\left(2\pi\right)^3}} \int_{-\infty}^{\infty} d^3r A\left(\boldsymbol{\lambda}, \boldsymbol{\Omega}\right) e^{i\sigma_t \left(\boldsymbol{\lambda} \cdot \mathbf{r}\right)}. \tag{69}$$

We apply the Fourier transforms, Eqs. (68) and (69), to the general geometry analytic source iteration equations:

$$\boldsymbol{\Omega} \cdot \boldsymbol{\nabla} \psi^{(l+\frac{1}{2})}\left(\mathbf{r}, \boldsymbol{\Omega}\right) + \sigma_t\left(\mathbf{r}\right) \psi^{(l+\frac{1}{2})}\left(\mathbf{r}, \boldsymbol{\Omega}\right) = \frac{1}{4\pi}\sigma_s\left(\mathbf{r}\right) \int_{4\pi} d\Omega \psi^{(l)}\left(\mathbf{r}, \boldsymbol{\Omega}\right) + Q\left(\mathbf{r}\right). \tag{70}$$

Assuming a homogeneous medium we subtract Eq. (70) from the converged transport equation with the following definitions,

$$\hat{\psi}^{(l+\frac{1}{2})}\left(\mathbf{r}, \boldsymbol{\Omega}\right) = \psi\left(\mathbf{r}, \boldsymbol{\Omega}\right) - \psi^{(l+\frac{1}{2})}\left(\mathbf{r}, \boldsymbol{\Omega}\right), \tag{71}$$

$$\hat{\psi}^{(l)}\left(\mathbf{r}, \boldsymbol{\Omega}\right) = \psi\left(\mathbf{r}, \boldsymbol{\Omega}\right) - \psi^{(l)}\left(\mathbf{r}, \boldsymbol{\Omega}\right), \tag{72}$$

yields,

$$\boldsymbol{\Omega} \cdot \boldsymbol{\nabla} \hat{\psi}^{(l+\frac{1}{2})}\left(\mathbf{r}, \boldsymbol{\Omega}\right) + \sigma_t\left(\mathbf{r}\right) \hat{\psi}^{(l+\frac{1}{2})}\left(\mathbf{r}, \boldsymbol{\Omega}\right) = \frac{1}{4\pi}\sigma_s\left(\mathbf{r}\right) \int_{4\pi} d\Omega \hat{\psi}^{(l)}\left(\mathbf{r}, \boldsymbol{\Omega}\right). \tag{73}$$

We substitute the ansatz, Eq. (69) into Eq. (73) which results in,

$$\int_{-\infty}^{\infty} d^3\lambda \left[\sigma_t\left(\boldsymbol{\Omega} \cdot i\boldsymbol{\lambda} + 1\right) A^{(l+\frac{1}{2})}\left(\boldsymbol{\lambda}, \boldsymbol{\Omega}\right) - \frac{1}{4\pi}\sigma_s\left(\mathbf{r}\right) \int_{4\pi} d\Omega' A^{(l)}\left(\boldsymbol{\lambda}, \boldsymbol{\Omega}'\right)\right] e^{i\sigma_t \left(\boldsymbol{\lambda} \cdot \mathbf{r}\right)} = 0. \tag{74}$$

The orthogonality of the Fourier modes $e^{i\sigma_t \left(\boldsymbol{\lambda} \cdot \mathbf{r}\right)}$ implies,

$$A^{(l+\frac{1}{2})}\left(\boldsymbol{\lambda}, \boldsymbol{\Omega}\right) = \frac{c}{4\pi\left(\boldsymbol{\Omega} \cdot i\boldsymbol{\lambda} + 1\right)} \int_{4\pi} d\Omega' A^{(l)}\left(\boldsymbol{\lambda}, \boldsymbol{\Omega}'\right), \quad -\infty < \lambda < \infty, \tag{75}$$

where,

$$c = \frac{\sigma_s}{\sigma_t} \{ \text{ Scattering Ratio} . \tag{76}$$

Integrating Eq. (75) over Ω results in,

$$\int_{4\pi} d\Omega' A^{(l+\frac{1}{2})}\left(\lambda,\Omega'\right) = \left[\frac{c}{4\pi}\int_{4\pi}\frac{d\Omega}{(\Omega\cdot\lambda+1)}\right]\int_{4\pi} d\Omega' A^{(l)}\left(\lambda,\Omega'\right). \tag{77}$$

Subsequently,

$$\omega\left(\lambda\right) = \frac{c}{4\pi}\int_{4\pi}\frac{d\Omega}{(\Omega\cdot\lambda+1)}, \tag{78}$$

is the set of eigenvalues for the system and $A^{(l+\frac{1}{2})}\left(\lambda,\Omega'\right)$ are the associated eigenvectors of the iteration scheme. The meaning of the eigenvalues is the rate at which the error is reduced in frequency space. Similar to the definition of the spectral radius in Eq. (44) for the general iteration scheme, we define the spectral radius for the general geometry equation of transfer as the absolute value of the maximum eigenvalue,

$$\rho \equiv \max_{-\infty<\lambda<\infty}\left|\omega\left(\lambda\right)\right|. \tag{79}$$

We will now analyze source iteration applied to the slab geometry equations of transfer. We will reiterate the original presentation of Larsen in 1982 [LM82] [Lar82a] [Lar82b]. We start by assuming the problem of interest is an infinite homogeneous medium. The slab geometry transport equation is,

$$\mu\frac{\partial}{\partial x}\psi\left(x,\mu\right) + \sigma_t\psi\left(x,\mu\right) = \frac{\sigma_s}{2}\int_{-1}^{1}d\mu\psi\left(x,\mu\right) + Q\left(x\right). \tag{80}$$

When iteratively solved with source iteration the equation becomes,

$$\mu\frac{\partial}{\partial x}\psi^{(l+\frac{1}{2})}\left(x,\mu\right) + \sigma_t\psi^{(l+\frac{1}{2})}\left(x,\mu\right) = \frac{\sigma_s}{2}\phi^{(l)}\left(x\right) + Q\left(x\right), \tag{81}$$

where,

$$\phi^{(l+1)}\left(x\right) = \int_{-1}^{1}d\mu\psi^{(l+\frac{1}{2})}\left(x,\mu\right). \tag{82}$$

We rewrite Eqs. (81) (82) in terms of the converged solution to the system so that,

$$\mu\frac{\partial}{\partial x}\hat{\psi}^{(l+\frac{1}{2})}\left(x,\mu\right) + \sigma_t\left(x\right)\hat{\psi}^{(l+\frac{1}{2})}\left(x,\mu\right) = \frac{\sigma_s\left(x\right)}{2}\hat{\phi}^{(l)}\left(x\right) + Q\left(x\right), \tag{83}$$

$$\hat{\phi}^{(l+1)}(x) = \int_{-1}^{1} d\mu \hat{\psi}^{(l+\frac{1}{2})}(x,\mu) , \tag{84}$$

where,

$$\hat{\psi}^{(l+\frac{1}{2})}(x,\mu) = \psi(x,\mu) - \psi^{(l+\frac{1}{2})}(x,\mu) , \tag{85}$$

$$\hat{\phi}^{(l)}(x) = \phi(x) - \phi^{(l)}(x) . \tag{86}$$

The separation of variable *ansatz* for Fourier analysis are,

$$\hat{\phi}^{(l)}(x) = \omega^{(l)}(\lambda) A(\lambda) e^{i\sigma_t \lambda x} , \tag{87}$$

$$\hat{\psi}^{(l+\frac{1}{2})}(x,\mu) = \omega^{(l)}(\lambda) b(\lambda,\mu) e^{i\sigma_t \lambda x} , \tag{88}$$

where,

$$i = \sqrt{-1}, -\infty < \lambda < \infty . \tag{89}$$

The eigenfunctions are the set $A(\lambda) e^{i\sigma_t \lambda x}$ and the eigenvalues are $\omega^{(l)}(\lambda)$. Substituting the ansatz, Eqs. (87) and (88) into Eqs. (83) and (84) we arrive at the following equations,

$$b(\lambda,\mu) = \frac{c}{2} \left[\frac{1}{1 + i\lambda\mu} \right] A(\lambda) , \tag{90}$$

$$\omega(\lambda,\mu) = \frac{c}{2} \int_{-1}^{1} \frac{d\mu}{1 + \lambda^2 \mu^2} = c \int_{0}^{1} \frac{d\mu}{1 + \lambda^2 \mu^2} = \frac{c}{\lambda} \tan^{-1}\lambda . \tag{91}$$

Figure (3) is a plot of of Eq. (91) and shows that the maximum spectral radius, ρ_{max}, for the slab geometry infinite homogeneous medium source iteration case with $c = 1.0$ occurs at the zero mode and is equal to,

$$\rho = \max_{\lambda} |\omega(\lambda)| = \omega(0) = c \equiv \{ \text{ Scattering Ratio} . \tag{92}$$
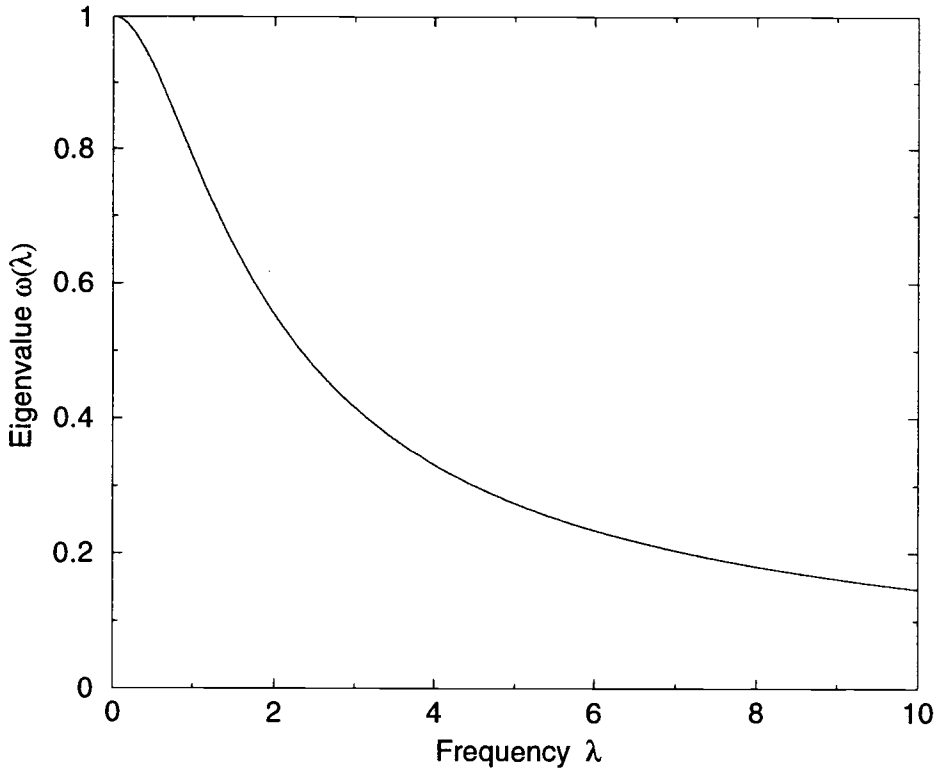
Fig. 3: Source iteration (SI) eigenvalues $\omega(\lambda)$ as a function of λ for analytic slab geometry.

This Fourier analysis is for the analytic in space problem and as such, the $\lambda = 0$ mode is present and is the slowest converging mode. For a finite problem this mode, $\lambda = 0$, does not exist and so a problem with $c \leq 1.0$ will be stable and will always converge. It is important, however, to keep in mind the concept of false convergence in problems when c is very near unity. It is also important to note the shape of this eigenvalue versus frequency curve. We can see that source iteration very effectively removes the error in the high frequency domain but does not damp low frequency error modes. This data will be useful in determining an appropriate *low-order* operator for accelerating source iteration.

2.3.5 Diffusion Synthetic Acceleration

We know from the above analytic analysis that the slowest converging error modes of source iteration are the spatially smooth, slowly changing modes. This means that the acceleration method that we apply should dampen these error modes. These slowly changing modes have an angular dependence which is nearly linearly anisotropic. The diffusion operator approximates the transport operator when the angular intensity is linearly anisotropic. It could be used to remove or at least dampen the low frequency, slowly converging error modes from the source iteration sweep. By removing these slowly converging source iteration error modes on each iteration, the iterative convergence rate may be improved.

If we recall the requirements for the *low-order* operator **L** in Section (2.3.2), we see that the diffusion operator is an *approximation* to the transport operator and is usually far less *costly* to invert.

Applying a diffusion correction to source iteration yields the following iterative system,

$$\mathbf{\Omega} \cdot \mathbf{\nabla} \psi^{(l+\frac{1}{2})} (\mathbf{r}, \mathbf{\Omega}) + \sigma_t (\mathbf{r}) \psi^{(l+\frac{1}{2})} (\mathbf{r}, \mathbf{\Omega}) = \frac{1}{4\pi} \sigma_s (\mathbf{r}) \phi^{(l)} (\mathbf{r}) + Q (\mathbf{r}) , \qquad (93)$$

$$\phi^{(l+\frac{1}{2})} (\mathbf{r}) = \int_{4\pi} d\mathbf{\Omega} \psi^{(l+\frac{1}{2})} (\mathbf{r}, \mathbf{\Omega}) , \qquad (94)$$

with,

$$\mathbf{\nabla} \cdot \frac{1}{3\sigma_t (\mathbf{r})} \mathbf{\nabla} f^{(l+1)} (\mathbf{r}) + \sigma_a (\mathbf{r}) f^{(l+1)} (\mathbf{r}) = \sigma_s (\mathbf{r}) \left[\phi^{(l+\frac{1}{2})} (\mathbf{r}) - \phi^{(l)} (\mathbf{r}) \right] , \qquad (95)$$

$$f^{(l+1)} (\mathbf{r}) = \phi^{(l+1)} (\mathbf{r}) - \phi^{(l+\frac{1}{2})} (\mathbf{r}) , \qquad (96)$$

where Eq. (95) yields the correction f_0 to the scalar intensity.

We can Fourier analyze this new iteration scheme in a similar fashion to source iteration. Starting with the single energy, isotropic scattering analytic slab geometry

equation of transfer written in terms of the error we have,

$$\mu \frac{\partial}{\partial x}\hat{\psi}^{(l+\frac{1}{2})}(x,\mu) + \sigma_t(x)\,\hat{\psi}^{(l+\frac{1}{2})}(x,\mu) = \frac{\sigma_s(x)}{2}\hat{\phi}^{(l)}(x) + Q(x)\ , \qquad (97)$$

$$\hat{\phi}^{(l+1)}(x) = \int_{-1}^{1} d\mu \hat{\psi}^{(l+\frac{1}{2})}(x,\mu)\ . \qquad (98)$$

The low order diffusion equations are,

$$-\frac{\partial}{\partial x}\frac{1}{3\sigma_t(x)}\frac{\partial}{\partial x}\hat{f}^{(l+1)}(x) + \sigma_a(x)\,\hat{f}^{(l+1)}(x) = \sigma_s(x)\left(\hat{\phi}^{(l+\frac{1}{2})}(x) - \hat{\phi}^{(l)}(x)\right)\ , \qquad (99)$$

The Fourier ansatz are defined as,

$$\hat{\phi}^{(l)} = \omega^{(l)}(\lambda)\,a(\lambda)\,e^{i\sigma_t\lambda x}\ , \qquad (100)$$

$$\hat{\psi}^{(l+\frac{1}{2})} = \omega^{(l)}(\lambda)\,b(\lambda,\mu)\,e^{i\sigma_t\lambda x}\ , \qquad (101)$$

$$\hat{\phi}^{(l+\frac{1}{2})} = \omega^{(l)}(\lambda)\,c(\lambda)\,e^{i\sigma_t\lambda x}\ , \qquad (102)$$

$$\hat{f}^{(l+1)} = \omega^{(l)}(\lambda)\,d(\lambda)\,e^{i\sigma_t\lambda x}\ . \qquad (103)$$

If we substitute Eqs. (100)-(103) into Eqs. (93)-(96) we find that the iteration eigenvalue becomes,

$$\omega(\lambda) = c\left[\frac{\lambda^2}{\lambda^2 + 3(1-c)}\right]\int_0^1 d\mu\left(\frac{1 - 3\mu^2}{1 + \lambda^2\mu^2}\right)$$

$$= \frac{3c}{\lambda^2 + 3(1-c)}\left[\left(\frac{\lambda^2}{3} + 1\right)\frac{\tan^{-1}\lambda}{\lambda} - 1\right]\ . \qquad (104)$$

Looking at Figure (4) we can see how the eigenvalues of the accelerated system compare to that of the unaccelerated system. The low order diffusion equations
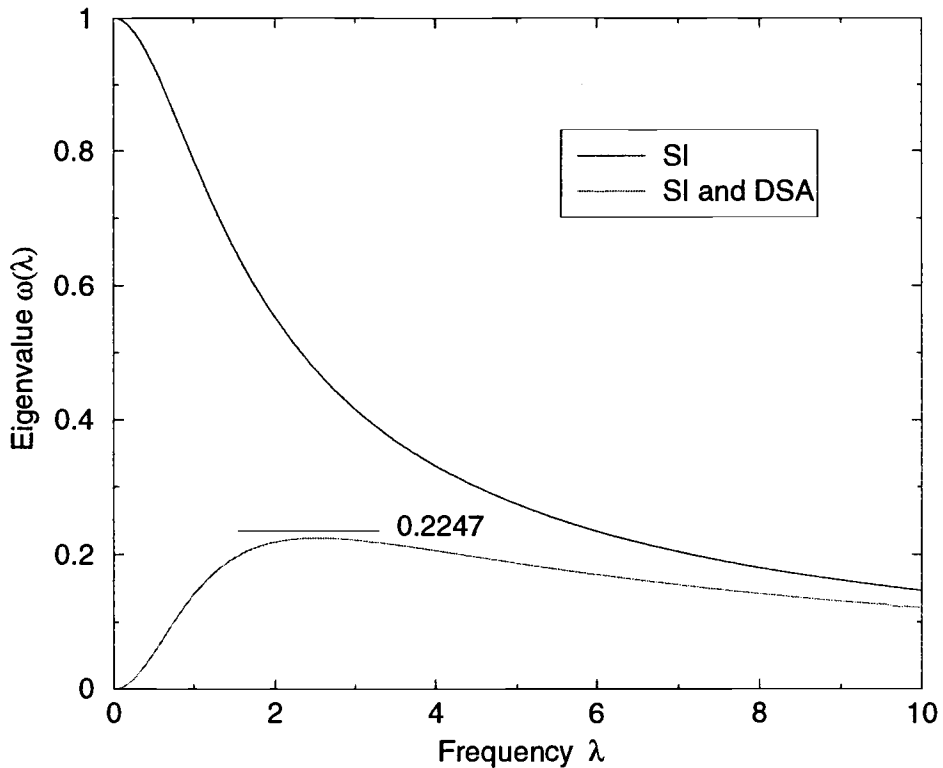
Fig. 4: Eigenvalues $\omega(\lambda)$ as a function of λ for diffusion synthetic acceleration (DSA) in slab geometry.

rapidly accelerate the *rate* of convergence for the iteration scheme. We determine the spectral radius for the accelerated iteration scheme by solving for the maximum eigenvalue,

$$\rho \leq \max_{\lambda} \left| c \int_0^1 d\mu \frac{1 - 3\mu^2}{1 + \lambda^2 \mu^2} \right| < 0.2247c. \tag{105}$$

This means that for $c = 1.0$, the slowest converging error mode is reduced approximately by a factor of 77% on each iteration.

2.4 Summary

In this chapter we have reviewed some concepts important to the work being performed within this thesis. We started by introducing the system of interest and

the equation of transfer that describes the flow of radiation in this system. We also reviewed general iterative techniques and their application to solving the equation of transfer. We discussed general ways of accelerating iterative methods and some of the desirable properties of iterative accelerators. We then introduced source iteration, a specific iterative technique used for solving the equation of transfer and then discussed a method called Fourier analysis used to analyze the convergence rates of source iteration. Fourier analysis will be used extensively to investigate iterative schemes in this thesis. Based on the results of the Fourier analysis of source iteration we motivated our look at acceleration techniques. We showed how and why a diffusion equation can be used to accelerate the iterative rate of convergence of source iteration. A specific means of deriving the diffusion equations was introduced called the Four-Step procedure. A modification to the Four-Step procedure will be used to derive the diffusion acceleration equations used in this thesis. We ended by using Fourier analysis to determine the convergence rates of source iteration accelerated by the 4-step diffusion synthetic acceleration procedure.

3 SLAB GEOMETRY DISCRETIZED TRANSPORT

3.1 Introduction

In this section we discuss the methodology used to discretize the seven independent variables in the equation of transfer. First we review methods for discretizing the frequency dependence of the equation of transfer. More specifically we will introduce the commonly used multi-group technique. We then introduce a method for treating the temporal variable. We will make the observation that the equation of transfer, discretized in energy using the multi-group approximation, and discretized in time using a backward Euler technique, is very similar to a neutron transport equation with a fission source. At this point we explain our rationale for considering, in the remainder of the thesis, an energy-independent steady-state transport equation with isotropic scattering and an isotropic source. From here we describe the discrete ordinates method for discretizing the angular unknown.

Next we introduce the two spatial discretizations that we are concerned with in this thesis, simple corner balance (SCB), and upstream corner balance (UCB). Both of these discretizations impose particle conservation over sub-cell volumes (corners) of a cell and are thus coined *corner balance* discretizations. We will then look at how to derive the modified 4-step DSA equations from the SCB balance equations.

We will next discuss how to analyze these discretization and acceleration schemes. Using Fourier analysis we will compute the theoretical rates of convergence for our scheme. We also use an implementation code, a code the implements the method to verify the results of the Fourier analysis. The results of this analysis will determine whether or not in slab geometry the SCB derived modified 4-step DSA equations can be used to unconditionally accelerate UCB.

3.2 Discrete Transport

The solution to the general geometry equation of transfer is a function of seven independent variables: three spatial variables (x, y, z), two angular variables $(\mu \rightarrow (polar), \gamma \rightarrow (azimuthal))$, one frequency variable (ν), and one time variable (t). In order to numerically solve this equation in a deterministic way, we must discretize each of these independent variables.

3.2.1 Frequency Discretization

In our discussion so far, we have treated the radiation frequency, as a continuous variable ν. The most common technique for discretizing the transfer equation in frequency is the *multi-group* technique. The photon frequency range is divided into G frequency groups. Figure 5 shows the continuous frequency spectrum broken into a finite number of *groups*. These frequency groups are typically numbered in a backwards fashion, $\nu = 0$ being the highest frequency and $\nu = G$ being the lowest. This frequency indexing treatment coincides with that of the neutronics community where neutrons tend to *slow down* in energy as they interact with the matter. We define ψ_g, the total specific intensity in frequency group g, as

$$\psi_g(\mathbf{r}, \mathbf{\Omega}, t) = \int_{\nu_g}^{\nu_{g-1}} d\nu \psi(\mathbf{r}, \nu, \mathbf{\Omega}, t) . \tag{106}$$

The total direction-integrated intensity between frequency ν_{g-1} and ν_g is,

$$\phi_g(\mathbf{r}, t) = \int_{\nu_g}^{\nu_{g-1}} d\nu \phi(\mathbf{r}, \nu, t) . \tag{107}$$

This means that the total specific intensity ψ for all frequency groups is defined as,

$$\psi(\mathbf{r}, \mathbf{\Omega}, t) = \int_0^\infty d\nu \psi(\mathbf{r}, \nu, \mathbf{\Omega}, t) = \sum_{g'=0}^{G} \int_{g'} d\nu' \psi(\mathbf{r}, \nu', \mathbf{\Omega}, t) , \tag{108}$$

and that the the total direction-integrated intensity is defined as,

$$\phi\left(\mathbf{r}, t\right) = \int_0^\infty d\nu \phi\left(\mathbf{r}, \nu, t\right) = \sum_{g'=0}^{G} \int_{g'} d\nu' \phi\left(\mathbf{r}, \nu', t\right) . \tag{109}$$

The frequency dependent Plankian, Eq. (12) is integrated over frequency to give an expression for the group-averaged Plank spectrum:

$$B_g\left(T\right) = \int_{\nu_g}^{\nu_{g-1}} d\nu \frac{2h\nu^3}{c^2} \left[e^{\left[\frac{h\nu}{kT}\right]} - 1 \right]^{-1} . \tag{110}$$

The cross-sections $(\sigma_s, \sigma_a, \sigma_t)$ are normally defined by assuming a known spectrum within each group (either Plankian or Rosseland mean) [Pal93] such as,

$$\sigma_{a,g} = \frac{\int_{\nu_g} \nu_{g-1} d\nu \sigma_a\left(\nu\right) f\left(\nu\right)}{\int_{\nu_g} \nu_{g-1} d\nu f\left(\nu\right)} . \tag{111}$$
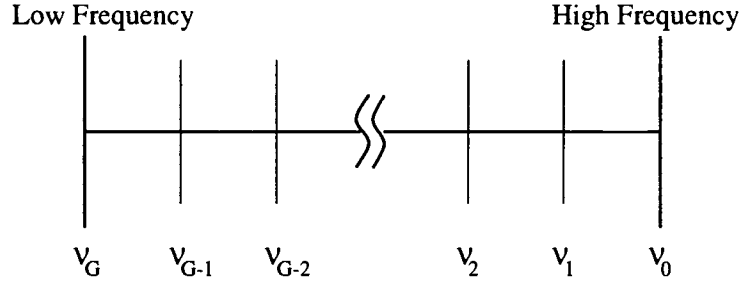
Fig. 5: Frequency division into G frequency groups.

With the above definitions the equation of transfer becomes,

$$\frac{1}{c} \frac{\partial}{\partial t} \psi_g + \mathbf{\Omega} \cdot \nabla \psi_g + \sigma_{t,g} \psi_g = \frac{1}{4\pi} \sigma_{s,g} \phi_g + \sigma_{a,g} B_g\left(T\right) , \tag{112}$$

The material temperature equation becomes,

$$C_v \frac{\partial T}{\partial t} = \sum_{g'=0}^{G} \sigma_{a,g}\left(\phi_g - 4\pi B_g\left(T\right)\right) + Q_g . \tag{113}$$

3.2.2 Time Discretization

To discretize the transfer equation in time we apply the standard backward Euler method to Eqs. (10)- (13). This results in,

$$\frac{1}{c\Delta t^n}\left[\psi_g^{n+\frac{1}{2}} - \psi_g^{n-\frac{1}{2}}\right] + \boldsymbol{\Omega}\cdot\boldsymbol{\nabla}\psi_g^{n+\frac{1}{2}} + \sigma_{t,g}^n\psi_g^{n+\frac{1}{2}} = \frac{1}{4\pi}\sigma_{s,g}^n\phi_g^{n+\frac{1}{2}} + \sigma_{a,g}^n B_g\left(T^{n+\frac{1}{2}}\right),\tag{114}$$

$$\phi_g^{n+\frac{1}{2}}(\mathbf{r}) = \int_{4\pi} d\Omega\,\psi_g^{n+\frac{1}{2}}(\mathbf{r},\boldsymbol{\Omega}),\tag{115}$$

$$\frac{C_v^n}{\Delta t^n}\left(T^{n+\frac{1}{2}} - T^{n-\frac{1}{2}}\right) = \sum_{g=1}^{G}\sigma_{a,g}^n\left(\phi_g^{n+\frac{1}{2}} - 4\pi B_g\left(T^{n+\frac{1}{2}}\right)\right) + Q_g,\tag{116}$$

where,

n = time index

Δt = time step

g = frequency group index

G = total number of photon frequency groups.

Eqs. (114)- (116) are nonlinear with respect to temperature. The Plankian function is linearized in temperature enabling us to substitute an expression for the material temperature into the transport equation. This results in a linear transport equation representing a single Newton iteration on a nonlinear system [MWS96]. The linearization begins by assuming that,

$$B^{n+\frac{1}{2}} \approx B^{n-\frac{1}{2}} + \frac{\partial B^{n-\frac{1}{2}}}{\partial t}\left(T^{n+\frac{1}{2}} - T^{n-\frac{1}{2}}\right).\tag{117}$$

The linearization assumption, Eq. (117), is substituted into Eq. (116). Rearranging we find:

$$T^{n+\frac{1}{2}} - T^{n-\frac{1}{2}} = \frac{\displaystyle\sum_{k=1}^{G} \sigma_{a,k}^n \phi_k^{n+\frac{1}{2}} - 4\pi \sum_{k=1}^{G} \sigma_{a,k}^n B_k^{n-\frac{1}{2}} + Q_g}{\left[\dfrac{C_v^n}{\Delta t^n} + 4\pi \displaystyle\sum_{k=1}^{G} \sigma_{a,k}^n \dfrac{\partial B_k^{n-\frac{1}{2}}}{\partial T} \right]} \cdot \qquad (118)$$

Eq. (118) is used to determine the material temperature at the next time iteration by solving for $T^{n+\frac{1}{2}}$ based on $T^{n-\frac{1}{2}}$. Substituting Eq. (118) back into the discretized radiative transfer equation (114) and performing some simple algebra results in the following,

$$\mathbf{\Omega} \cdot \mathbf{\nabla} \psi_g^{n+\frac{1}{2}} + \hat{\sigma}_{t,g}^n \psi_g^{n+\frac{1}{2}} = \frac{1}{4\pi} \sigma_{s,g}^n \phi_g^{n+\frac{1}{2}} + q_g + \frac{\eta \chi_g}{4\pi} \sum_{k=1}^{G} \sigma_{a,k}^n \phi_k^{n+\frac{1}{2}} + \frac{1}{c \Delta t^n} \psi_g^{n-\frac{1}{2}}, \quad (119)$$

where the quantities with no time index n are assumed to be evaluated at the previous time step $n - \frac{1}{2}$,

$$\hat{\sigma}_{t,g} = \left[\sigma_{t,g}^{n-\frac{1}{2}} + \frac{1}{c\Delta t} \right], \qquad (120)$$

$$\eta = \frac{\left[4\pi \displaystyle\sum_{k=1}^{G} \sigma_{a,k} \dfrac{\partial B_k}{\partial T} \right]}{\left[\dfrac{C_v}{\Delta t} + 4\pi \displaystyle\sum_{k=1}^{G} \sigma_{a,k} \dfrac{\partial B_k}{\partial T} \right]}, \qquad (121)$$

$$\chi_g = \frac{\left[\sigma_{a,g} \dfrac{\partial B_g}{\partial T} \right]}{\left[\displaystyle\sum_{k=1}^{G} \sigma_{a,k} \dfrac{\partial B_k}{\partial T} \right]}, \qquad (122)$$

$$q_g = \sigma_{a,g} B_g + \frac{1}{4\pi} \eta \chi_g \left[Q - 4\pi \frac{\partial B_g}{\partial T} \right], \qquad (123)$$

$$B_g = \int_{\nu_g}^{\nu_{g-1}} d\nu \frac{2h\nu^3}{c^2} \left[e^{\left[\frac{h\nu}{kT}\right]} - 1 \right]^{-1}, \tag{124}$$

$$\frac{\partial B_g}{\partial T} = \int_{\nu_g}^{\nu_{g-1}} d\nu \frac{2h^2\nu^4}{c^2 k(T)^2} \frac{e^{\left[\frac{h\nu}{kT}\right]}}{\left[e^{\left[\frac{h\nu}{kT}\right]} - 1 \right]^2}. \tag{125}$$

Eq. (119) is dependent only the material temperature at the previous time step. Eliminating the current time step temperature has left us with a system that couples the frequency groups through an effective emission source. This source is analogous to a neutron fission source [MWS96]. The multigroup technique consists of a number of one-group results. At each stage in a multigroup problem we have a one-group problem to solve. For this reason we will restrict ourselves to a simpler one-group approximation of Eq. (119) for the duration of this thesis. If the acceleration methods that we investigate fail on the one-group system then they will almost surely fail on the far more complicated multigroup system. For these reasons we will use the following one-group general geometry transport equation with isotropic scattering,

$$\boldsymbol{\Omega} \cdot \boldsymbol{\nabla}\psi + \sigma_t\psi = \frac{1}{4\pi}\sigma_s\phi + Q, \tag{126}$$

where the group index has been omitted for convenience.

3.2.3 Angular Discretization

There are several methods for treating the angular dependence of the equation of transfer. In order to solve the equation of transfer, integrals over direction must be computed. To properly handle these integrals we will concentrate on one of the more popular methods known as discrete ordinates or S_n. The discrete ordinates

approximation requires the equation of transfer to hold true only for a finite number of angles Ω. With this assumption we can numerically approximate the integral in angle by applying a quadrature rule. In slab geometry the S_n equation of transfer becomes,

$$\mu_m \frac{\partial}{\partial x} \psi_m(x) + \sigma_t(x) \psi_m(x) = \frac{1}{2} \sigma_s(x) \phi(x) + \frac{Q(x)}{2}, \quad m = 1, 2, 3 \ldots, N, \quad (127)$$

where the the direction-integrated intensity is defined as,

$$\phi(x) = \sum_{m=1}^{N} w_m \psi_m(x) . \quad (128)$$

The quadrature weights, w_m are normalized based on the dimensionality of the problem. In slab geometry we choose this to be,

$$\sum_{m=1}^{N} w_m = 2 . \quad (129)$$

3.2.4   Spatial Discretization

Spatially discretizing the equation of transfer requires that we divide the problem domain into a finite number of cells, over which material properties are held constant. Dividing the problem into a finite number of cells is the same as laying a mesh or grid on the problem. The mesh allows us to understand the connectivity of the problem and devise discretizations with which to solve the equation of transfer. A variety of different discretization techniques have been created, each of which possesses different characteristics. Overall, the goal is to have a discretization that will allow for the quick but accurate solution to a given problem. There are a variety of different families of discretizations and we can group most of them into three primary categories. These categories are Characteristic Methods (CM), Finite Element Methods (FEM) and Finite Volume Methods (FVM) [Ada97]. In this work we will concentrate on Cartesian geometry corner balance discretizations in slab and x-y geometries.
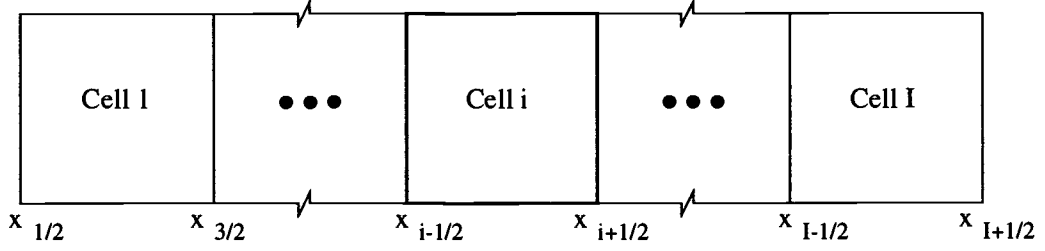
Fig. 6: Slab-geometry problem in which the slab has been broken into I discrete cells.

3.3 Corner Balance

We consider a slab geometry problem, shown in Figure 6, and divide cell i into two *corners* represented in Figure 7.
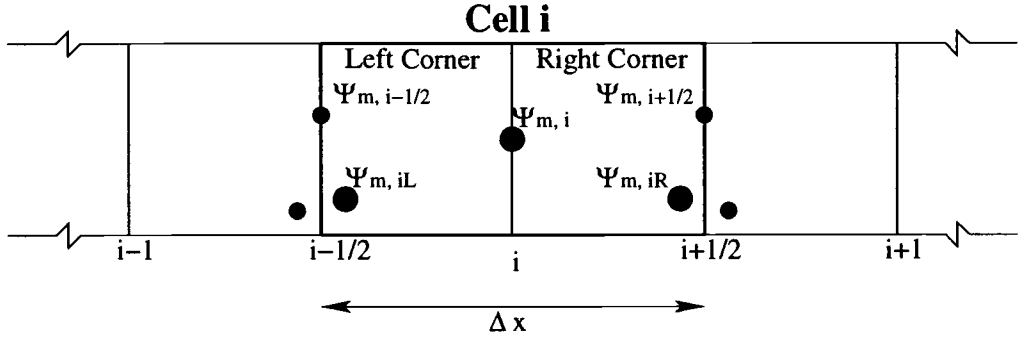
Fig. 7: Cell i divided into left and right corners.

Corner balance is a finite volume technique in which we impose particle *balance* over each *corner*. We integrate the discrete-ordinates equation of transfer, Eq. (127), over each corner (from $x_{i-\frac{1}{2}}$ to x_i for the left corner and x_i to $x_{i+\frac{1}{2}}$ for the right corner):

$$\int_{x_{i-\frac{1}{2}}}^{x_i} \left[\mu_m \frac{\partial}{\partial x} \psi_m\left(x\right) + \sigma_t\left(x\right) \psi_m\left(x\right) = \frac{1}{2}\sigma_s\left(x\right) \phi_m\left(x\right) + \frac{Q\left(x\right)}{2} \right] , \qquad (130)$$

$$\int_{x_i}^{x_{i+\frac{1}{2}}} \left[\mu_m \frac{\partial}{\partial x} \psi_m(x) + \sigma_t(x) \psi_m(x) = \frac{1}{2} \sigma_s(x) \phi_m(x) + \frac{Q(x)}{2} \right]. \qquad (131)$$

The result is two equations, one for the left corner,

$$\frac{\mu_m}{\Delta x_i} \left(\psi_{m,i} - \psi_{m,i-\frac{1}{2}} \right) + \sigma_{t,i} \psi_{m,iL} = \frac{\sigma_{s,iL}}{2} \phi_{iL} + \frac{Q_{iL}}{2}, \qquad (132)$$

and one for the right corner,

$$\frac{\mu_m}{\Delta x_i} \left(\psi_{m,i+\frac{1}{2}} - \psi_{m,i} \right) + \sigma_{t,i} \psi_{m,iR} = \frac{\sigma_{s,iR}}{2} \phi_{iR} + \frac{Q_{iR}}{2}. \qquad (133)$$

These *exact* balance equations, Eqs. (132) (133), for the left and right corners, need to be closed with two additional expressions as there are currently four unknowns: two corner average scalar intensities $\psi_{m,iL}$ and $\psi_{m,iR}$, a cell-edge scalar intensity, either $\psi_{m,i-\frac{1}{2}}$ or $\psi_{m,i+\frac{1}{2}}$, and a cell-midpoint scalar intensity $\psi_{m,i}$. An upstream closure is chosen for the cell-edge unknown,

$$\left. \begin{array}{l} \psi_{m,i+1/2} = \psi_{m,i,R} \\ \psi_{m,i-1/2} = \psi_{m,i-1,R} \end{array} \right\} \quad , \quad \mu > 0, \qquad (134)$$

$$\left. \begin{array}{l} \psi_{m,i+1/2} = \psi_{m,i+1,L} \\ \psi_{m,i-1/2} = \psi_{m,i,L} \end{array} \right\} \quad , \quad \mu < 0. \qquad (135)$$

We need a relationship between the cell midpoint and the corner and cell-edge scalar intensities. The two closures that we will investigate in this thesis, simple corner balance (SCB) [Ada91] and upstream corner balance (UCB) [Ada97] differ subtly in their form.

3.4   Slab Geometry Simple Corner Balance

The cell-center angular intensity is replaced by a *simple* average of the angular intensities on the left and right corners,

$$\psi_{m,i} = \left(\frac{\psi_{m,i,L} + \psi_{m,i,R}}{2} \right) \left\{ \begin{array}{l} \mu > 0 \quad , \\ \mu < 0 \quad . \end{array} \right. \qquad (136)$$

The result is two equations, one for the left corner,

$$\frac{\mu_m}{\Delta x_i}\left(\psi_{m,iL} + \psi_{m,iR} - 2\psi_{m,i-\frac{1}{2}}\right) + \sigma_{t,i}\psi_{m,iL} = \frac{\sigma_{s,iL}}{2}\phi_{iL} + \frac{Q_{iL}}{2}, \qquad (137)$$

and one for the right corner,

$$\frac{\mu_m}{\Delta x_i}\left(2\psi_{m,i+\frac{1}{2}} - \psi_{m,iL} - \psi_{m,iR}\right) + \sigma_{t,i}\psi_{m,iR} = \frac{\sigma_{s,iR}}{2}\phi_{iR} + \frac{Q_{iR}}{2}. \qquad (138)$$

We can write Eqs. (137) and (138) in matrix form:

$$\begin{bmatrix} \sigma_{t,i}\Delta x_i + \mu & \mu \\ -\mu & \sigma_{t,i}\Delta x_i + \mu \end{bmatrix}\begin{bmatrix} \psi_{m,i,L} \\ \psi_{m,i,R} \end{bmatrix} + \begin{bmatrix} -2\mu & 0 \\ 0 & 0 \end{bmatrix}\begin{bmatrix} \psi_{m,i-1,R} \\ \psi_{m,i+1,L} \end{bmatrix}$$

$$= \begin{bmatrix} \dfrac{\sigma_{s,i}\Delta x_i}{2} & 0 \\ 0 & \dfrac{\sigma_{s,i}\Delta x_i}{2} \end{bmatrix}\begin{bmatrix} \phi_{i,L} \\ \phi_{i,R} \end{bmatrix} + \begin{bmatrix} \dfrac{\Delta x_i}{2} & 0 \\ 0 & \dfrac{\Delta x_i}{2} \end{bmatrix}\begin{bmatrix} Q_{i,L} \\ Q_{i,R} \end{bmatrix}, \quad \mu > 0, \quad (139)$$

$$\begin{bmatrix} \sigma_{t,i}\Delta x_i - \mu & \mu \\ -\mu & \sigma_{t,i}\Delta x_i - \mu \end{bmatrix}\begin{bmatrix} \psi_{m,i,L} \\ \psi_{m,i,R} \end{bmatrix} + \begin{bmatrix} 0 & 0 \\ 0 & 2\mu \end{bmatrix}\begin{bmatrix} \psi_{m,i-1,R} \\ \psi_{m,i+1,L} \end{bmatrix}$$

$$= \begin{bmatrix} \dfrac{\sigma_{s,i}\Delta x_i}{2} & 0 \\ 0 & \dfrac{\sigma_{s,i}\Delta x_i}{2} \end{bmatrix}\begin{bmatrix} \phi_{i,L} \\ \phi_{i,R} \end{bmatrix} + \begin{bmatrix} \dfrac{\Delta x_i}{2} & 0 \\ 0 & \dfrac{\Delta x_i}{2} \end{bmatrix}\begin{bmatrix} Q_{i,L} \\ Q_{i,R} \end{bmatrix}, \quad \mu < 0. \quad (140)$$

Which can be expressed as,

$$\mathbf{T}_m^{\pm}\mathbf{\Psi}_{m,i}^{\pm} + \mathbf{H}_m^{\pm}\mathbf{\Psi}_{m,i\pm1}^{inc,\pm} = \mathbf{S}\Phi_i, \qquad (141)$$

where,

$$\Phi_i = \begin{bmatrix} \phi_{i,L} \\ \phi_{i,R} \end{bmatrix}, \qquad (142)$$

$$\mathbf{\Psi}_{m,i}^{\pm} = \begin{bmatrix} \psi_{m,i,L}^{\pm} \\ \psi_{m,i,R}^{\pm} \end{bmatrix}, \qquad (143)$$

$$\mathbf{\Psi}_{m,i\pm1}^{\pm} = \begin{bmatrix} \psi_{m,i,\pm1}^{\pm} \\ \psi_{m,i,\pm1}^{\pm} \end{bmatrix}, \qquad (144)$$

and $\psi^{\pm}$ represents positive and negative direction dependence on μ, of ψ.

The use of a simple average to close the system is the origin of the name of this corner balance discretization: Simple Corner Balance or SCB [Ada91]. When Adams introduced SCB it was a step in the right direction for radiative transfer problems. It has excellent behavior in optically thick diffusive problems, common for radiation transport problems, and it is easy to define and implement on arbitrary polygonal cells. By optically thick we mean that the distance a photon travels between interactions is very small compared to the size of the problem. However, the simple corner balance (SCB) closure couples the left and right half cell scalar intensities in both of the balance equations. This requires the solution of a 2×2 linear system in each zone for slab geometry transport sweeps.

3.5 Slab Geometry Upstream Corner Balance

During the last few years there has been an increased effort to use *unstructured* meshes consisting of arbitrarily connected grids of polygons. When we extend the SCB method to general 2D polygons, the transport sweep requires the inversion of an $N \times N$ matrix in each spatial cell where N is the number of corners of each polygon. Inverting an $N \times N$ matrix for the solution within each spatial cell becomes very expensive as the number of corners increases. A discretization method that maintains the favorable properties of SCB but eliminates the need to invert an $N \times N$ matrix for each cell would be a significant improvement. In 1997 Adams [Ada97] designed a modification to SCB that alleviates this inefficiency by replacing Eq. (136) with an *upstream* closure, eliminating the coupling between the corner balance equations. In

slab geometry this closure has the form:

$$\psi_{m,i} = \begin{cases} \psi_{m,i,L} + \dfrac{1}{4}\left[\left(\dfrac{\sigma_s\phi + Q}{\sigma_t}\right)_{i,R} - \left(\dfrac{\sigma_s\phi + Q}{\sigma_t}\right)_{i,L}\right] \\[2ex] \quad + \beta\left(\tau_{m,i,L}\right)\left(\psi_{m,i,L} - \psi_{m,i-1/2}\right), \quad \mu > 0, \\[3ex] \psi_{m,i,R} + \dfrac{1}{4}\left[\left(\dfrac{\sigma_s\phi + Q}{\sigma_t}\right)_{i,L} - \left(\dfrac{\sigma_s\phi + Q}{\sigma_t}\right)_{i,R}\right] \\[2ex] \quad + \beta\left(\tau_{m,i,R}\right)\left(\psi_{m,i,R} - \psi_{m,i+1/2}\right), \quad \mu < 0, \end{cases}$$

where,

$$\beta_{m,i}\left(\tau_{m,i}\right) = \frac{\alpha_{m,i}\left(\tau_{m,i}\right)}{\tau_{m,i}}, \tag{145}$$

$$\alpha_{m,i}\left(\tau_{m,i}\right) = \frac{3 + 4\tau_{m,i} + 4\alpha_0\tau_{m,i}^2}{2 + 2\tau_{m,i} + 4\tau_{m,i}^2}, \quad \alpha_0 = 0.455, \tag{146}$$

$$\tau_{m,i} = \frac{\sigma_{t,i}\Delta x}{2|\mu_m|}, \tag{147}$$

This closure eliminates the need for a matrix inversion in each zone. Furthermore, Eq. (145) helps UCB to limit to the same (or somewhat more accurate) discretized diffusion equation for optically thick and diffusive problems [Ada97]. This closure also provides improved accuracy for optically thin and intermediate regimes.

By combining the left and right corner balance Eqs. (132)- (133) with the upstream closure Eq. (145) we obtain,

$$
\begin{bmatrix} \dfrac{2\mu_m}{\Delta x_i}\left(1+\beta_{m,i,L}\right)+\sigma_{t,i,L} & 0 \\[2ex] -\dfrac{2\mu_m}{\Delta x_i}\left(1+\beta_{m,i,L}\right) & \dfrac{2\mu_m}{\Delta x_i}+\sigma_{t,i,L} \end{bmatrix} \begin{bmatrix} \psi_{m,i,L} \\[1ex] \psi_{m,i,R} \end{bmatrix}
$$

$$
-\begin{bmatrix} -\dfrac{2\mu_m}{\Delta x_i}\left(1+\beta_{m,i,L}\right) & 0 \\[2ex] 0 & -\dfrac{2\mu_m}{\Delta x_i}\left(-\beta_{m,i,L}\right) \end{bmatrix} \begin{bmatrix} \psi_{m,i-1,R} \\[1ex] \psi_{m,i-1,R} \end{bmatrix}
$$

$$
=\begin{bmatrix} \dfrac{\mu_m}{\Delta x_i}\dfrac{c}{4} & -\dfrac{\mu_m}{\Delta x_i}\dfrac{c}{4}+\dfrac{\sigma_s}{2} \\[2ex] -\dfrac{\mu_m}{\Delta x_i}\dfrac{c}{4}+\dfrac{\sigma_s}{2} & \dfrac{\mu_m}{\Delta x_i}\dfrac{c}{4} \end{bmatrix} \begin{bmatrix} \phi_{i,L} \\[1ex] \phi_{i,R} \end{bmatrix}
$$

$$
+\begin{bmatrix} \dfrac{\mu_m}{\Delta x_i}\dfrac{1}{4\sigma_t} & -\dfrac{\mu_m}{\Delta x_i}\dfrac{c}{4\sigma_t}+\dfrac{1}{2} \\[2ex] \dfrac{\mu_m}{\Delta x_i}\dfrac{c}{4\sigma_t}+\dfrac{1}{2} & -\dfrac{\mu_m}{\Delta x_i}\dfrac{c}{4\sigma_t} \end{bmatrix} \begin{bmatrix} Q_{i,L} \\[1ex] Q_{i,R} \end{bmatrix}, \quad \mu>0, \tag{148}
$$

$$
\begin{bmatrix} \dfrac{2\mu_m}{\Delta x_i}+\sigma_{t,i,L} & -\dfrac{2\mu_m}{\Delta x_i}\left(1+\beta_{m,i,L}\right) \\[2ex] 0 & \dfrac{2\mu_m}{\Delta x_i}\left(1+\beta_{m,i,L}\right)+\sigma_{t,i,L} \end{bmatrix} \begin{bmatrix} \psi_{m,i,L} \\[1ex] \psi_{m,i,R} \end{bmatrix}
$$

$$
-\begin{bmatrix} -\dfrac{2\mu_m}{\Delta x_i}\left(-\beta_{m,i,L}\right) & 0 \\[2ex] 0 & -\dfrac{2\mu_m}{\Delta x_i}\left(1+\beta_{m,i,L}\right) \end{bmatrix} \begin{bmatrix} \psi_{m,i+1,L} \\[1ex] \psi_{m,i+1,L} \end{bmatrix}
$$

$$
=\begin{bmatrix} -\dfrac{\mu_m}{\Delta x_i}\dfrac{c}{4}+\dfrac{\sigma_s}{2} & \dfrac{\mu_m}{\Delta x_i}\dfrac{c}{4} \\[2ex] \dfrac{\mu_m}{\Delta x_i}\dfrac{c}{4} & -\dfrac{\mu_m}{\Delta x_i}\dfrac{c}{4}+\dfrac{\sigma_s}{2} \end{bmatrix} \begin{bmatrix} \phi_{i,L} \\[1ex] \phi_{i,R} \end{bmatrix}
$$

$$
+\begin{bmatrix} -\dfrac{\mu_m}{\Delta x_i}\dfrac{c}{4\sigma_t}+\dfrac{1}{2} & \dfrac{\mu_m}{\Delta x_i}\dfrac{1}{4\sigma_t} \\[2ex] -\dfrac{\mu_m}{\Delta x_i}\dfrac{c}{4\sigma_t} & -\dfrac{\mu_m}{\Delta x_i}\dfrac{c}{4\sigma_t}+\dfrac{1}{2} \end{bmatrix} \begin{bmatrix} Q_{i,L} \\[1ex] Q_{i,R} \end{bmatrix}, \quad \mu<0. \tag{149}
$$

The UCB system can be expressed, with the appropriate matrix substitutions, as

$$
\mathbf{T}_m^{\pm}\Psi_{m,i}^{\pm,\left(l+\frac{1}{2}\right)}+\mathbf{H}_m^{\pm}\Psi_{m,i\pm1}^{inc,\pm,\left(l+\frac{1}{2}\right)}=\mathbf{S}_m\Phi_i^{(l)}, \tag{150}
$$

where,

$$
\Phi_i=\begin{bmatrix} \phi_{i,L} \\[1ex] \phi_{i,R} \end{bmatrix}, \tag{151}
$$

$$\Psi_{m,i}^{\pm} = \left[\begin{array}{c} \psi_{m,i,L}^{\pm} \\ \psi_{m,i,R}^{\pm} \end{array} \right] , \qquad (152)$$

$$\Psi_{m,i\pm1}^{\pm} = \left[\begin{array}{c} \psi_{m,i,\pm1}^{\pm} \\ \psi_{m,i,\pm1}^{\pm} \end{array} \right] , \qquad (153)$$

and $\psi^{\pm}$ represents positive and negative direction dependence on μ, of ψ.

3.6   1D SCB Derived Modified-4-Step DSA

Source iteration applied to the SCB and UCB transport differencings will converge prohibitively slowly for optically thick and diffusive problems. In fact, the spectral radius for source iteration will be c, the scattering ratio. As was discussed in Section 2, diffusion synthetic acceleration (DSA) can be used to alleviate this problem and has been shown to unconditionally reduce the spectral radius from c to approximately $c/3$ (for isotropic scattering), provided the discretized diffusion equations are consistently derived from the discretized transport equations [AM92]. The Modified Four-Step (M4S) DSA scheme of Adams and Martin [AM92] yields a diffusion equation that is *not* strictly consistent with the transport discretization. M4S, in contrast to the traditional Four-Step procedure, enables researchers to readily derive acceleration diffusion equations for multi-dimensional systems. M4S was initially developed for FE discretizations. Adams [Ada97] showed that SCB is *exactly* equivalent to lumped linear discontinuous (LLD) FE. This means that the M4S procedure can be applied to SCB to yield acceleration equations.

Starting with the slab geometry SCB Eqs. (137)- (138), the following steps are followed to derive the M4S DSA equations:

1. Take the 0th and 1st angular moments of SCB transport Eqs. (137) - (138).

2. Change iteration indices to $(l+1)$ except on second and higher moment terms.

3. Subtract the resulting equations from the converged system to obtain a new system of equations for the additive corrections to the scalar flux resulting from source iteration.

4. Eliminate 1st moments from system, leaving a discretized diffusion equation. To do this we have to make the within-cell approximation to the cell-edge scalar flux correction and we have to eliminate all currents in favor of the left and right half-cell flux corrections.

Taking the 0th moment $\sum_m w_m$ of Eqs. (137) - (138) yields,

$$\left(\frac{J_{i,L}+J_{i,R}}{2}\right)^{(l+\frac{1}{2})} - J_{i-\frac{1}{2}}^{(l+\frac{1}{2})} + \frac{\sigma_{t,i}\Delta x_i}{2}\phi_{i,L}^{(l+\frac{1}{2})} = \frac{\sigma_{s,i}\Delta x_i}{2}\phi_{i,L}^{(l)}, \qquad (154)$$

$$J_{i+\frac{1}{2}}^{(l+\frac{1}{2})} - \left(\frac{J_{i,L}+J_{i,R}}{2}\right)^{(l+\frac{1}{2})} + \frac{\sigma_{t,i}\Delta x_i}{2}\phi_{i,R}^{(l+\frac{1}{2})} = \frac{\sigma_{s,i}\Delta x_i}{2}\phi_{i,R}^{(l)}. \qquad (155)$$

In order to take the 1st moment of Eqs. (137) - (138) we recall that,

$$\mu_m^2 = \frac{2}{3}\left[\frac{1}{2}\left(3\mu_m^2-1\right)\right] + \frac{1}{3} = \frac{2}{3}P_2\left(\mu_m\right) + \frac{1}{3}P_0\left(\mu_m\right). \qquad (156)$$

Then

$$\sum_m \mu_m^2 w_m \psi = \frac{2}{3}\Phi + \frac{1}{3}\phi, \qquad (157)$$

where,

$$\Phi = \sum_m w_m P_2\left(\mu_m\right)\psi_m. \qquad (158)$$

Taking the 1st moment $\sum_m w_m \mu_m$ of Eqs. (137) (138) yields,

$$\frac{2}{3}\left[\left(\frac{\Phi_{i,L}+\Phi_{i,R}}{2}\right)^{(l+\frac{1}{2})} - \Phi_{i-\frac{1}{2}}^{(l+\frac{1}{2})}\right] + \frac{1}{3}\left[\left(\frac{\phi_{i,L}+\phi_{i,R}}{2}\right)^{(l+\frac{1}{2})} - \phi_{i-\frac{1}{2}}^{(l+\frac{1}{2})}\right]$$

$$+ \frac{\sigma_{t,i}\Delta x_i}{2}J_{i,L}^{(l+\frac{1}{2})} = 0, \qquad (159)$$

$$\frac{2}{3}\left[\Phi_{i+\frac{1}{2}}^{\left(l+\frac{1}{2}\right)} - \left(\frac{\Phi_{i,L}+\Phi_{i,R}}{2}\right)^{\left(l+\frac{1}{2}\right)}\right] + \frac{1}{3}\left[\phi_{i+\frac{1}{2}}^{\left(l+\frac{1}{2}\right)} - \left(\frac{\phi_{i,L}+\phi_{i,R}}{2}\right)^{\left(l+\frac{1}{2}\right)}\right]$$

$$+\frac{\sigma_{t,i}\Delta x_i}{2}J_{i,R}^{\left(l+\frac{1}{2}\right)} = 0\,. \qquad (160)$$

Now, we rewrite Eqs. (154) - (155) and (159) - (160) promoting all iteration indices to the $(l+1)$ iterate except those of Φ:

$$\left(\frac{J_{i,L}+J_{i,R}}{2}\right)^{(l+1)} - J_{i-\frac{1}{2}}^{(l+1)} + \frac{\sigma_{t,i}\Delta x_i}{2}\phi_{i,L}^{(l+1)} = \frac{\sigma_{s,i}\Delta x_i}{2}\phi_{i,L}^{(l+1)}\,, \qquad (161)$$

$$J_{i+\frac{1}{2}}^{(l+1)} - \left(\frac{J_{i,L}+J_{i,R}}{2}\right)^{(l+1)} + \frac{\sigma_{t,i}\Delta x_i}{2}\phi_{i,R}^{(l+1)} = \frac{\sigma_{s,i}\Delta x_i}{2}\phi_{i,R}^{(l+1)}\,, \qquad (162)$$

$$\frac{2}{3}\left[\left(\frac{\Phi_{i,L}+\Phi_{i,R}}{2}\right)^{\left(l+\frac{1}{2}\right)} - \Phi_{i-\frac{1}{2}}^{\left(l+\frac{1}{2}\right)}\right] + \frac{1}{3}\left[\left(\frac{\phi_{i,L}+\phi_{i,R}}{2}\right)^{(l+1)} - \phi_{i-\frac{1}{2}}^{(l+1)}\right]$$

$$+\frac{\sigma_{t,i}\Delta x_i}{2}J_{i,L}^{(l+1)} = 0\,, \qquad (163)$$

$$\frac{2}{3}\left[\Phi_{i+\frac{1}{2}}^{\left(l+\frac{1}{2}\right)} - \left(\frac{\Phi_{i,L}+\Phi_{i,R}}{2}\right)^{\left(l+\frac{1}{2}\right)}\right] + \frac{1}{3}\left[\phi_{i+\frac{1}{2}}^{(l+1)} - \left(\frac{\phi_{i,L}+\phi_{i,R}}{2}\right)^{(l+1)}\right]$$

$$+\frac{\sigma_{t,i}\Delta x_i}{2}J_{i,R}^{(l+1)} = 0\,. \qquad (164)$$

We define the following corrections:

$$f_{i,L}^{(l+1)} = \phi_{i,L}^{(l+1)} - \phi_{i,L}^{\left(l+\frac{1}{2}\right)}\,, \qquad (165)$$

$$f_{i,R}^{(l+1)} = \phi_{i,R}^{(l+1)} - \phi_{i,R}^{\left(l+\frac{1}{2}\right)}\,, \qquad (166)$$

$$g_{i,L}^{(l+1)} = J_{i,L}^{(l+1)} - J_{i,L}^{\left(l+\frac{1}{2}\right)}\,, \qquad (167)$$

$$g_{i,R}^{(l+1)} = J_{i,R}^{(l+1)} - J_{i,R}^{\left(l+\frac{1}{2}\right)}\,. \qquad (168)$$

Substitute in the corrections, Eqs. (165) - (166) and (167) - (168) and subtract Eqs. (154), (155), (159), (160) from Eqs. (161), (162), (163), and (164) to yield:

$$\left(\frac{g_{i,L} + g_{i,R}}{2}\right)^{(l+1)} - g_{i-\frac{1}{2}}^{(l+1)} + \frac{\sigma_{t,i}\Delta x_i}{2}f_{i,L}^{(l+1)} = \frac{\sigma_{s,i}\Delta x_i}{2}\phi_{i,L}^{(l+1)} - \left(\phi_{i,L}^{(l)}\right), \qquad (169)$$

$$g_{i+\frac{1}{2}}^{(l+1)} - \left(\frac{g_{i,L} + g_{i,R}}{2}\right)^{(l+1)} + \frac{\sigma_{t,i}\Delta x_i}{2}f_{i,R}^{(l+1)} = \frac{\sigma_{s,i}\Delta x_i}{2}\phi_{i,R}^{(l+1)} - \left(\phi_{i,R}^{(l)}\right), \qquad (170)$$

$$\frac{1}{3}\left[\left(\frac{f_{i,L} + f_{i,R}}{2}\right)^{(l+1)} - f_{i-\frac{1}{2}}^{(l+1)}\right] + \frac{\sigma_{t,i}\Delta x_i}{2}g_{i,L}^{(l+1)} = 0, \qquad (171)$$

$$\frac{1}{3}\left[f_{i+\frac{1}{2}}^{(l+1)} - \left(\frac{f_{i,L} + f_{i,R}}{2}\right)^{(l+1)}\right] + \frac{\sigma_{t,i}\Delta x_i}{2}g_{i,R}^{(l+1)} = 0. \qquad (172)$$

We simplify the right hand side of Eqs. (169) and (170) using the fact that

$$\frac{\sigma_{s,i}\Delta x_i}{2}\left(\phi_{i,L/R}^{(l+1)} - \phi_{i,L/R}^{(l)}\right) = \frac{\sigma_{s,i}\Delta x_i}{2}\left(\phi_{i,L/R}^{(l+1)} - \phi_{i,L/R}^{\left(l+\frac{1}{2}\right)}\right) + \frac{\sigma_{s,i}\Delta x_i}{2}\left(\phi_{i,L/R}^{\left(l+\frac{1}{2}\right)} - \phi_{i,L/R}^{(l)}\right), \qquad (173)$$

which yields,

$$\left(\frac{g_{i,L} + g_{i,R}}{2}\right)^{(l+1)} - g_{i-\frac{1}{2}}^{(l+1)} + \frac{\sigma_{a,i}\Delta x_i}{2}f_{i,L}^{(l+1)} = \frac{\sigma_{s,i}\Delta x_i}{2}\left(\phi_{i,L}^{\left(l+\frac{1}{2}\right)} - \phi_{i,L}^{(l)}\right), \qquad (174)$$

$$g_{i+\frac{1}{2}}^{(l+1)} - \left(\frac{g_{i,L} + g_{i,R}}{2}\right)^{(l+1)} + \frac{\sigma_{a,i}\Delta x_i}{2}f_{i,R}^{(l+1)} = \frac{\sigma_{s,i}\Delta x_i}{2}\left(\phi_{i,R}^{\left(l+\frac{1}{2}\right)} - \phi_{i,R}^{(l)}\right). \qquad (175)$$

We next remove the dependencies on the edges $i + \frac{1}{2}, i - \frac{1}{2}$ by first obtaining,

$$g_{i+\frac{1}{2}}^{(l+1)} = \sum_{\mu>0} w_m\mu_m\left[\psi_{i,R}^{(l+1)} - \psi_{i,R}^{\left(l+\frac{1}{2}\right)}\right] + \sum_{\mu<0} w_m\mu_m\left[\psi_{i+1,L}^{(l+1)} - \psi_{i+1,L}^{\left(l+\frac{1}{2}\right)}\right], \qquad (176)$$

which, if we use a P_1 expansion of the angular intensity becomes,

$$g_{i+\frac{1}{2}}^{(l+1)} = \sum_{\mu>0} w_m\mu_m\left[\left(\frac{\phi_{i,R}}{2} + \frac{3\mu_m J_{i,R}}{2}\right)^{(l+1)} - \left(\frac{\phi_{i,R}}{2} + \frac{3\mu_m J_{i,R}}{2}\right)^{\left(l+\frac{1}{2}\right)}\right]$$

$$+ \sum_{\mu<0} w_m\mu_m\left[\left(\frac{\phi_{i+1,L}}{2} + \frac{3\mu_m J_{i+1,L}}{2}\right)^{(l+1)} - \left(\frac{\phi_{i+1,L}}{2} + \frac{3\mu_m J_{i+1,L}}{2}\right)^{\left(l+\frac{1}{2}\right)}\right] \qquad (177)$$

This reduces to,

$$g_{i+\frac{1}{2}}^{(l+1)} = \frac{\gamma}{2}\left(f_{i,R}^{(l+1)} - f_{i+1,L}^{(l+1)}\right) + \frac{1}{2}\left(g_{i,R}^{(l+1)} - g_{i+1,L}^{(l+1)}\right) . \tag{178}$$

Similarly, we find,

$$g_{i-\frac{1}{2}}^{(l+1)} = \frac{\gamma}{2}\left(f_{i-1,R}^{(l+1)} - f_{i,L}^{(l+1)}\right) + \frac{1}{2}\left(g_{i,L}^{(l+1)} - g_{i-1,R}^{(l+1)}\right) , \tag{179}$$

where γ is the quadrature normalization defined as the sum of the quadrature weights,

$$\gamma = \sum_{n=1}^{N/2} w_n . \tag{180}$$

We substitute Eqs. (178) and (179) into Eqs. (174) and (175) which yields,

$$\left(\frac{g_{i,L} + g_{i,R}}{2}\right)^{(l+1)} - \left[\frac{\gamma}{2}\left(f_{i-1,R}^{(l+1)} - f_{i,L}^{(l+1)}\right) + \frac{1}{2}\left(g_{i,L}^{(l+1)} - g_{i-1,R}^{(l+1)}\right)\right]$$

$$+ \frac{\sigma_{a,i}\Delta x_i}{2}f_{i,L}^{(l+1)} = \frac{\sigma_{s,i}\Delta x_i}{2}\left[\phi_{i,L}^{\left(l+\frac{1}{2}\right)} - \phi_{i,L}^{(l)}\right] , \tag{181}$$

$$\left[\frac{\gamma}{2}\left(f_{i,R}^{(l+1)} - f_{i+1,L}^{(l+1)}\right) + \frac{1}{2}\left(g_{i,R}^{(l+1)} - g_{i+1,L}^{(l+1)}\right)\right] - \left(\frac{g_{i,L} + g_{i,R}}{2}\right)^{(l+1)}$$

$$+ \frac{\sigma_{a,i}\Delta x_i}{2}f_{i,R}^{(l+1)} = \frac{\sigma_{s,i}\Delta x_i}{2}\left[\phi_{i,R}^{\left(l+\frac{1}{2}\right)} - \phi_{i,R}^{(l)}\right] . \tag{182}$$

We use a very simple approximation to eliminate the $f_{i+\frac{1}{2}}^{(l+1)}$; it is:

$$f_{i+\frac{1}{2}}^{(l+1)} = f_{i,R}^{(l+1)} \quad , \quad f_{i-\frac{1}{2}}^{(l+1)} = f_{i,L}^{(l+1)} . \tag{183}$$

These are local approximations to the edge direction integrated intensity quantities. These allow us to reduce Eqs. (171) and (172) to:

$$g_{i,L}^{(l+1)} = g_{i,R}^{(l+1)} = -\left(\frac{1}{3\sigma_{t,i}}\right)\left(\frac{f_{i,R}^{(l+1)} - f_{i,L}^{(l+1)}}{\Delta x_i}\right) . \tag{184}$$

By using Eq. (184) we arrive at two equations containing only the corner direction-integrated intensity corrections:

$$-\frac{1}{2}(\frac{1}{3\sigma_{t,i}})(\frac{f_{i,R}^{\ell+1} - f_{i,L}^{\ell+1}}{\Delta x_i}) - \frac{\gamma}{2}(f_{i-1,R}^{\ell+1} - f_{i,L}^{\ell+1})$$

$$+\frac{1}{2}(\frac{1}{3\sigma_{t,i-1}})(\frac{f_{i-1,R}^{\ell+1} - f_{i-1,L}^{\ell+1}}{\Delta x_{i-1}}) + \frac{\sigma_{a,i}\Delta x_i}{2}f_{i,L}^{\ell+1} = \frac{\sigma_{s,i}\Delta x_i}{2}(\phi_{i,L}^{\ell+\frac{1}{2}} - \phi_{i,L}^{\ell}), \tag{185}$$

and

$$\frac{1}{2}(\frac{1}{3\sigma_{t,i}})(\frac{f_{i,R}^{\ell+1} - f_{i,L}^{\ell+1}}{\Delta x_i}) + \frac{\gamma}{2}(f_{i,R}^{\ell+1} - f_{i+1,L}^{\ell+1})$$

$$-\frac{1}{2}(\frac{1}{3\sigma_{t,i+1}})(\frac{f_{i+1,R}^{\ell+1} - f_{i+1,L}^{\ell+1}}{\Delta x_{i+1}}) + \frac{\sigma_{a,i}\Delta x_i}{2}f_{i,R}^{\ell+1} = \frac{\sigma_{s,i}\Delta x_i}{2}(\phi_{i,R}^{\ell+\frac{1}{2}} - \phi_{i,R}^{\ell}) . \quad (186)$$

These equations, valid only in the interior of the domain, can be written in matrix form as a banded seven-stripe matrix. We can write Eqs. (185)- (186) in matrix form as,

$$\mathbf{D}\begin{bmatrix} f_{i-1,L}^{(l+\frac{1}{2})} \\ f_{i-1,R}^{(l+\frac{1}{2})} \\ f_{i,L}^{(l+\frac{1}{2})} \\ f_{i,R}^{(l+\frac{1}{2})} \\ f_{i+1,L}^{(l+\frac{1}{2})} \\ f_{i+1,R}^{(l+\frac{1}{2})} \end{bmatrix} = \mathbf{P}\begin{bmatrix} \phi_{i-1,L}^{(l+\frac{1}{2})} & - & \phi_{i-1,L}^{(l)} \\ \phi_{i-1,R}^{(l+\frac{1}{2})} & - & \phi_{i-1,R}^{(l)} \\ \phi_{i,L}^{(l+\frac{1}{2})} & - & \phi_{i,L}^{(l)} \\ \phi_{i,R}^{(l+\frac{1}{2})} & - & \phi_{i,R}^{(l)} \\ \phi_{i+1,L}^{(l+\frac{1}{2})} & - & \phi_{i+1,L}^{(l)} \\ \phi_{i+1,R}^{(l+\frac{1}{2})} & - & \phi_{i+1,R}^{(l)} \end{bmatrix} , \quad (187)$$

where,

$$\mathbf{D} = \begin{bmatrix} m & n & o & p & 0 & 0 \\ 0 & 0 & q & r & s & t \end{bmatrix} , \quad (188)$$

$$m = -\frac{1}{2}\left(\frac{1}{3\sigma_{t,i-1}\Delta x_{i-1}}\right) , \quad (189)$$

$$n = -\frac{\gamma}{2} + \frac{1}{2}\left(\frac{1}{3\sigma_{t,i-1}\Delta x_{i-1}}\right) , \quad (190)$$

$$o = \frac{1}{2}\left(\frac{1}{3\sigma_{t,i}\Delta x_i}\right) + \frac{\gamma}{2} + \frac{\sigma_{a,i}\Delta x_i}{2} , \quad (191)$$

$$p = -\frac{1}{2}\left(\frac{1}{3\sigma_{t,i}\Delta x_i}\right) , \quad (192)$$

$$q = -\frac{1}{2}\left(\frac{1}{3\sigma_{t,i}\Delta x_i}\right) , \quad (193)$$

$$r = \frac{1}{2}\left(\frac{1}{3\sigma_{t,i}\Delta x_i}\right) + \frac{\gamma}{2} + \frac{\sigma_{a,i}\Delta x_i}{2}, \tag{194}$$

$$s = -\frac{\gamma}{2} + \frac{1}{2}\left(\frac{1}{3\sigma_{t,i+1}\Delta x_{i+1}}\right), \tag{195}$$

$$t = -\frac{1}{2}\left(\frac{1}{3\sigma_{t,i+1}\Delta x_{i+1}}\right). \tag{196}$$

$$\mathbf{P} = \frac{\sigma_{s,i}\Delta x_i}{2}\mathbf{I}, \tag{197}$$

where $\mathbf{I}$ is the identity matrix.

In contrast to SCB, the non-conventional form of the UCB closure, Eq. (145), makes deriving a set of discontinuous acceleration equations using M4S DSA a difficult task. Palmer [Pal93] while analyzing curvilinear geometries applied a procedure called asymptotic analysis [LMM89] that determines specific characteristics about discretizations in particular limits. Palmer noted that SCB and UCB have *identical* thick diffusion limits. Palmer observed, that SCB derived M4S diffusion equations appeared to effectively accelerate UCB source iteration.

3.7 Slab Geometry Fourier Analysis

To determine the effectiveness of accelerating UCB with SCB derived M4S DSA equations we will perform a Fourier analysis similar to that described in Section 2.

3.7.1 Fourier Analysis of Source Iterations: SCB

The Fourier analysis source iteration applied to SCB begins with Eqs. (139) and (140) written in terms of the iteration errors. We assume an infinite medium

with zero source which results in,

$$
\begin{bmatrix} \sigma_{t,i}\Delta x_i + \mu_m & \mu_m \\ -\mu_m & \sigma_{t,i}\Delta x_i + \mu_m \end{bmatrix} \begin{bmatrix} \hat{\psi}_{m,i,L}^{(l+1)} \\ \hat{\psi}_{m,i,R}^{(l+1)} \end{bmatrix} + \begin{bmatrix} -2\mu_m & 0 \\ 0 & 0 \end{bmatrix} \begin{bmatrix} \hat{\psi}_{m,i-1,R}^{(l+1)} \\ \hat{\psi}_{m,i+1,L}^{(l+1)} \end{bmatrix}
$$

$$
= \begin{bmatrix} \dfrac{\sigma_{s,i}\Delta x_i}{2} & 0 \\ 0 & \dfrac{\sigma_{s,i}\Delta x_i}{2} \end{bmatrix} \begin{bmatrix} \hat{\phi}_{i,L}^{(l)} \\ \hat{\phi}_{i,R}^{(l)} \end{bmatrix} , \mu > 0 , \quad (198)
$$

and

$$
\begin{bmatrix} \sigma_{t,i}\Delta x_i - \mu & \mu_m \\ -\mu_m & \sigma_{t,i}\Delta x_i - \mu_m \end{bmatrix} \begin{bmatrix} \hat{\psi}_{m,i,L}^{(l+1)} \\ \hat{\psi}_{m,i,R}^{(l+1)} \end{bmatrix} + \begin{bmatrix} 0 & 0 \\ 0 & 2\mu_m \end{bmatrix} \begin{bmatrix} \hat{\psi}_{m,i-1,R}^{(l+1)} \\ \hat{\psi}_{m,i+1,L}^{(l+1)} \end{bmatrix}
$$

$$
= \begin{bmatrix} \dfrac{\sigma_{s,i}\Delta x_i}{2} & 0 \\ 0 & \dfrac{\sigma_{s,i}\Delta x_i}{2} \end{bmatrix} \begin{bmatrix} \hat{\phi}_{i,L}^{(l)} \\ \hat{\phi}_{i,R}^{(l)} \end{bmatrix} , \mu < 0 , \quad (199)
$$

where,

$$
\begin{bmatrix} \hat{\phi}_{i,L} \\ \hat{\phi}_{i,R} \end{bmatrix}^{(l)} = \sum_m w_m \begin{bmatrix} \hat{\psi}_{m,i,L} \\ \hat{\psi}_{m,i,R} \end{bmatrix}^{(l+1)} . \quad (200)
$$

The discrete Fourier mode ansatz are,

$$
\begin{bmatrix} \hat{\psi}_{m,i,L} \\ \hat{\psi}_{m,i,R} \end{bmatrix}^{(l)} = \omega^l e^{i\lambda x_i} \begin{bmatrix} a_{m,L} \\ a_{m,R} \end{bmatrix} , \quad (201)
$$

$$
\begin{bmatrix} \hat{\phi}_{i,L} \\ \hat{\phi}_{i,R} \end{bmatrix}^{(l)} = \omega^l e^{i\lambda x_i} \begin{bmatrix} A_{m,L} \\ A_{m,R} \end{bmatrix} . \quad (202)
$$

Substituting the Fourier ansatz into Eqs. (198) and (199) yields the following equations,

$$
\omega \mathbf{L}_m^+ \begin{bmatrix} a_{m,L} \\ a_{m,R} \end{bmatrix} = \mathbf{P}\mathbf{s} \begin{bmatrix} A_L \\ A_R \end{bmatrix} , \mu > 0 , \quad (203)
$$

$$
\omega \mathbf{L}_m^- \begin{bmatrix} a_{m,L} \\ a_{m,R} \end{bmatrix} = \mathbf{P}\mathbf{s} \begin{bmatrix} A_L \\ A_R \end{bmatrix} , \mu < 0 , \quad (204)
$$

where $\mathbf{L}_m^+$ and $\mathbf{L}_m^-$, the matrices corresponding to positive and negative μ, are equal to,

$$\mathbf{L}_m^+ = \begin{bmatrix} \dfrac{\mu_m}{2} + \dfrac{\sigma_{t,i}\Delta x_i}{2} & \dfrac{\mu_m}{2} - \mu_m e^{-i\lambda \Delta x_i} \\ \dfrac{-\mu_m}{2} & \dfrac{\mu_m}{2} - \dfrac{\sigma_{t,i}\Delta x_i}{2} \end{bmatrix}, \tag{205}$$

$$\mathbf{L}_m^- = \begin{bmatrix} \dfrac{\mu_m}{2} - \dfrac{\sigma_{t,i}\Delta x_i}{2} & \dfrac{-\mu_m}{2} \\ \mu_m e^{i\lambda \Delta x_i} - \dfrac{\mu_m}{2} & \dfrac{-\mu_m}{2} + \dfrac{\sigma_{t,i}\Delta x_i}{2} \end{bmatrix}, \tag{206}$$

with,

$$\mathbf{P_s} = \begin{bmatrix} \dfrac{\sigma_{s,i}\Delta x_i}{4} & 0 \\ 0 & \dfrac{\sigma_{s,i}\Delta x_i}{4} \end{bmatrix}. \tag{207}$$

Rearranging Eqs. (203) and (204) we arrive at,

$$\omega \begin{bmatrix} a_{m,L} \\ a_{m,R} \end{bmatrix} = \sum_m w_m \left[(\mathbf{L}_m^+)^{-1} + (\mathbf{L}_m^-)^{-1} \right] \mathbf{P_s} \begin{bmatrix} A_L \\ A_R \end{bmatrix} = \Lambda_{SCB} \begin{bmatrix} A_L \\ A_R \end{bmatrix}. \tag{208}$$

3.7.2 Fourier Analysis of Source Iteration: UCB

The Fourier analysis of source iteration applied to UCB begins with Eqs. (148) and (149) written in terms of the iteration errors. We assume an infinite medium with zero source which results in,

$$\begin{bmatrix} \dfrac{2\mu_m}{\Delta x_i}(1 + \beta_{m,i,L}) + \sigma_{t,i,L} & 0 \\ -\dfrac{2\mu_m}{\Delta x_i}(1 + \beta_{m,i,L}) & \dfrac{2\mu_m}{\Delta x_i} + \sigma_{t,i,L} \end{bmatrix} \begin{bmatrix} \hat{\psi}_{m,i,L}^{(l+1)} \\ \hat{\psi}_{m,i,R}^{(l+1)} \end{bmatrix}$$

$$- \begin{bmatrix} -\dfrac{2\mu_m}{\Delta x_i}(1 + \beta_{m,i,L}) & 0 \\ 0 & -\dfrac{2\mu_m}{\Delta x_i}(-\beta_{m,i,L}) \end{bmatrix} \begin{bmatrix} \hat{\psi}_{m,i-1,R}^{(l+1)} \\ \hat{\psi}_{m,i-1,R}^{(l+1)} \end{bmatrix}$$

$$= \dfrac{1}{2}\left[\mathbf{S}_s - \dfrac{\mu_m}{\Delta x_i}\mathbf{MD}_m\mathbf{S}_s\mathbf{S}_t^{-1} \right] \begin{bmatrix} \hat{\phi}_{i,L}^{(l)} \\ \hat{\phi}_{i,R}^{(l)} \end{bmatrix}, \mu > 0, \tag{209}$$

$$\begin{bmatrix} \dfrac{2\mu_m}{\Delta x_i} + \sigma_{t,i,L} & -\dfrac{2\mu_m}{\Delta x_i}\left(1 + \beta_{m,i,L}\right) \\ 0 & \dfrac{2\mu_m}{\Delta x_i}\left(1 + \beta_{m,i,L}\right) + \sigma_{t,i,L} \end{bmatrix} \begin{bmatrix} \hat{\psi}_{m,i,L}^{(l+1)} \\ \hat{\psi}_{m,i,R}^{(l+1)} \end{bmatrix}$$

$$- \begin{bmatrix} -\dfrac{2\mu_m}{\Delta x_i}\left(-\beta_{m,i,L}\right) & 0 \\ 0 & -\dfrac{2\mu_m}{\Delta x_i}\left(1 + \beta_{m,i,L}\right) \end{bmatrix} \begin{bmatrix} \hat{\psi}_{m,i+1,R}^{(l+1)} \\ \hat{\psi}_{m,i+1,R}^{(l+1)} \end{bmatrix}$$

$$= \frac{1}{2}\left[\mathbf{S}_s - \frac{\mu_m}{\Delta x_i}\mathbf{MD}_m\mathbf{S}_s\mathbf{S}_t^{-1}\right] \begin{bmatrix} \hat{\phi}_{i,L}^{(l)} \\ \hat{\phi}_{i,R}^{(l)} \end{bmatrix} , \mu < 0 , \tag{210}$$

where,

$$\begin{bmatrix} \hat{\phi}_{i,L} \\ \hat{\phi}_{i,R} \end{bmatrix}^{(l)} = \sum_m w_m \begin{bmatrix} \hat{\psi}_{m,i,L} \\ \hat{\psi}_{m,i,R} \end{bmatrix}^{(l+1)} . \tag{211}$$

The discrete Fourier mode ansatz are,

$$\begin{bmatrix} \hat{\psi}_{m,i,L} \\ \hat{\psi}_{m,i,R} \end{bmatrix}^{(l)} = \omega^l e^{i\lambda x_i} \begin{bmatrix} a_{m,L} \\ a_{m,R} \end{bmatrix} , \tag{212}$$

$$\begin{bmatrix} \hat{\phi}_{i,L} \\ \hat{\phi}_{i,R} \end{bmatrix}^{(l)} = \omega^l e^{i\lambda x_i} \begin{bmatrix} A_L \\ A_R \end{bmatrix} . \tag{213}$$

Introducing the Fourier ansatz yields,

$$\omega \mathbf{L}_m^+ \begin{bmatrix} a_{m,L} \\ a_{m,R} \end{bmatrix} = \mathbf{P}_{U,m}^+ \begin{bmatrix} A_L \\ A_R \end{bmatrix} , \mu > 0 , \tag{214}$$

$$\omega \mathbf{L}_m^- \begin{bmatrix} a_{m,L} \\ a_{m,R} \end{bmatrix} = \mathbf{P}_{U,m}^- \begin{bmatrix} A_L \\ A_R \end{bmatrix} , \mu < 0 , \tag{215}$$

which we notice is identical to Eqs. (203) and (204) except for $\mathbf{P}_{U,m}^{\pm}$ which in the UCB discretization, is now a function of angle. We define $\mathbf{L}_m^+$, $\mathbf{L}_m^+$ and $\mathbf{P}_{U,m}^{\pm}$ as,

$$\mathbf{L}_m^+ = \begin{bmatrix} \dfrac{2\mu_m}{\Delta x_i}\left(1 + \beta_{m,i,L}\right) + \sigma_{t,i,L} & -\dfrac{2\mu_m}{\Delta x_i}\left(1 + \beta_{m,i,L}\right)e^{-i\lambda\Delta x_i} \\ -\dfrac{2\mu_m}{\Delta x_i}\left(1 + \beta_{m,i,L}\right) & \dfrac{2\mu_m}{\Delta x_i}\left(1 + \beta_{m,i,L}\right)e^{-i\lambda\Delta x_i} + \sigma_{t,i,L} \end{bmatrix} , \tag{216}$$

$$\mathbf{L}_m^+ = \begin{bmatrix} \dfrac{2\mu_m}{\Delta x_i}(1+\beta_{m,i,R})\,e^{i\lambda\Delta x_i}+\sigma_{t,i,R} & -\dfrac{2\mu_m}{\Delta x_i}(1+\beta_{m,i,L}) \\ -\dfrac{2\mu_m}{\Delta x_i}(1+\beta_{m,i,R})\,e^{i\lambda\Delta x_i} & \dfrac{2\mu_m}{\Delta x_i}(1+\beta_{m,i,R})+\sigma_{t,i,R} \end{bmatrix}, \qquad (217)$$

$$\mathbf{P_{U}}_m^\pm = \begin{bmatrix} \dfrac{\sigma_{s,i,L}}{2}+\dfrac{\mu_m c}{2\Delta x_i} & -\dfrac{\mu_m c}{2\Delta x_i} \\ -\dfrac{\mu_m c}{2\Delta x_i} & \dfrac{\sigma_{s,i,R}}{2}+\dfrac{\mu_m c}{2\Delta x_i} \end{bmatrix}, \qquad (218)$$

where c is equal to the scattering ratio $\frac{\sigma_s}{\sigma_t}$.

Rearranging Eqs. (214) and (215) we arrive at,

$$\omega \begin{bmatrix} a_{m,L} \\ a_{m,R} \end{bmatrix} = \left[\sum_{m=1}^{N/2} w_m \left[(\mathbf{L}_m^+)^{-1}\,\mathbf{P_{U}}_m \right] + \sum_{m=N/2}^{N} w_m \left[(\mathbf{L}_m^-)^{-1}\,\mathbf{P_{U}}_m \right] \right] \begin{bmatrix} A_L \\ A_R \end{bmatrix}$$

$$= \Lambda_{UCB} \begin{bmatrix} A_L \\ A_R \end{bmatrix}. \quad (219)$$

3.7.3 Fourier Analysis of Modified 4-Step Diffusion Equations

The Fourier analysis of the slab geometry SCB derived M4S DSA equations begins with Eqs. (185) and (186). The discrete Fourier mode ansatz are,

$$\begin{bmatrix} f_{i,L} \\ f_{i,R} \end{bmatrix}^{(l+1)} = \omega^{(l)} e^{i\lambda x_i} \begin{bmatrix} a_L \\ a_R \end{bmatrix}, \qquad (220)$$

$$\begin{bmatrix} \hat{\phi}_{i,L} \\ \hat{\phi}_{i,R} \end{bmatrix}^{(l)} = \omega^{(l)} e^{i\lambda x_i} \begin{bmatrix} A_L \\ A_R \end{bmatrix}. \qquad (221)$$

Substituting the Fourier ansatz into Eq. (187) yields the following matrix eigenvalue/eigenvector system:

$$\mathbf{D} \begin{bmatrix} a_L \\ a_R \end{bmatrix} = \mathbf{P_D} \begin{bmatrix} A_L \\ A_R \end{bmatrix}, \qquad (222)$$

where **D** is equal to,

$$
\begin{bmatrix}
\left[\frac{1}{3\sigma_t\Delta x}\right] + \gamma - \left[\frac{1}{3\sigma_t\Delta x}\right]e^{-i\lambda\Delta x} + \sigma_a\Delta x & -\left[\frac{1}{3\sigma_t\Delta x}\right] - \gamma e^{-i\lambda\Delta x} + \left[\frac{1}{3\sigma_t\Delta x}\right]e^{-i\lambda\Delta x} \\
-\left[\frac{1}{3\sigma_t\Delta x}\right] - \gamma e^{i\lambda\Delta x} + \left[\frac{1}{3\sigma_t\Delta x}\right]e^{i\lambda\Delta x} & \left[\frac{1}{3\sigma_t\Delta x}\right] + \gamma - \left[\frac{1}{3\sigma_t\Delta x}\right]e^{i\lambda\Delta x} + \sigma_a\Delta x
\end{bmatrix},
$$

$$(223)$$

and **P$_D$** is equal to,

$$
\mathbf{P_D} = \begin{bmatrix} \dfrac{\sigma_s\Delta x}{4} & 0 \\ 0 & \dfrac{\sigma_s\Delta x}{4} \end{bmatrix}.
$$

$$(224)$$

The Fourier analysis of the SCB system accelerated with the SCB derived modified 4-step equations and the UCB system accelerated with SCB derived modified 4-step equations can be represented in the following in matrix notation,

$$
\omega \begin{bmatrix} A_L \\ A_R \end{bmatrix} = [\Lambda_{SCB,UCB} + \mathbf{E}\left(\Lambda_{SCB,UCB} - \mathbf{I}\right)] \begin{bmatrix} A_L \\ A_R \end{bmatrix},
$$

$$(225)$$

where,

$$
\mathbf{E} = \mathbf{D}^{-1}\mathbf{P_D},
$$

$$(226)$$

where ω is an eigenvalue, $A_{L,R}$ is an eigenfunction and **I** is the identity matrix.

3.8   Numerical Results

3.8.1   Fourier Analysis Results

A Fourier analysis of SCB and UCB transport accelerated with SCB derived modified 4-step equations was performed using a S_{32} Gaussian quadrature set. The iterative scheme was also implemented to verify the results of the Fourier analysis. Figure (8) shows the results of the Fourier analysis and implementation code. It shows the spectral radii as a function of mesh spacing for the SCB and UCB discretization using SCB derived DSA corrections. The SCB-accelerated UCB discretization has

a maximum spectral radius of 0.2950, for $c = 0.999999$ and an optical thickness of approximately 0.93 mean-free-paths (mfp). The expected spectral radius in the thin limit is approximately 0.2247 at 0.01 mean-free-paths (mfp). The plot also shows a spectral radius approaching zero for very optically thick cells. Numerical results were generated for slabs with 100 cells, an S_{32} quadrature set and vacuum boundary conditions for a range of optical thicknesses matching that of the Fourier analysis. To get the most accurate results, all of the Fourier modes were excited by picking a random initial guess for the angular intensity. We choose a zero source and let the solution converge toward the exact results: $\psi = 0$. The problem is run until a stable spectral radius is achieved. Figure 8 shows that our implementation code agrees well with our analysis: SCB-derived DSA effectively accelerates the UCB discretization. It is important to note that the implementation results should be equal to or less than the Fourier analysis. This is because the implementation code is modeling a *finite* system while the Fourier analysis is modeling an *infinite* system. We can clearly see that the implementation results are just slightly less than the Fourier analysis results. This means that the implemented method is behaving exactly as predicted by the analysis.

3.8.2 Implementation Code Model Problem

To complement the Fourier analysis the implementation code was run on a representative slab geometry problem. The implementation code serves two primary purposes. First it is a separate means of determining the convergence properties of the iterative scheme as shown in Figure 8. Second, it is a good way of verifying the that the DSA is converging to the correct answer.

We begin by describing a slab geometry model problem that was chosen to verify

SCB/UCB WITH "MODIFIED 4–STEP" DSA
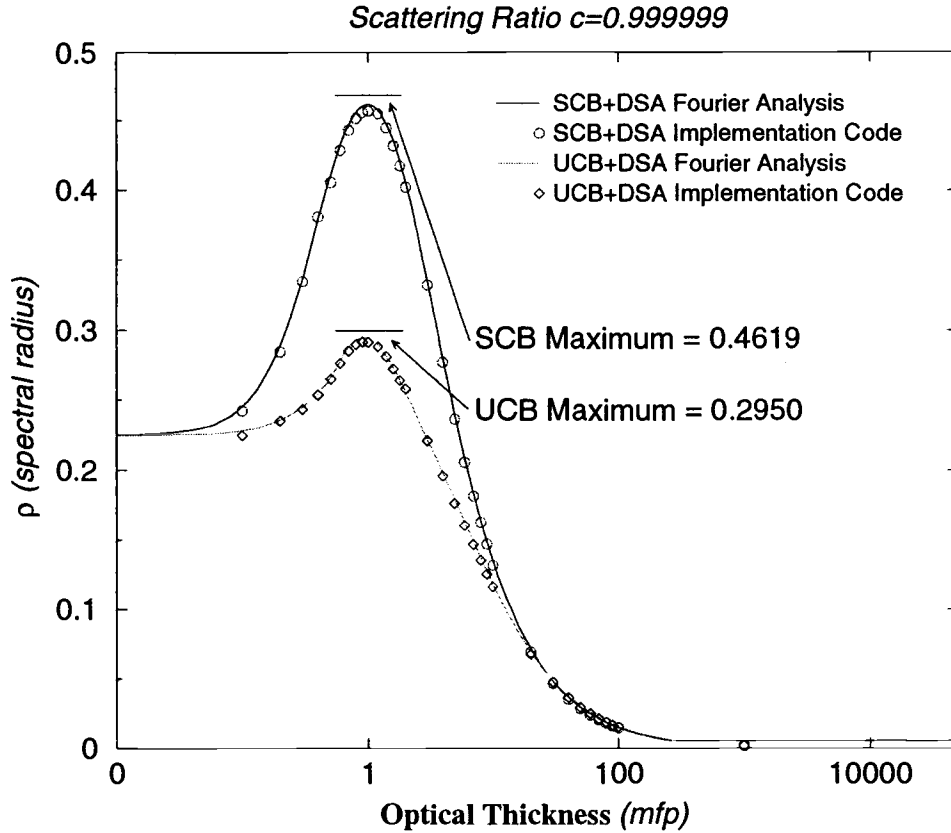
Fig. 8: Maximum Eigenvalues $\omega(\lambda)$ as a function of Δx for SCB and UCB slab geometry with "Modified 4-Step" diffusion synthetic acceleration (DSA).

the proper operation of the acceleration technique. Figure 9 illustrates the model problem.

In Figures 10 and 11 we see that the SCB and UCB solutions both with and without the DSA. One of the properties of an acceleration technique is that it yields the same solution as the unaccelerated solution. We see that the SCB solution, with and without DSA, converges to the same solution. We also see that the UCB solution, with and without DSA, converge to same solution.

| Reflecting Boundary | $\sigma_t = 50\,\mathrm{cm}^{-1}$ $\sigma_s = 0.0\ \mathrm{cm}^{-1}$ $Q = 1000$ | $\sigma_t = 1.0$ $\sigma_s = 0.0$ $Q = 0.0$ | $\sigma_t = 1.0\ \mathrm{cm}^{-1}$ $\sigma_s = 1.0\ \mathrm{cm}^{-1}$ $Q = 0.0$ | $\sigma_t = 1.0$ $\sigma_s = 1.0$ $Q = 1.0$ | $\sigma_t = 1.0\ \mathrm{cm}^{-1}$ $\sigma_s = 0.9\ \mathrm{cm}^{-1}$ $Q = 0.0$ | Vacuum Boundary |

0 ⟷ 10 ⟷ 15 ⟷ 25 ⟷ 30 ⟷ 40

x (cm)

Fig. 9: SCB and UCB slab model stencil.

Table 1 shows some convergence metrics for the model problem. It is clear to see that the DSA scheme is highly effective in reducing the number of iterations required to converge to the same result. The SCB and UCB 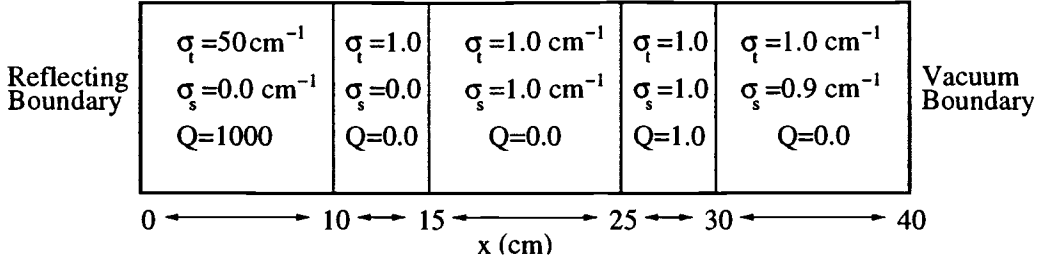model problem results have spectral radii that are less than the Fourier analysis. Since the Fourier analysis is for an infinite system, any finite system, such as the model problem, will have a smaller spectral radius.

Table 1: Slab Model Problem Results

Discretization:	$Iterations_{SI}$:	$Iterations_{DSA}$:	ρ_{SI}:	ρ_{DSA}:	ϵ:
SCB	2639	34	0.993	0.452	$1.0e^{-16}$
UCB	2629	24	0.989	0.252	$1.0e^{-16}$

3.9 Summary

In this chapter we considered strategies for discretizing the slab geometry equation of transfer in frequency, time, angle and space. In particular, we focused on the form of the corner balance family of spatial discretizations. We reviewed the simple corner balance and upstream corner balance closures and the equations that are iteratively solved when using source iteration.

We then introduced the technique for deriving the M4S DSA equations and applied
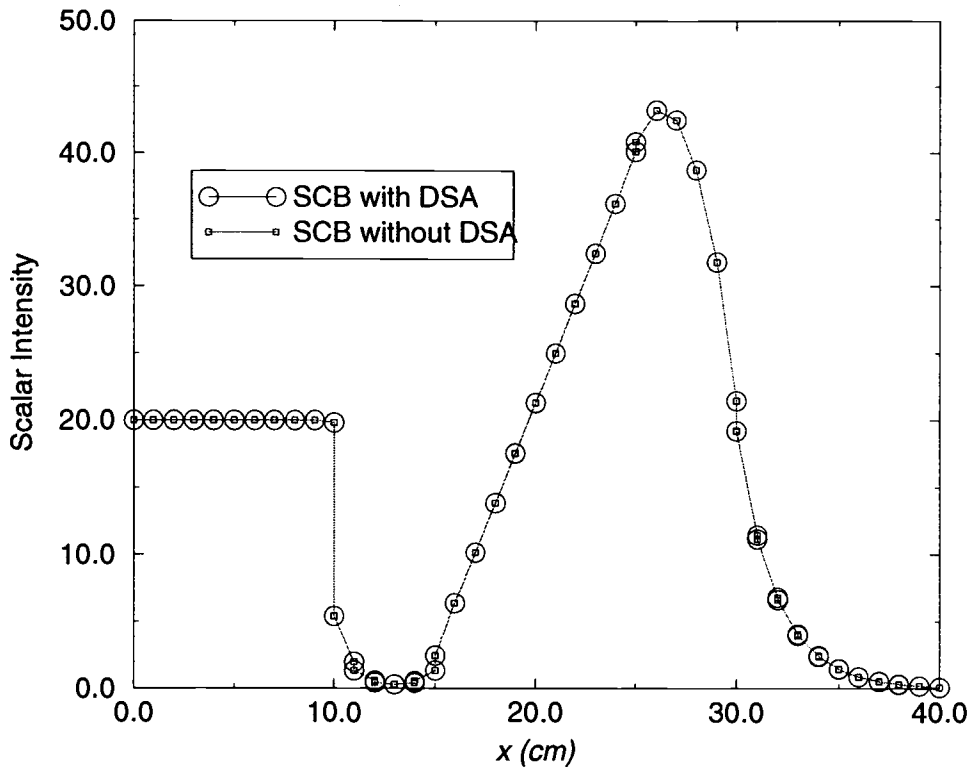
Fig. 10: SCB model problem results with and without acceleration.

this technique to derive acceleration equations for slab geometry SCB transport.

We then performed a Fourier analysis of the SCB, UCB, and M4S DSA equations. These Fourier analysis results have been verified by implementing this acceleration scheme and observing convergence rates for several model problems. The results clearly showed that SCB derived diffusion acceleration equations are very effective at increasing the rate of iterative convergence of UCB. We have also solved an interesting model problem to test our implementation code for accuracy. The results of this problem indicate that our accelerated system converges to the unaccelerated results, and that the coarse mesh results agree with high spatial resolution benchmark results.
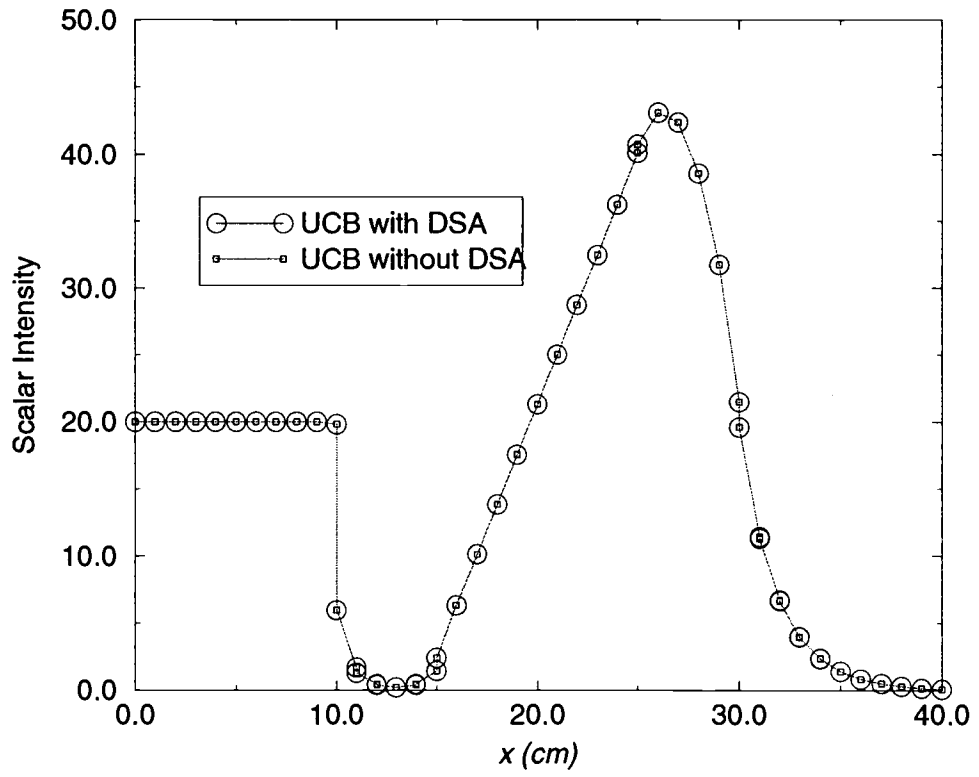
Fig. 11: UCB model problem results with and without and without acceleration.

4 X-Y GEOMETRY DISCRETIZED TRANSPORT

4.1 Introduction

We begin by discussing the methodology used to discretize the seven independent variables of the equation of transfer. In x-y geometry the only discretizations that are different from the slab geometry cases are the angular and spatial discretizations. We discuss the angular discretization changes and then apply SCB and UCB in x-y geometry. This includes reviewing the form of the SCB derived M4S DSA equations.

We perform a Fourier analysis in x-y geometry in a manner consistent with that in Section 3. We find that only subtle differences exist between the slab geometry and x-y geometry Fourier analyses.

Having established the SCB, UCB and SCB derived M4S DSA schemes we will look at the results of the Fourier analyses and the associated implementation code.

4.2 Discrete Transport

In x-y geometry, the solution to the equation of transfer is a function comprised of six independent variables: two spatial variables (x, y), two angular variables $(\mu \rightarrow (polar), \gamma \rightarrow (azimuthal))$, one frequency variable (ν), and one time variable (t).

4.2.1 Frequency Discretization

In x-y geometry we use the same multigroup frequency discretization that we used in slab geometry. [See Section 3.2.1]

4.2.2   Time Discretization

In x-y geometry we use the identical temporal discretization that we used in slab geometry. [See Section 3.2.2]

4.2.3   Angular Discretization

In x-y geometry we again use discrete ordinates to discretize the angular variable. The discrete-ordinates equation of transfer becomes,

$$\mu_m \frac{\partial}{\partial x} \psi_m (x, y) + \eta_m \frac{\partial}{\partial y} \psi_m (x, y) + \sigma_t (x, y) \psi_m (x, y)$$

$$= \frac{1}{4} \sigma_s (x, y) \phi_m (x, y) + \frac{Q(x, y)}{4} , \quad m = 1, 2, 3..., N , \tag{227}$$

where the direction-integrated intensity is defined as,

$$\phi (x, y) = \sum_{m=1}^{N} w_m \psi_m (x, y) . \tag{228}$$

The normalization of the quadrature weights, w_m, changes in x-y geometry:

$$\sum_{m=1}^{N} w_m = 4 . \tag{229}$$

4.2.4   Spatial Discretization

Just as we divided the problem domain into a finite number of cells in the slab geometry system, we must divide up the plane in x-y geometry into a finite number of cells, over which material properties are held constant.
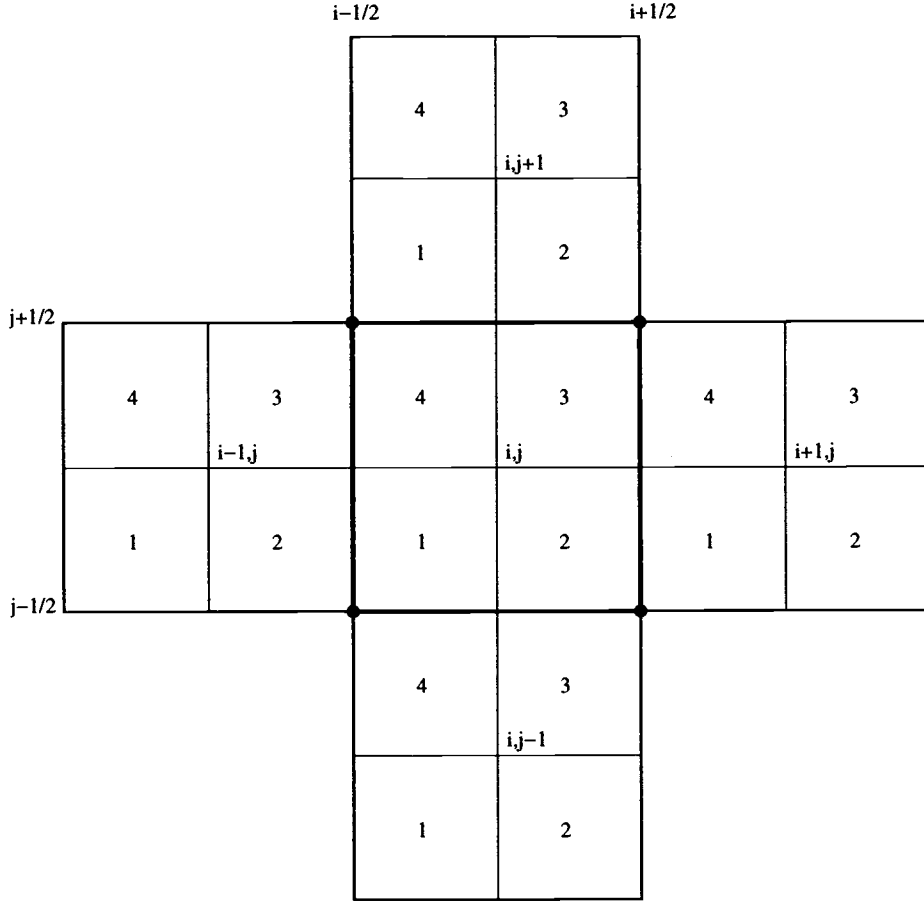
Fig. 12: Cell i, j and its neighbors with their corner subcell volumes.

4.3 Corner Balance

We consider the x-y geometry orthogonal mesh stencil, shown in Figure 12. The relationship of cell i, j to its neighboring cells are shown.

Figure 12 illustrates cell (i, j) with four *corners* labeled 1, 2, 3, 4. In corner balance, we impose particle balance over each corner. We integrate the x-y geometry discrete-ordinates equation of transfer, Eq. (227) over each corner:

Corner 1:

$$\int_{x_{i-\frac{1}{2}}}^{x_i} dx \int_{y_{i-\frac{1}{2}}}^{y_i} dy \left[\mu_m \frac{\partial}{\partial x} \psi_m(x,y) + \eta_m \frac{\partial}{\partial y} \psi_m(x,y) + \sigma_t(x,y) \psi_m(x,y) \right.$$

$$\left. = \frac{1}{4} \sigma_s(x,y) \phi_m(x,y) + \frac{Q(x,y)}{4} \right] , \quad (230)$$

Corner 2:

$$\int_{x_i}^{x_{i-\frac{1}{2}}} dx \int_{y_{i-\frac{1}{2}}}^{y_i} dy \left[\mu_m \frac{\partial}{\partial x} \psi_m(x,y) + \eta_m \frac{\partial}{\partial y} \psi_m(x,y) + \sigma(x,y) \psi_m(x,y) \right.$$

$$\left. = \frac{1}{4} \sigma_s(x,y) \phi_m(x,y) + \frac{Q(x,y)}{4} \right] , \quad (231)$$

Corner 3:

$$\int_{x_i}^{x_{i+\frac{1}{2}}} dx \int_{y_i}^{y_{i+\frac{1}{2}}} dy \left[\mu_m \frac{\partial}{\partial x} \psi_m(x,y) + \eta_m \frac{\partial}{\partial y} \psi_m(x,y) + \sigma_t(x,y) \psi_m(x,y) \right.$$

$$\left. = \frac{1}{4} \sigma_s(x,y) \phi_m(x,y) + \frac{Q(x,y)}{4} \right] , \quad (232)$$

Corner 4:

$$\int_{x_{i-\frac{1}{2}}}^{x_i} dx \int_{y_i}^{y_{i+\frac{1}{2}}} dy \left[\mu_m \frac{\partial}{\partial x} \psi_m(x,y) + \eta_m \frac{\partial}{\partial y} \psi_m(x,y) + \sigma_t(x,y) \psi_m(x,y) \right.$$

$$\left. = \frac{1}{4} \sigma_s(x,y) \phi_m(x,y) + \frac{Q(x,y)}{4} \right] . \quad (233)$$

The result is four equations for each of the four corners of each cell. Figure 13 illustrates the cell unknowns and locations.

$$\frac{\mu_m}{\Delta x_i} (\psi_{m,i,j,B} - \psi_{m,i,j,1-}) + \frac{\eta_m}{\Delta y_i} (\psi_{m,i,j,L} - \psi_{m,i,j,1+})$$

$$+ \sigma_{t,i,j} \psi_{m,i,j,1} = \frac{1}{4} \sigma_{s,i,j} \phi_{i,j,1} + \frac{Q_{i,j,1}}{4} , \quad (234)$$
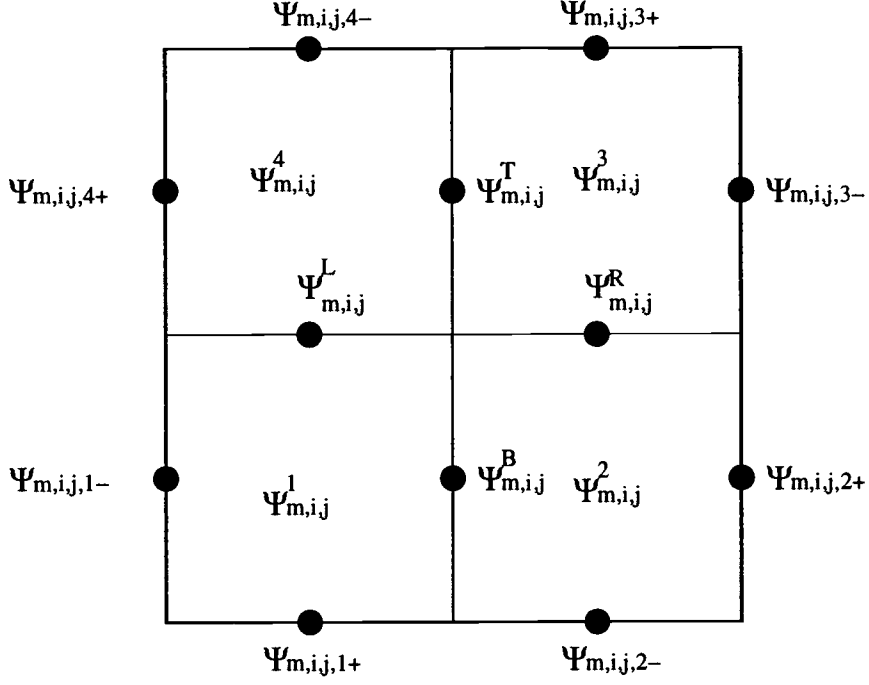
Fig. 13: X-Y geometry stencil for cell i, j.

$$\frac{\mu_m}{\Delta x_i} \left(\psi_{m,i,j,2+} - \psi_{m,i,j,B}\right) + \frac{\eta_m}{\Delta y_i} \left(\psi_{m,i,j,R} - \psi_{m,i,j,2-}\right)$$

$$+ \sigma_{t,i,j} \psi_{m,i,j,2} = \frac{1}{4} \sigma_{s,i,j} \phi_{i,j,2} + \frac{Q_{i,j,2}}{4} , \tag{235}$$

$$\frac{\mu_m}{\Delta x_i} \left(\psi_{m,i,j,3-} - \psi_{m,i,j,T}\right) + \frac{\eta_m}{\Delta y_i} \left(\psi_{m,i,j,3+} - \psi_{m,i,j,R}\right)$$

$$+ \sigma_{t,i,j} \psi_{m,i,j,3} = \frac{1}{4} \sigma_{s,i,j} \phi_{i,j,3} + \frac{Q_{i,j,3}}{4} , \tag{236}$$

$$\frac{\mu_m}{\Delta x_i} \left(\psi_{m,i,j,T} - \psi_{m,i,j,4+}\right) + \frac{\eta_m}{\Delta y_i} \left(\psi_{m,i,j,4-} - \psi_{m,i,j,L}\right)$$

$$+ \sigma_{t,i,j} \psi_{m,i,j,4} = \frac{1}{4} \sigma_{s,i,j} \phi_{i,j,4} + \frac{Q_{i,j,4}}{4} . \tag{237}$$

Similar to slab geometry, an upstream closure is chosen,

$$\psi_{m,i,j,1-} = \begin{cases} \psi_{m,i-1,j,2} , & \mu > 0 \\ \psi_{m,i,j,1} , & \mu < 0 \end{cases} , \tag{238}$$

$$\psi_{m,i,j,1+} = \begin{cases} \psi_{m,i,j-1,4} \, , & \eta > 0 \\ \psi_{m,i,j,1} \, , & \eta < 0 \end{cases} \, , \qquad (239)$$

$$\psi_{m,i,j,2+} = \begin{cases} \psi_{m,i,j,2} \, , & \mu > 0 \\ \psi_{m,i+1,j,1} \, , & \mu < 0 \end{cases} \, , \qquad (240)$$

$$\psi_{m,i,j,2-} = \begin{cases} \psi_{m,i,j-1,3} \, , & \eta > 0 \\ \psi_{m,i,j,2} \, , & \eta < 0 \end{cases} \, , \qquad (241)$$

$$\psi_{m,i,j,3-} = \begin{cases} \psi_{m,i,j,3} \, , & \mu > 0 \\ \psi_{m,i+1,j,4} \, , & \mu < 0 \end{cases} \, , \qquad (242)$$

$$\psi_{m,i,j,3+} = \begin{cases} \psi_{m,i,j,3} \, , & \eta > 0 \\ \psi_{m,i,j+1,2} \, , & \eta < 0 \end{cases} \, , \qquad (243)$$

$$\psi_{m,i,j,4+} = \begin{cases} \psi_{m,i-1,j,3} \, , & \mu > 0 \\ \psi_{m,i,j,4} \, , & \mu < 0 \end{cases} \, , \qquad (244)$$

$$\psi_{m,i,j,4-} = \begin{cases} \psi_{m,i,j,4} \, , & \eta > 0 \\ \psi_{m,i,j+1,1} \, , & \eta < 0 \end{cases} \, . \qquad (245)$$

4.4 X-Y Geometry Simple Corner Balance

As before, the cell-center angular intensity is replaced by a *simple* average of the angular intensities across each internal boundary. In Figure 12, L, B, R, T represent the internal corner surface boundaries. The four expressions for the four internal corner surface fluxes are,

$$\psi_{m,i,j,L} = \left(\frac{\psi_{m,i,j,1} + \psi_{m,i,j,4}}{2} \right) \, , \qquad (246)$$

$$\psi_{m,i,j,B} = \left(\frac{\psi_{m,i,j,1} + \psi_{m,i,j,2}}{2} \right) \, , \qquad (247)$$

$$\psi_{m,i,j,R} = \left(\frac{\psi_{m,i,j,2} + \psi_{m,i,j,3}}{2} \right) \, , \qquad (248)$$

$$\psi_{m,i,j,T} = \left(\frac{\psi_{m,i,j,4} + \psi_{m,i,j,3}}{2} \right) . \tag{249}$$

Inserting these closures into Eqs. (234)- (237) yields,

$$\frac{\mu_m}{\Delta x_i} \left(\psi_{m,i,j,1} + \psi_{m,i,j,2} - 2\psi_{m,i,j,1-} \right) + \frac{\eta_m}{\Delta y_i} \left(\psi_{m,i,j,1} + \psi_{m,i,j,4} - 2\psi_{m,i,j,1+} \right)$$

$$+ \sigma_{t,i,j} \psi_{m,i,j,1} = \frac{1}{4} \sigma_{s,i,j} \phi_{i,j,1} + \frac{Q_{i,j,1}}{4} , \tag{250}$$

$$\frac{\mu_m}{\Delta x_i} \left(2\psi_{m,i,j,2+} - \psi_{m,i,j,2} - \psi_{m,i,j,1} \right) + \frac{\eta_m}{\Delta y_i} \left(\psi_{m,i,j,2} + \psi_{m,i,j,3} - 2\psi_{m,i,j,2-} \right)$$

$$+ \sigma_{t,i,j} \psi_{m,i,j,2} = \frac{1}{4} \sigma_{s,i,j} \phi_{i,j,2} + \frac{Q_{i,j,2}}{4} , \tag{251}$$

$$\frac{\mu_m}{\Delta x_i} \left(2\psi_{m,i,j,3-} - \psi_{m,i,j,4} - \psi_{m,i,j,3} \right) + \frac{\eta_m}{\Delta y_i} \left(2\psi_{m,i,j,3+} - \psi_{m,i,j,2} - \psi_{m,i,j,3} \right)$$

$$+ \sigma_{t,i,j} \psi_{m,i,j,3} = \frac{1}{4} \sigma_{s,i,j} \phi_{i,j,3} + \frac{Q_{i,j,3}}{4} , \tag{252}$$

$$\frac{\mu_m}{\Delta x_i} \left(\psi_{m,i,j,4} + \psi_{m,i,j,3} - 2\psi_{m,i,j,4+} \right) + \frac{\eta_m}{\Delta y_i} \left(2\psi_{m,i,j,4-} - \psi_{m,i,j,1} - \psi_{m,i,j,4} \right)$$

$$+ \sigma_{t,i,j} \psi_{m,i,j,4} = \frac{1}{4} \sigma_{s,i,j} \phi_{i,j,4} + \frac{Q_{i,j,4}}{4} . \tag{253}$$

If we insert the upstream closures into Eqs. (250)- (253) and write the system in matrix form, we have,

$$\mathbf{H}_m \begin{bmatrix} \psi_{m,i-1,j,2} \\ \psi_{m,i,j-1,4} \\ \psi_{m,i,j-1,3} \\ \psi_{m,i+1,j,1} \\ \psi_{m,i+1,j,4} \\ \psi_{m,i,j+1,2} \\ \psi_{m,i,j+1,1} \\ \psi_{m,i-1,j,3} \end{bmatrix} + \mathbf{T}_m \begin{bmatrix} \psi_{m,i,j,1} \\ \psi_{m,i,j,2} \\ \psi_{m,i,j,3} \\ \psi_{m,i,j,4} \end{bmatrix} = \frac{\sigma_{s,i,j}}{16} \mathbf{I} \begin{bmatrix} \phi_{i,j,1} \\ \phi_{i,j,2} \\ \phi_{i,j,3} \\ \phi_{i,j,4} \end{bmatrix} + \frac{\Delta x_i \Delta y i}{16} \mathbf{I} \begin{bmatrix} Q_{i,j,1} \\ Q_{i,j,2} \\ Q_{i,j,3} \\ Q_{i,j,4} \end{bmatrix} , \tag{254}$$

where the matrices $\mathbf{T}_m$ and $\mathbf{H}_m$ are direction dependent. If we define,

$$U = \frac{\mu_m \Delta y_i}{2} , \tag{255}$$

$$V = \frac{\eta_m \Delta x_i}{2} , \tag{256}$$

$$W = \frac{\mu_m \Delta y_i}{4} , \tag{257}$$

$$X = \frac{\eta_m \Delta x_i}{4} , \tag{258}$$

then for $\mu > 0$, $\eta > 0$,

$$\mathbf{H}_m = \begin{bmatrix} -U & -V & 0 & 0 & 0 & 0 & 0 & 0 \\ 0 & 0 & -V & 0 & 0 & 0 & 0 & 0 \\ 0 & 0 & 0 & 0 & 0 & 0 & 0 & 0 \\ 0 & 0 & 0 & 0 & 0 & 0 & 0 & -U \end{bmatrix} , \mu > 0 , \eta > 0 . \tag{259}$$

H can also be written in matrix form as

$$\mathbf{T}_m = \begin{bmatrix} G & W & 0 & X \\ -W & G & X & 0 \\ 0 & -X & G & -W \\ -X & 0 & W & G \end{bmatrix} , \tag{260}$$

where G, for $\mu > 0$, $\eta > 0$, is defined as,

$$G = \frac{\mu_m \Delta y_i}{4} + \frac{\eta_m \Delta x_i}{4} + \frac{\sigma_{t,i,j} \Delta x_i \Delta y_j}{4} . \tag{261}$$

For $\mu < 0$, $\eta > 0$,

$$\mathbf{H}_m = \begin{bmatrix} 0 & -V & 0 & 0 & 0 & 0 & 0 & 0 \\ 0 & 0 & -V & U & 0 & 0 & 0 & 0 \\ 0 & 0 & 0 & 0 & U & 0 & 0 & 0 \\ 0 & 0 & 0 & 0 & 0 & 0 & 0 & 0 \end{bmatrix} , \mu < 0 , \eta > 0 , \tag{262}$$

$$G = \frac{-\mu_m \Delta y_i}{4} + \frac{\eta_m \Delta x_i}{4} + \frac{\sigma_{t,i,j} \Delta x_i \Delta y_j}{4} . \tag{263}$$

For $\mu > 0$, $\eta < 0$,

$$\mathbf{H}_m = \begin{bmatrix} -U & 0 & 0 & 0 & 0 & 0 & 0 & 0 \\ 0 & 0 & 0 & 0 & 0 & 0 & 0 & 0 \\ 0 & 0 & 0 & 0 & 0 & V & 0 & 0 \\ 0 & 0 & 0 & 0 & 0 & 0 & V & -U \end{bmatrix} , \mu > 0 , \eta < 0 , \tag{264}$$

$$G = \frac{\mu_m \Delta y_i}{4} + \frac{-\eta_m \Delta x_i}{4} + \frac{\sigma_{t,i,j} \Delta x_i \Delta y_j}{4} \,. \tag{265}$$

For $\mu < 0$, $\eta < 0$,

$$\mathbf{H}_m = \begin{bmatrix} 0 & 0 & 0 & 0 & 0 & 0 & 0 & 0 \\ 0 & 0 & 0 & U & 0 & 0 & 0 & 0 \\ 0 & 0 & 0 & 0 & U & V & 0 & 0 \\ 0 & 0 & 0 & 0 & 0 & 0 & V & 0 \end{bmatrix} , \mu < 0 , \eta < 0 , \tag{266}$$

$$G = \frac{-\mu_m \Delta y_i}{4} + \frac{-\eta_m \Delta x_i}{4} + \frac{\sigma_{t,i,j} \Delta x_i \Delta y_j}{4} \,. \tag{267}$$

4.5   X-Y Geometry Upstream Corner Balance

Similar to SCB we replace the cell-centered angular intensity by the UCB closure. The x-y geometry UCB closures are,

$$\psi_{m,i,j,B} = \psi_{m,i,j,1} + \frac{1}{4} \left[\left(\frac{\sigma_s \phi + Q}{\sigma_t} \right)_{i,j,2} - \left(\frac{\sigma_s \phi + Q}{\sigma_t} \right)_{i,j,1} \right]$$
$$+ \beta \left(\tau_{m,i,j,1}^x \right) \left(\psi_{m,i,j,1} - \psi_{m,i,j,1-} \right) \,, \ \mu > 0 , \tag{268}$$

$$\psi_{m,i,j,B} = \psi_{m,i,j,2} + \frac{1}{4} \left[\left(\frac{\sigma_s \phi + Q}{\sigma_t} \right)_{i,j,1} - \left(\frac{\sigma_s \phi + Q}{\sigma_t} \right)_{i,j,2} \right]$$
$$+ \beta \left(\tau_{m,i,j,2}^x \right) \left(\psi_{m,i,j,2} - \psi_{m,i,j,2+} \right) \,, \ \mu < 0 , \tag{269}$$

$$\psi_{m,i,j,T} = \psi_{m,i,j,4} + \frac{1}{4} \left[\left(\frac{\sigma_s \phi + Q}{\sigma_t} \right)_{i,j,3} - \left(\frac{\sigma_s \phi + Q}{\sigma_t} \right)_{i,j,4} \right]$$
$$+ \beta \left(\tau_{m,i,j,4}^x \right) \left(\psi_{m,i,j,4} - \psi_{m,i,j,4+} \right) \,, \ \mu > 0 , \tag{270}$$

$$\psi_{m,i,j,B} = \psi_{m,i,j,3} + \frac{1}{4} \left[\left(\frac{\sigma_s \phi + Q}{\sigma_t} \right)_{i,j,4} - \left(\frac{\sigma_s \phi + Q}{\sigma_t} \right)_{i,j,3} \right]$$
$$+ \beta \left(\tau_{m,i,j,3}^x \right) \left(\psi_{m,i,j,3} - \psi_{m,i,j,3-} \right) \,, \ \mu < 0 , \tag{271}$$

$$\psi_{m,i,j,L} = \psi_{m,i,j,1} + \frac{1}{4} \left[\left(\frac{\sigma_s \phi + Q}{\sigma_t} \right)_{i,j,4} - \left(\frac{\sigma_s \phi + Q}{\sigma_t} \right)_{i,j,1} \right]$$

$$+ \beta \left(\tau^y_{m,i,j,1} \right) \left(\psi_{m,i,j,1} - \psi_{m,i,j,1+} \right) \ , \ \eta > 0 \,, \tag{272}$$

$$\psi_{m,i,j,L} = \psi_{m,i,j,4} + \frac{1}{4} \left[\left(\frac{\sigma_s \phi + Q}{\sigma_t} \right)_{i,j,1} - \left(\frac{\sigma_s \phi + Q}{\sigma_t} \right)_{i,j,4} \right]$$

$$+ \beta \left(\tau^y_{m,i,j,4} \right) \left(\psi_{m,i,j,4} - \psi_{m,i,j,4-} \right) \ , \ \eta < 0 \,, \tag{273}$$

$$\psi_{m,i,j,R} = \psi_{m,i,j,2} + \frac{1}{4} \left[\left(\frac{\sigma_s \phi + Q}{\sigma_t} \right)_{i,j,3} - \left(\frac{\sigma_s \phi + Q}{\sigma_t} \right)_{i,j,2} \right]$$

$$+ \beta \left(\tau^y_{m,i,j,2} \right) \left(\psi_{m,i,j,2} - \psi_{m,i,j,2-} \right) \ , \ \eta > 0 \,, \tag{274}$$

$$\psi_{m,i,j,B} = \psi_{m,i,j,3} + \frac{1}{4} \left[\left(\frac{\sigma_s \phi + Q}{\sigma_t} \right)_{i,j,2} - \left(\frac{\sigma_s \phi + Q}{\sigma_t} \right)_{i,j,3} \right]$$

$$+ \beta \left(\tau^y_{m,i,j,3} \right) \left(\psi_{m,i,j,3} - \psi_{m,i,j,3+} \right) \ , \ \eta < 0 \,, \tag{275}$$

where,

$$\beta^{x,y}_{m,i,j} \left(\tau^{x,y}_{m,i,j} \right) = \frac{\alpha^{x,y}_{m,i,j} \left(\tau^{x,y}_{m,i,j} \right)}{\tau^{x,y}_{m,i,j}} \,, \tag{276}$$

$$\alpha^{x,y}_{m,i,j} \left(\tau^{x,y} \right) = \frac{3 + 4\tau^{x,y}_{m,i,j} + 4\alpha_0 \tau^{x,y}_{m,i,j}{}^2}{2 + 2\tau^{x,y}_{m,i,j} + 4\tau^{x,y}_{m,i,j}{}^2} \ , \ \alpha_0 = 0.455 \,, \tag{277}$$

$$\tau^x_{m,i,j} = \frac{\sigma_{t,i,j} \Delta x}{2|\mu_m|} \,, \tag{278}$$

$$\tau^y_{m,i,j} = \frac{\sigma_{t,i,j} \Delta y}{2|\eta_m|} \,. \tag{279}$$

We can write this system in matrix notation to simplify the presentation. The

resultant matrix system is,

$$
\left[\frac{2\mu}{\Delta x_i}\mathbf{A}_m + \frac{2\eta}{\Delta y_j}\mathbf{B}_m + \mathbf{C}\right]\begin{bmatrix}\psi_{m,i,j,1}\\\psi_{m,i,j,2}\\\psi_{m,i,j,4}\\\psi_{m,i,j,3}\end{bmatrix} - \frac{2\mu}{\Delta x_i}\mathbf{D}_m\begin{bmatrix}\psi_{m,i+1,j,1}\\\psi_{m,i-1,j,2}\\\psi_{m,i+1,j,4}\\\psi_{m,i-1,j,3}\end{bmatrix} - \frac{2\mu}{\Delta x_i}\mathbf{E}_m\begin{bmatrix}\psi_{m,i,j+1,1}\\\psi_{m,i,j+1,2}\\\psi_{m,i,j-1,4}\\\psi_{m,i,j-1,3}\end{bmatrix}
$$

$$
= \frac{1}{4}\mathbf{F}_m\begin{bmatrix}\phi_{i,j,1}\\\phi_{i,j,2}\\\phi_{i,j,4}\\\phi_{i,j,3}\end{bmatrix} + \frac{1}{4}\mathbf{G}_m\begin{bmatrix}Q_{i,j,1}\\Q_{i,j,2}\\Q_{i,j,4}\\Q_{i,j,3}\end{bmatrix}, \tag{280}
$$

where, for $\mu > 0, \eta > 0$,

$$
\mathbf{A}_m = \begin{bmatrix}1+\beta^x & 0 & 0 & 0\\-1-\beta^x & 1 & 0 & 0\\0 & 0 & 1+\beta^x & 0\\0 & 0 & -1-\beta^x & 1\end{bmatrix}, \tag{281}
$$

$$
\mathbf{B}_m = \begin{bmatrix}1+\beta^y & 0 & 0 & 0\\0 & 1+\beta^y & 0 & 0\\-1-\beta^y & 0 & 1 & 0\\0 & -1-\beta^y & 0 & 1\end{bmatrix}, \tag{282}
$$

$$
\mathbf{C} = \sigma_{t,i,j}\mathbf{I}, \tag{283}
$$

$$
\mathbf{D}_m = \begin{bmatrix}0 & 1+\beta^x & 0 & 0\\0 & -\beta^x & 0 & 0\\0 & 0 & 0 & 1+\beta^x\\0 & 0 & 0 & -\beta^x\end{bmatrix}, \tag{284}
$$

$$
\mathbf{E}_m = \begin{bmatrix}0 & 0 & 1+\beta^y & 0\\0 & 0 & 0 & 1+\beta^y\\0 & 0 & -\beta^y & 0\\0 & 0 & 0 & -\beta^x\end{bmatrix}, \tag{285}
$$

$$
\mathbf{F}_m = \begin{bmatrix}\frac{\mu_m c}{\Delta x_i}+\frac{\eta_m c}{\Delta y_j}+\sigma_s & -\frac{\mu_m c}{\Delta x_i} & -\frac{\eta_m c}{\Delta y_j} & 0\\-\frac{\mu_m c}{\Delta x_i} & \frac{\mu_m c}{\Delta x_i}+\frac{\eta_m c}{\Delta y_j}+\sigma_s & 0 & -\frac{\eta_m c}{\Delta y_j}\\-\frac{\eta_m c}{\Delta y_j} & 0 & \frac{\mu_m c}{\Delta x_i}+\frac{\eta_m c}{\Delta y_j}+\sigma_s & -\frac{\mu_m c}{\Delta x_i}\\0 & -\frac{\eta_m c}{\Delta y_j} & -\frac{\mu_m c}{\Delta x_i} & \frac{\mu_m c}{\Delta x_i}+\frac{\eta_m c}{\Delta y_j}+\sigma_s\end{bmatrix}, \tag{286}
$$

$$\mathbf{G}_m = \begin{bmatrix} Diag & -\frac{\mu_m}{\Delta x_i}\frac{1}{\sigma_t} & -\frac{\eta_m}{\Delta y_j}\frac{1}{\sigma_t} & 0 \\ -\frac{\mu_m}{\Delta x_i}\frac{1}{\sigma_t} & Diag & 0 & -\frac{\eta_m}{\Delta y_j}\frac{1}{\sigma_t} \\ -\frac{\eta_m}{\Delta y_j}\frac{1}{\sigma_t} & 0 & Diag & -\frac{\mu_m}{\Delta x_i}\frac{1}{\sigma_t} \\ 0 & -\frac{\eta_m}{\Delta y_j}\frac{1}{\sigma_t} & -\frac{\mu_m}{\Delta x_i}\frac{1}{\sigma_t} & Diag \end{bmatrix}, \tag{287}$$

where c is equal to the scattering ratio $\frac{\sigma_s}{\sigma_t}$ and,

$$Diag = \frac{\mu_m}{\Delta x_i}\frac{1}{\sigma_t} + \frac{\eta_m}{\Delta y_j}\frac{1}{\sigma_t} + \frac{1}{2}. \tag{288}$$

For $\mu < 0, \eta > 0$,

$$\mathbf{A}_m = \begin{bmatrix} 1 & -1-\beta^x & 0 & 0 \\ 0 & 1+\beta^x & 0 & 0 \\ 0 & 0 & 1 & -1-\beta^x \\ 0 & 0 & 0 & 1+\beta^x \end{bmatrix}, \tag{289}$$

$$\mathbf{B}_m = \begin{bmatrix} 1+\beta^y & 0 & 0 & 0 \\ 0 & 1+\beta^y & 0 & 0 \\ -1-\beta^y & 0 & 1 & 0 \\ 0 & -1-\beta^y & 0 & 1 \end{bmatrix}, \tag{290}$$

$$\mathbf{C} = \sigma_{t,i,j}\mathbf{I}, \tag{291}$$

$$\mathbf{D}_m = \begin{bmatrix} -\beta^x & 0 & 0 & 0 \\ 1+\beta^x & 0 & 0 & 0 \\ 0 & 0 & -\beta^x & 0 \\ 0 & 0 & 1+\beta^x & 0 \end{bmatrix}, \tag{292}$$

$$\mathbf{E}_m = \begin{bmatrix} 0 & 0 & 1+\beta^y & 0 \\ 0 & 0 & 0 & 1+\beta^y \\ 0 & 0 & -\beta^y & 0 \\ 0 & 0 & 0 & -\beta^x \end{bmatrix}, \tag{293}$$

$$\mathbf{F}_m = \begin{bmatrix} \frac{\mu_m c}{\Delta x_i}+\frac{\eta_m c}{\Delta y_j}+\sigma_s & -\frac{\mu_m c}{\Delta x_i} & -\frac{\eta_m c}{\Delta y_j} & 0 \\ -\frac{\mu_m c}{\Delta x_i} & \frac{\mu_m c}{\Delta x_i}+\frac{\eta_m c}{\Delta y_j}+\sigma_s & 0 & -\frac{\eta_m c}{\Delta y_j} \\ -\frac{\eta_m c}{\Delta y_j} & 0 & \frac{\mu_m c}{\Delta x_i}+\frac{\eta_m c}{\Delta y_j}+\sigma_s & -\frac{\mu_m c}{\Delta x_i} \\ 0 & -\frac{\eta_m c}{\Delta y_j} & -\frac{\mu_m c}{\Delta x_i} & \frac{\mu_m c}{\Delta x_i}+\frac{\eta_m c}{\Delta y_j}+\sigma_s \end{bmatrix}, \tag{294}$$

$$\mathbf{G}_m = \begin{bmatrix} Diag & -\frac{\mu_m}{\Delta x_i}\frac{1}{\sigma_t} & -\frac{\eta_m}{\Delta y_j}\frac{1}{\sigma_t} & 0 \\ -\frac{\mu_m}{\Delta x_i}\frac{1}{\sigma_t} & Diag & 0 & -\frac{\eta_m}{\Delta y_j}\frac{1}{\sigma_t} \\ -\frac{\eta_m}{\Delta y_j}\frac{1}{\sigma_t} & 0 & Diag & -\frac{\mu_m}{\Delta x_i}\frac{1}{\sigma_t} \\ 0 & -\frac{\eta_m}{\Delta y_j}\frac{1}{\sigma_t} & -\frac{\mu_m}{\Delta x_i}\frac{1}{\sigma_t} & Diag \end{bmatrix}, \tag{295}$$

for $\mu > 0, \eta < 0$,

$$\mathbf{A}_m = \begin{bmatrix} 1+\beta^x & 0 & 0 & 0 \\ -1-\beta^x & 1 & 0 & 0 \\ 0 & 0 & 1+\beta^x & 0 \\ 0 & 0 & -1-\beta^x & 1 \end{bmatrix}, \tag{296}$$

$$\mathbf{B}_m = \begin{bmatrix} 1 & 0 & -1-\beta^y & 0 \\ 0 & 1 & 0 & -1-\beta^y \\ 0 & 0 & 1+\beta^y & 0 \\ 0 & 0 & & 1+\beta^y \end{bmatrix}, \tag{297}$$

$$\mathbf{C} = \sigma_{t,i,j}\mathbf{I}, \tag{298}$$

$$\mathbf{D}_m = \begin{bmatrix} 0 & 1+\beta^x & 0 & 0 \\ 0 & -\beta^x & 0 & 0 \\ 0 & 0 & 0 & 1+\beta^x \\ 0 & 0 & 0 & -\beta^x \end{bmatrix}, \tag{299}$$

$$\mathbf{E}_m = \begin{bmatrix} -\beta^y & 0 & 0 & 0 \\ 0 & -\beta^y & 0 & 0 \\ 1+\beta^y & 0 & 0 & 0 \\ 0 & 1+\beta^y & 0 & 0 \end{bmatrix}, \tag{300}$$

$$\mathbf{F}_m = \begin{bmatrix} \frac{\mu_m c}{\Delta x_i} + \frac{\eta_m c}{\Delta y_j} + \sigma_s & -\frac{\mu_m c}{\Delta x_i} & -\frac{\eta_m c}{\Delta y_j} & 0 \\ -\frac{\mu_m c}{\Delta x_i} & \frac{\mu_m c}{\Delta x_i} + \frac{\eta_m c}{\Delta y_j} + \sigma_s & 0 & -\frac{\eta_m c}{\Delta y_j} \\ -\frac{\eta_m c}{\Delta y_j} & 0 & \frac{\mu_m c}{\Delta x_i} + \frac{\eta_m c}{\Delta y_j} + \sigma_s & -\frac{\mu_m c}{\Delta x_i} \\ 0 & -\frac{\eta_m c}{\Delta y_j} & -\frac{\mu_m c}{\Delta x_i} & \frac{\mu_m c}{\Delta x_i} + \frac{\eta_m c}{\Delta y_j} + \sigma_s \end{bmatrix}, \tag{301}$$

$$\mathbf{G}_m = \begin{bmatrix} Diag & -\frac{\mu_m}{\Delta x_i}\frac{1}{\sigma_t} & -\frac{\eta_m}{\Delta y_j}\frac{1}{\sigma_t} & 0 \\ -\frac{\mu_m}{\Delta x_i}\frac{1}{\sigma_t} & Diag & 0 & -\frac{\eta_m}{\Delta y_j}\frac{1}{\sigma_t} \\ -\frac{\eta_m}{\Delta y_j}\frac{1}{\sigma_t} & 0 & Diag & -\frac{\mu_m}{\Delta x_i}\frac{1}{\sigma_t} \\ 0 & -\frac{\eta_m}{\Delta y_j}\frac{1}{\sigma_t} & -\frac{\mu_m}{\Delta x_i}\frac{1}{\sigma_t} & Diag \end{bmatrix}, \tag{302}$$

for $\mu < 0, \eta < 0$,

$$\mathbf{A}_m = \begin{bmatrix} 1 & -1-\beta^x & 0 & 0 \\ 0 & 1+\beta^x & 0 & 0 \\ 0 & 0 & 1 & -1-\beta^x \\ 0 & 0 & 0 & 1+\beta^x \end{bmatrix}, \tag{303}$$

$$\mathbf{B}_m = \begin{bmatrix} 1 & 0 & -1-\beta^y & 0 \\ 0 & 1 & 0 & -1-\beta^y \\ 0 & 0 & 1+\beta^y & 0 \\ 0 & 0 & & 1+\beta^y \end{bmatrix}, \tag{304}$$

$$\mathbf{C} = \sigma_{t,i,j}\mathbf{I}, \tag{305}$$

$$\mathbf{D}_m = \begin{bmatrix} -\beta^x & 0 & 0 & 0 \\ 1+\beta^x & 0 & 0 & 0 \\ 0 & 0 & -\beta^x & 0 \\ 0 & 0 & 1+\beta^x & 0 \end{bmatrix}, \tag{306}$$

$$\mathbf{E}_m = \begin{bmatrix} -\beta^y & 0 & 0 & 0 \\ 0 & -\beta^y & 0 & 0 \\ 1+\beta^y & 0 & 0 & 0 \\ 0 & 1+\beta^y & 0 & 0 \end{bmatrix}, \tag{307}$$

$$\mathbf{F}_m = \begin{bmatrix} \frac{\mu_m c}{\Delta x_i} + \frac{\eta_m c}{\Delta y_j} + \sigma_s & -\frac{\mu_m c}{\Delta x_i} & -\frac{\eta_m c}{\Delta y_j} & 0 \\ -\frac{\mu_m c}{\Delta x_i} & \frac{\mu_m c}{\Delta x_i} + \frac{\eta_m c}{\Delta y_j} + \sigma_s & 0 & -\frac{\eta_m c}{\Delta y_j} \\ -\frac{\eta_m c}{\Delta y_j} & 0 & \frac{\mu_m c}{\Delta x_i} + \frac{\eta_m c}{\Delta y_j} + \sigma_s & -\frac{\mu_m c}{\Delta x_i} \\ 0 & -\frac{\eta_m c}{\Delta y_j} & -\frac{\mu_m c}{\Delta x_i} & \frac{\mu_m c}{\Delta x_i} + \frac{\eta_m c}{\Delta y_j} + \sigma_s \end{bmatrix}, \tag{308}$$

$$\mathbf{G}_m = \begin{bmatrix} Diag & -\frac{\mu_m}{\Delta x_i}\frac{1}{\sigma_t} & -\frac{\eta_m}{\Delta y_j}\frac{1}{\sigma_t} & 0 \\ -\frac{\mu_m}{\Delta x_i}\frac{1}{\sigma_t} & Diag & 0 & -\frac{\eta_m}{\Delta y_j}\frac{1}{\sigma_t} \\ -\frac{\eta_m}{\Delta y_j}\frac{1}{\sigma_t} & 0 & Diag & -\frac{\mu_m}{\Delta x_i}\frac{1}{\sigma_t} \\ 0 & -\frac{\eta_m}{\Delta y_j}\frac{1}{\sigma_t} & -\frac{\mu_m}{\Delta x_i}\frac{1}{\sigma_t} & Diag \end{bmatrix}, \tag{309}$$

We can write this system in matrix notation to simplify the presentation. With the proper definition of $\mathbf{H_m}$ the resultant matrix system is,

$$\mathbf{H}_m \begin{bmatrix} \psi_{m,i-1,j,2} \\ \psi_{m,i,j-1,4} \\ \psi_{m,i+1,j-1,3} \\ \psi_{m,i+1,j,1} \\ \psi_{m,i+1,j,4} \\ \psi_{m,i,j+1,2} \\ \psi_{m,i,j+1,1} \\ \psi_{m,i-1,j,3} \end{bmatrix} + \mathbf{T}_m \begin{bmatrix} \psi_{m,i,j,1} \\ \psi_{m,i,j,2} \\ \psi_{m,i,j,3} \\ \psi_{m,i,j,4} \end{bmatrix} = \frac{\sigma_{s,i,j}}{16}\mathbf{I} \begin{bmatrix} \phi_{i,j,1} \\ \phi_{i,j,2} \\ \phi_{i,j,3} \\ \phi_{i,j,4} \end{bmatrix} + \frac{\Delta x_i \Delta yi}{16}\mathbf{I} \begin{bmatrix} Q_{i,j,1} \\ Q_{i,j,2} \\ Q_{i,j,3} \\ Q_{i,j,4} \end{bmatrix}. \tag{310}$$

4.6   2D SCB Derived Modified 4-Step DSA

To derive the modified 4-step DSA equations in x-y geometry, we follow exactly the same procedure as in slab geometry:

1. Take the 0th and 1st angular moments of the SCB transport equations, Eqs. (250)-(253).

2. Change iteration indices to $(l+1)$ except on second and higher moment terms.

3. Subtract the resulting equations from the converged system to obtain a new system of equations for the additive corrections to the scalar flux resulting from source iteration.

4. Eliminate the 1st moments from the system, leaving a discretized diffusion equation. To do this we have to make the within-cell approximation to the cell-edge scalar flux correction and we have to eliminate all currents in favor of the left and right half-cell flux corrections.

We can derive the low order equations using the modified 4-step method by first taking the 0th and 1st moments of the discretized SCB equations, Eqs. (250) - (253). Taking the 0th angular moment, $\sum_m w_m$ yields,

$$\frac{\Delta y_j}{2} \left[\left(\frac{J_{i,j,1}^{x,\left(l+\frac{1}{2}\right)} + J_{i,j,2}^{x,\left(l+\frac{1}{2}\right)}}{2} \right) - J_{i,j,1-}^{x,\left(l+\frac{1}{2}\right)} \right]$$

$$+ \frac{\Delta x_i}{2} \left[\left(\frac{J_{i,j,1}^{y,\left(l+\frac{1}{2}\right)} + J_{i,j,4}^{y,\left(l+\frac{1}{2}\right)}}{2} \right) - J_{i,j,1+}^{y,\left(l+\frac{1}{2}\right)} \right]$$

$$+ \sigma_{t,i,j} \phi_{i,j,1}^{\left(l+\frac{1}{2}\right)} \frac{\Delta x_i \Delta y_j}{4} = \sigma_{s,i,j} \phi_{i,j,1}^{(l)} \frac{\Delta x_i \Delta y_j}{4} + Q_{i,j,1} \frac{\Delta x_i \Delta y_j}{4}, \qquad (311)$$

$$\frac{\Delta y_j}{2}\left[J_{i,j,2+}^{x,\left(l+\frac{1}{2}\right)} - \left(\frac{J_{i,j,1}^{x,\left(l+\frac{1}{2}\right)} + J_{i,j,2}^{x,\left(l+\frac{1}{2}\right)}}{2}\right)\right]$$

$$+\frac{\Delta x_i}{2}\left[\left(\frac{J_{i,j,3}^{y,\left(l+\frac{1}{2}\right)} + J_{i,j,2}^{y,\left(l+\frac{1}{2}\right)}}{2}\right) - J_{i,j,2-}^{y,\left(l+\frac{1}{2}\right)}\right]$$

$$+\sigma_{t,i,j}\phi_{i,j,2}^{\left(l+\frac{1}{2}\right)}\frac{\Delta x_i \Delta y_j}{4} = \sigma_{s,i,j}\phi_{i,j,2}^{(l)}\frac{\Delta x_i \Delta y_j}{4} + Q_{i,j,2}\frac{\Delta x_i \Delta y_j}{4}, \qquad (312)$$

$$\frac{\Delta y_j}{2}\left[J_{i,j,3-}^{x,\left(l+\frac{1}{2}\right)} - \left(\frac{J_{i,j,3}^{x,\left(l+\frac{1}{2}\right)} + J_{i,j,4}^{x,\left(l+\frac{1}{2}\right)}}{2}\right)\right]$$

$$+\frac{\Delta x_i}{2}\left[J_{i,j,3+}^{y,\left(l+\frac{1}{2}\right)} - \left(\frac{J_{i,j,3}^{y,\left(l+\frac{1}{2}\right)} + J_{i,j,2}^{y,\left(l+\frac{1}{2}\right)}}{2}\right)\right]$$

$$+\sigma_{t,i,j}\phi_{i,j,3}^{\left(l+\frac{1}{2}\right)}\frac{\Delta x_i \Delta y_j}{4} = \sigma_{s,i,j}\phi_{i,j,3}^{(l)}\frac{\Delta x_i \Delta y_j}{4} + Q_{i,j,3}\frac{\Delta x_i \Delta y_j}{4}, \qquad (313)$$

$$\frac{\Delta y_j}{2}\left[\left(\frac{J_{i,j,3}^{x,\left(l+\frac{1}{2}\right)} + J_{i,j,4}^{x,\left(l+\frac{1}{2}\right)}}{2}\right) - J_{i,j,4+}^{x,\left(l+\frac{1}{2}\right)}\right]$$

$$+\frac{\Delta x_i}{2}\left[J_{i,j,4-}^{y,\left(l+\frac{1}{2}\right)} - \left(\frac{J_{i,j,1}^{y,\left(l+\frac{1}{2}\right)} + J_{i,j,4}^{y,\left(l+\frac{1}{2}\right)}}{2}\right)\right]$$

$$+\sigma_{t,i,j}\phi_{i,j,4}^{\left(l+\frac{1}{2}\right)}\frac{\Delta x_i \Delta y_j}{4} = \sigma_{s,i,j}\phi_{i,j,4}^{(l)}\frac{\Delta x_i \Delta y_j}{4} + Q_{i,j,4}\frac{\Delta x_i \Delta y_j}{4}, \qquad (314)$$

where $1-, 1+, 2-, 2+, 3-, 3+, 4-, 4-$ refer to cell boundary currents (see Figure 13). In order to take the 1st moment of Eqs. (250) - (253) we recall that,

$$\mu_m^2 = \frac{2}{3}\left[\frac{1}{2}\left(3\mu_m^2 - 1\right)\right] + \frac{1}{3} = \frac{2}{3}P_2\left(\mu_m\right) + \frac{1}{3}P_0\left(\mu_m\right), \qquad (315)$$

and,

$$\eta_m^2 = \frac{2}{3}\left[\frac{1}{2}\left(3\eta_m^2 - 1\right)\right] + \frac{1}{3} = \frac{2}{3}P_2\left(\eta_m\right) + \frac{1}{3}P_0\left(\eta_m\right). \qquad (316)$$

Then

$$\sum_m \mu_m^2 w_m \psi = \frac{2}{3}\Phi + \frac{1}{3}\phi, \tag{317}$$

where,

$$\Phi = \sum_m w_m P_2\left(\mu_m\right)\psi_m, \tag{318}$$

and

$$\sum_m \eta_m^2 w_m \psi = \frac{2}{3}\Phi + \frac{1}{3}\phi, \tag{319}$$

where,

$$\Phi = \sum_m w_m P_2\left(\eta_m\right)\psi_m. \tag{320}$$

Taking the 1st moment $\sum_m w_m \mu_m$ of Eqs. (250) - (253) yields,

$$\frac{\Delta y_j}{2}\left(\frac{2}{3}\right)\left[\left(\frac{\Phi_{i,j,1}^{\left(l+\frac{1}{2}\right)} + \Phi_{i,j,2}^{\left(l+\frac{1}{2}\right)}}{2}\right) - \Phi_{i,j,1-}^{\left(l+\frac{1}{2}\right)}\right]$$

$$+\frac{\Delta y_j}{2}\left(\frac{1}{3}\right)\left[\left(\frac{\phi_{i,j,1}^{\left(l+\frac{1}{2}\right)} + \phi_{i,j,2}^{\left(l+\frac{1}{2}\right)}}{2}\right) - \phi_{i,j,1-}^{\left(l+\frac{1}{2}\right)}\right] + \sigma_{t,i,j}J_{i,j,1}^{x,\left(l+\frac{1}{2}\right)}\frac{\Delta x_i \Delta y_j}{4} = 0, \tag{321}$$

$$\frac{\Delta y_j}{2}\left(\frac{2}{3}\right)\left[\Phi_{i,j,2+}^{\left(l+\frac{1}{2}\right)} - \left(\frac{\Phi_{i,j,1}^{\left(l+\frac{1}{2}\right)} + \Phi_{i,j,2}^{\left(l+\frac{1}{2}\right)}}{2}\right)\right]$$

$$+\frac{\Delta y_j}{2}\left(\frac{1}{3}\right)\left[\phi_{i,j,2+}^{\left(l+\frac{1}{2}\right)} - \left(\frac{\phi_{i,j,1}^{\left(l+\frac{1}{2}\right)} + \phi_{i,j,2}^{\left(l+\frac{1}{2}\right)}}{2}\right)\right] + \sigma_{t,i,j}J_{i,j,2}^{x,\left(l+\frac{1}{2}\right)}\frac{\Delta x_i \Delta y_j}{4} = 0, \tag{322}$$

$$\frac{\Delta y_j}{2}\left(\frac{2}{3}\right)\left[\Phi_{i,j,3-}^{\left(l+\frac{1}{2}\right)} - \left(\frac{\Phi_{i,j,3}^{\left(l+\frac{1}{2}\right)} + \Phi_{i,j,4}^{\left(l+\frac{1}{2}\right)}}{2}\right)\right]$$

$$+\frac{\Delta y_j}{2}\left(\frac{1}{3}\right)\left[\phi_{i,j,3-}^{\left(l+\frac{1}{2}\right)} - \left(\frac{\phi_{i,j,3}^{\left(l+\frac{1}{2}\right)} + \phi_{i,j,4}^{\left(l+\frac{1}{2}\right)}}{2}\right)\right] + \sigma_{t,i,j}J_{i,j,3}^{x,\left(l+\frac{1}{2}\right)}\frac{\Delta x_i \Delta y_j}{4} = 0, \tag{323}$$

$$\frac{\Delta y_j}{2}\left(\frac{2}{3}\right)\left[\left(\frac{\Phi_{i,j,3}^{\left(l+\frac{1}{2}\right)}+\Phi_{i,j,4}^{\left(l+\frac{1}{2}\right)}}{2}\right)-\Phi_{i,j,4+}^{\left(l+\frac{1}{2}\right)}\right]$$

$$+\frac{\Delta y_j}{2}\left(\frac{1}{3}\right)\left[\left(\frac{\phi_{i,j,3}^{\left(l+\frac{1}{2}\right)}+\phi_{i,j,4}^{\left(l+\frac{1}{2}\right)}}{2}\right)-\phi_{i,j,4+}^{\left(l+\frac{1}{2}\right)}\right]+\sigma_{t,i,j}J_{i,j,4}^{x,\left(l+\frac{1}{2}\right)}\frac{\Delta x_i\Delta y_j}{4}=0\,,\quad(324)$$

$$\frac{\Delta x_i}{2}\left(\frac{2}{3}\right)\left[\left(\frac{\Phi_{i,j,1}^{\left(l+\frac{1}{2}\right)}+\Phi_{i,j,4}^{\left(l+\frac{1}{2}\right)}}{2}\right)-\Phi_{i,j,1+}^{\left(l+\frac{1}{2}\right)}\right]$$

$$+\frac{\Delta x_i}{2}\left(\frac{1}{3}\right)\left[\left(\frac{\phi_{i,j,1}^{\left(l+\frac{1}{2}\right)}+\phi_{i,j,4}^{\left(l+\frac{1}{2}\right)}}{2}\right)-\phi_{i,j,1+}^{\left(l+\frac{1}{2}\right)}\right]+\sigma_{t,i,j}J_{i,j,1}^{y,\left(l+\frac{1}{2}\right)}\frac{\Delta x_i\Delta y_j}{4}=0\,,\quad(325)$$

$$\frac{\Delta x_i}{2}\left(\frac{2}{3}\right)\left[\left(\frac{\Phi_{i,j,3}^{\left(l+\frac{1}{2}\right)}+\Phi_{i,j,2}^{\left(l+\frac{1}{2}\right)}}{2}\right)-\Phi_{i,j,2-}^{\left(l+\frac{1}{2}\right)}\right]$$

$$+\frac{\Delta x_i}{2}\left(\frac{1}{3}\right)\left[\left(\frac{\phi_{i,j,3}^{\left(l+\frac{1}{2}\right)}+\phi_{i,j,2}^{\left(l+\frac{1}{2}\right)}}{2}\right)-\phi_{i,j,2-}^{\left(l+\frac{1}{2}\right)}\right]+\sigma_{t,i,j}J_{i,j,2}^{y,\left(l+\frac{1}{2}\right)}\frac{\Delta x_i\Delta y_j}{4}=0\,,\quad(326)$$

$$\frac{\Delta x_i}{2}\left(\frac{2}{3}\right)\left[\Phi_{i,j,3+}^{\left(l+\frac{1}{2}\right)}-\left(\frac{\Phi_{i,j,3}^{\left(l+\frac{1}{2}\right)}+\Phi_{i,j,2}^{\left(l+\frac{1}{2}\right)}}{2}\right)\right]$$

$$+\frac{\Delta x_i}{2}\left(\frac{1}{3}\right)\left[\phi_{i,j,3+}^{\left(l+\frac{1}{2}\right)}-\left(\frac{\phi_{i,j,3}^{\left(l+\frac{1}{2}\right)}+\phi_{i,j,2}^{\left(l+\frac{1}{2}\right)}}{2}\right)\right]+\sigma_{t,i,j}J_{i,j,3}^{y,\left(l+\frac{1}{2}\right)}\frac{\Delta x_i\Delta y_j}{4}=0\,,\quad(327)$$

$$\frac{\Delta x_i}{2}\left(\frac{2}{3}\right)\left[\Phi_{i,j,4-}^{\left(l+\frac{1}{2}\right)}-\left(\frac{\Phi_{i,j,1}^{\left(l+\frac{1}{2}\right)}+\Phi_{i,j,4}^{\left(l+\frac{1}{2}\right)}}{2}\right)\right]$$

$$+\frac{\Delta x_i}{2}\left(\frac{1}{3}\right)\left[\phi_{i,j,4-}^{\left(l+\frac{1}{2}\right)}-\left(\frac{\phi_{i,j,1}^{\left(l+\frac{1}{2}\right)}+\phi_{i,j,4}^{\left(l+\frac{1}{2}\right)}}{2}\right)\right]+\sigma_{t,i,j}J_{i,j,4}^{y,\left(l+\frac{1}{2}\right)}\frac{\Delta x_i\Delta y_j}{4}=0\,.\quad(328)$$

W now rewrite Eqs. (311) - (314), Eqs. (321) - (321), and Eqs. (325) - (325), promoting all iteration indices to the $(l+1)$ iterate except those of Φ:

$$\frac{\Delta y_j}{2}\left[\left(\frac{J_{i,j,1}^{x,(l+1)} + J_{i,j,2}^{x,(l+1)}}{2}\right) - J_{i,j,1-}^{x,(l+1)}\right]$$

$$+\frac{\Delta x_i}{2}\left[\left(\frac{J_{i,j,1}^{y,(l+1)} + J_{i,j,4}^{y,(l+1)}}{2}\right) - J_{i,j,1+}^{y,(l+1)}\right]$$

$$+\sigma_{t,i,j}\phi_{i,j,1}^{(l+1)}\frac{\Delta x_i \Delta y_j}{4} = \sigma_{s,i,j}\phi_{i,j,1}^{(l+1)}\frac{\Delta x_i \Delta y_j}{4}\,, \tag{329}$$

$$\frac{\Delta y_j}{2}\left[J_{i,j,2+}^{x,(l+1)} - \left(\frac{J_{i,j,1}^{x,(l+1)} + J_{i,j,2}^{x,(l+1)}}{2}\right)\right]$$

$$+\frac{\Delta x_i}{2}\left[\left(\frac{J_{i,j,3}^{y,(l+1)} + J_{i,j,2}^{y,(l+1)}}{2}\right) - J_{i,j,2-}^{y,(l+1)}\right]$$

$$+\sigma_{t,i,j}\phi_{i,j,2}^{(l+1)}\frac{\Delta x_i \Delta y_j}{4} = \sigma_{s,i,j}\phi_{i,j,2}^{(l+1)}\frac{\Delta x_i \Delta y_j}{4}\,, \tag{330}$$

$$\frac{\Delta y_j}{2}\left[J_{i,j,3-}^{x,(l+1)} - \left(\frac{J_{i,j,3}^{x,(l+1)} + J_{i,j,4}^{x,(l+1)}}{2}\right)\right]$$

$$+\frac{\Delta x_i}{2}\left[J_{i,j,3+}^{y,(l+1)} - \left(\frac{J_{i,j,3}^{y,(l+1)} + J_{i,j,2}^{y,(l+1)}}{2}\right)\right]$$

$$+\sigma_{t,i,j}\phi_{i,j,3}^{(l+1)}\frac{\Delta x_i \Delta y_j}{4} = \sigma_{s,i,j}\phi_{i,j,3}^{(l+1)}\frac{\Delta x_i \Delta y_j}{4}\,, \tag{331}$$

$$\frac{\Delta y_j}{2}\left[\left(\frac{J_{i,j,3}^{x,(l+1)} + J_{i,j,4}^{x,(l+1)}}{2}\right) - J_{i,j,4+}^{x,(l+1)}\right]$$

$$+\frac{\Delta x_i}{2}\left[J_{i,j,4-}^{y,(l+1)} - \left(\frac{J_{i,j,1}^{y,(l+1)} + J_{i,j,4}^{y,(l+1)}}{2}\right)\right]$$

$$+\sigma_{t,i,j}\phi_{i,j,4}^{(l+1)}\frac{\Delta x_i \Delta y_j}{4} = \sigma_{s,i,j}\phi_{i,j,4}^{(l+1)}\frac{\Delta x_i \Delta y_j}{4}\,, \tag{332}$$

$$\frac{\Delta y_j}{2}\left(\frac{2}{3}\right)\left[\left(\frac{\Phi_{i,j,1}^{(l+1)}+\Phi_{i,j,2}^{(l+1)}}{2}\right)-\Phi_{i,j,1-}^{(l+1)}\right]$$

$$+\frac{\Delta y_j}{2}\left(\frac{1}{3}\right)\left[\left(\frac{\phi_{i,j,1}^{(l+1)}+\phi_{i,j,2}^{(l+1)}}{2}\right)-\phi_{i,j,1-}^{(l+1)}\right]$$

$$+\sigma_{t,i,j}J_{i,j,1}^{x,(l+1)}\frac{\Delta x_i\Delta y_j}{4}=0\,,\qquad(333)$$

$$\frac{\Delta y_j}{2}\left(\frac{2}{3}\right)\left[\Phi_{i,j,2+}^{(l+\frac{1}{2})}-\left(\frac{\Phi_{i,j,1}^{(l+\frac{1}{2})}+\Phi_{i,j,2}^{(l+\frac{1}{2})}}{2}\right)\right]$$

$$+\frac{\Delta y_j}{2}\left(\frac{1}{3}\right)\left[\phi_{i,j,2+}^{(l+1)}-\left(\frac{\phi_{i,j,1}^{(l+1)}+\phi_{i,j,2}^{(l+1)}}{2}\right)\right]$$

$$+\sigma_{t,i,j}J_{i,j,2}^{x,(l+1)}\frac{\Delta x_i\Delta y_j}{4}=0\,,\qquad(334)$$

$$\frac{\Delta y_j}{2}\left(\frac{2}{3}\right)\left[\Phi_{i,j,3-}^{(l+\frac{1}{2})}-\left(\frac{\Phi_{i,j,3}^{(l+\frac{1}{2})}+\Phi_{i,j,4}^{(l+\frac{1}{2})}}{2}\right)\right]$$

$$+\frac{\Delta y_j}{2}\left(\frac{1}{3}\right)\left[\phi_{i,j,3-}^{(l+1)}-\left(\frac{\phi_{i,j,3}^{(l+1)}+\phi_{i,j,4}^{(l+1)}}{2}\right)\right]$$

$$+\sigma_{t,i,j}J_{i,j,3}^{x,(l+1)}\frac{\Delta x_i\Delta y_j}{4}=0\,,\qquad(335)$$

$$\frac{\Delta y_j}{2}\left(\frac{2}{3}\right)\left[\left(\frac{\Phi_{i,j,3}^{(l+\frac{1}{2})}+\Phi_{i,j,4}^{(l+\frac{1}{2})}}{2}\right)-\Phi_{i,j,4+}^{(l+\frac{1}{2})}\right]$$

$$+\frac{\Delta y_j}{2}\left(\frac{1}{3}\right)\left[\left(\frac{\phi_{i,j,3}^{(l+1)}+\phi_{i,j,4}^{(l+1)}}{2}\right)-\phi_{i,j,4+}^{(l+1)}\right]$$

$$+\sigma_{t,i,j}J_{i,j,4}^{x,(l+1)}\frac{\Delta x_i\Delta y_j}{4}=0\,,\qquad(336)$$

$$\frac{\Delta x_i}{2}\left(\frac{2}{3}\right)\left[\left(\frac{\Phi_{i,j,1}^{\left(l+\frac{1}{2}\right)}+\Phi_{i,j,4}^{\left(l+\frac{1}{2}\right)}}{2}\right)-\Phi_{i,j,1+}^{\left(l+\frac{1}{2}\right)}\right]$$

$$+\frac{\Delta x_i}{2}\left(\frac{1}{3}\right)\left[\left(\frac{\phi_{i,j,1}^{(l+1)}+\phi_{i,j,4}^{(l+1)}}{2}\right)-\phi_{i,j,1+}^{(l+1)}\right]$$

$$+\sigma_{t,i,j}J_{i,j,1}^{y,(l+1)}\frac{\Delta x_i\Delta y_j}{4}=0\,,\tag{337}$$

$$\frac{\Delta x_i}{2}\left(\frac{2}{3}\right)\left[\left(\frac{\Phi_{i,j,3}^{\left(l+\frac{1}{2}\right)}+\Phi_{i,j,2}^{\left(l+\frac{1}{2}\right)}}{2}\right)-\Phi_{i,j,2-}^{\left(l+\frac{1}{2}\right)}\right]$$

$$+\frac{\Delta x_i}{2}\left(\frac{1}{3}\right)\left[\left(\frac{\phi_{i,j,3}^{(l+1)}+\phi_{i,j,2}^{(l+1)}}{2}\right)-\phi_{i,j,2-}^{(l+1)}\right]$$

$$+\sigma_{t,i,j}J_{i,j,2}^{y,(l+1)}\frac{\Delta x_i\Delta y_j}{4}=0\,,\tag{338}$$

$$\frac{\Delta x_i}{2}\left(\frac{2}{3}\right)\left[\Phi_{i,j,3+}^{\left(l+\frac{1}{2}\right)}-\left(\frac{\Phi_{i,j,3}^{\left(l+\frac{1}{2}\right)}+\Phi_{i,j,2}^{\left(l+\frac{1}{2}\right)}}{2}\right)\right]$$

$$+\frac{\Delta x_i}{2}\left(\frac{1}{3}\right)\left[\phi_{i,j,3+}^{(l+1)}-\left(\frac{\phi_{i,j,3}^{(l+1)}+\phi_{i,j,2}^{(l+1)}}{2}\right)\right]$$

$$+\sigma_{t,i,j}J_{i,j,3}^{y,(l+1)}\frac{\Delta x_i\Delta y_j}{4}=0\,,\tag{339}$$

$$\frac{\Delta x_i}{2}\left(\frac{2}{3}\right)\left[\Phi_{i,j,4-}^{\left(l+\frac{1}{2}\right)}\left(\frac{\Phi_{i,j,1}^{\left(l+\frac{1}{2}\right)}+\Phi_{i,j,4}^{\left(l+\frac{1}{2}\right)}}{2}\right)\right]$$

$$+\frac{\Delta x_i}{2}\left(\frac{1}{3}\right)\left[\phi_{i,j,4-}^{(l+1)}-\left(\frac{\phi_{i,j,1}^{(l+1)}+\phi_{i,j,4}^{(l+1)}}{2}\right)\right]$$

$$+\sigma_{t,i,j}J_{i,j,4}^{y,(l+1)}\frac{\Delta x_i\Delta y_j}{4}=0\,.\tag{340}$$

If we subtract Eqs. (311) - (314), (321) - (324), and (325) - (328) from Eqs. (329) - (332), (333) - (336), and (337) - (340) we find:

$$\frac{\Delta y_j}{2}\left[\left(\frac{g_{i,j,1}^{x,(l+1)} + g_{i,j,2}^{x,(l+1)}}{2}\right) - g_{i,j,1-}^{x,(l+1)}\right]$$

$$+\frac{\Delta x_i}{2}\left[\left(\frac{g_{i,j,1}^{y,(l+1)} + g_{i,j,4}^{y,(l+1)}}{2}\right) - g_{i,j,1+}^{y,(l+1)}\right]$$

$$+\sigma_{t,i,j}f_{i,j,1}^{(l+1)}\frac{\Delta x_i\Delta y_j}{4} = \sigma_{s,i,j}\frac{\Delta x_i\Delta y_j}{4}\left(\phi_{i,j,1}^{(l+1)} - \phi_{i,j,1}^{(l)}\right), \qquad (341)$$

$$\frac{\Delta y_j}{2}\left[g_{i,j,2+}^{x,(l+1)} - \left(\frac{g_{i,j,1}^{x,(l+1)} + g_{i,j,2}^{x,(l+1)}}{2}\right)\right]$$

$$+\frac{\Delta x_i}{2}\left[\left(\frac{g_{i,j,3}^{y,(l+1)} + g_{i,j,2}^{y,(l+1)}}{2}\right) - g_{i,j,2-}^{y,(l+1)}\right]$$

$$+\sigma_{t,i,j}f_{i,j,2}^{(l+1)}\frac{\Delta x_i\Delta y_j}{4} = \sigma_{s,i,j}\frac{\Delta x_i\Delta y_j}{4}\left(\phi_{i,j,2}^{(l+1)} - \phi_{i,j,2}^{(l)}\right), \qquad (342)$$

$$\frac{\Delta y_j}{2}\left[g_{i,j,3-}^{x,(l+1)} - \left(\frac{g_{i,j,3}^{x,(l+1)} + g_{i,j,4}^{x,(l+1)}}{2}\right)\right]$$

$$+\frac{\Delta x_i}{2}\left[g_{i,j,3+}^{y,(l+1)} - \left(\frac{g_{i,j,3}^{y,(l+1)} + g_{i,j,2}^{y,(l+1)}}{2}\right)\right]$$

$$+\sigma_{t,i,j}f_{i,j,3}^{(l+1)}\frac{\Delta x_i\Delta y_j}{4} = \sigma_{s,i,j}\frac{\Delta x_i\Delta y_j}{4}\left(\phi_{i,j,3}^{(l+1)} - \phi_{i,j,3}^{(l)}\right), \qquad (343)$$

$$\frac{\Delta y_j}{2}\left[\left(\frac{g_{i,j,3}^{x,(l+1)} + g_{i,j,4}^{x,(l+1)}}{2}\right) - g_{i,j,4+}^{x,(l+1)}\right]$$

$$+\frac{\Delta x_i}{2}\left[g_{i,j,4-}^{y,(l+1)} - \left(\frac{g_{i,j,1}^{y,(l+1)} + g_{i,j,4}^{y,(l+1)}}{2}\right)\right]$$

$$+\sigma_{t,i,j}f_{i,j,4}^{(l+1)}\frac{\Delta x_i\Delta y_j}{4} = \sigma_{s,i,j}\frac{\Delta x_i\Delta y_j}{4}\left(\phi_{i,j,4}^{(l+1)} - \phi_{i,j,4}^{(l)}\right), \qquad (344)$$

$$\frac{\Delta y_j}{2}\left(\frac{1}{3}\right)\left[\left(\frac{f_{i,j,1}^{(l+1)}+f_{i,j,2}^{(l+1)}}{2}\right)-f_{i,j,1-}^{(l+1)}\right]+\sigma_{t,i,j}g_{i,j,1}^{x,(l+1)}\frac{\Delta x_i \Delta y_j}{4}=0\,, \qquad (345)$$

$$\frac{\Delta y_j}{2}\left(\frac{1}{3}\right)\left[f_{i,j,2+}^{(l+1)}-\left(\frac{f_{i,j,1}^{(l+1)}+f_{i,j,2}^{(l+1)}}{2}\right)\right]+\sigma_{t,i,j}g_{i,j,2}^{x,(l+1)}\frac{\Delta x_i \Delta y_j}{4}=0\,, \qquad (346)$$

$$\frac{\Delta y_j}{2}\left(\frac{1}{3}\right)\left[f_{i,j,3-}^{(l+1)}-\left(\frac{f_{i,j,3}^{(l+1)}+f_{i,j,4}^{(l+1)}}{2}\right)\right]+\sigma_{t,i,j}g_{i,j,3}^{x,(l+1)}\frac{\Delta x_i \Delta y_j}{4}=0\,, \qquad (347)$$

$$\frac{\Delta y_j}{2}\left(\frac{1}{3}\right)\left[\left(\frac{f_{i,j,3}^{(l+1)}+f_{i,j,4}^{(l+1)}}{2}\right)-f_{i,j,4+}^{(l+1)}\right]+\sigma_{t,i,j}g_{i,j,4}^{x,(l+1)}\frac{\Delta x_i \Delta y_j}{4}=0\,, \qquad (348)$$

$$\frac{\Delta x_i}{2}\left(\frac{1}{3}\right)\left[\left(\frac{f_{i,j,1}^{(l+1)}+f_{i,j,4}^{(l+1)}}{2}\right)-f_{i,j,1+}^{(l+1)}\right]+\sigma_{t,i,j}g_{i,j,1}^{y,(l+1)}\frac{\Delta x_i \Delta y_j}{4}=0\,, \qquad (349)$$

$$\frac{\Delta x_i}{2}\left(\frac{1}{3}\right)\left[\left(\frac{f_{i,j,3}^{(l+1)}+f_{i,j,2}^{(l+1)}}{2}\right)-f_{i,j,2-}^{(l+1)}\right]+\sigma_{t,i,j}g_{i,j,2}^{y,(l+1)}\frac{\Delta x_i \Delta y_j}{4}=0\,, \qquad (350)$$

$$\frac{\Delta x_i}{2}\left(\frac{1}{3}\right)\left[f_{i,j,3+}^{(l+1)}-\left(\frac{f_{i,j,3}^{(l+1)}+f_{i,j,2}^{(l+1)}}{2}\right)\right]+\sigma_{t,i,j}g_{i,j,3}^{y,(l+1)}\frac{\Delta x_i \Delta y_j}{4}=0\,, \qquad (351)$$

$$\frac{\Delta x_i}{2}\left(\frac{1}{3}\right)\left[f_{i,j,4-}^{(l+1)}-\left(\frac{f_{i,j,1}^{(l+1)}+f_{i,j,4}^{(l+1)}}{2}\right)\right]+\sigma_{t,i,j}g_{i,j,4}^{y,(l+1)}\frac{\Delta x_i \Delta y_j}{4}=0\,. \qquad (352)$$

We simplify the right hand side of Eqs. (341) - (342) using the fact that

$$\frac{\sigma_{s,i}\Delta x_i}{2}\left(\phi_{i,N}^{(l+1)}-\phi_{i,N}^{(l)}\right)=\frac{\sigma_{s,i}\Delta x_i}{2}\left(\phi_{i,N}^{(l+1)}-\phi_{i,N}^{\left(l+\frac{1}{2}\right)}\right)$$

$$+\frac{\sigma_{s,i}\Delta x_i}{2}\left(\phi_{i,N}^{\left(l+\frac{1}{2}\right)}-\phi_{i,N}^{(l)}\right)\;N=1,2,3,4\,, \qquad (353)$$

which yields,

$$\frac{\Delta y_j}{2}\left[\left(\frac{g_{i,j,1}^{x,(l+1)}-g_{i,j,2}^{x,(l+1)}}{2}\right)-g_{i,j,1-}^{x,(l+1)}\right]$$

$$+\frac{\Delta x_i}{2}\left[\left(\frac{g_{i,j,1}^{y,(l+1)}-g_{i,j,4}^{y,(l+1)}}{2}\right)-g_{i,j,1+}^{y,(l+1)}\right]$$

$$+\sigma_{a,i,j}f_{i,j,1}^{(l+1)}\frac{\Delta x_i \Delta y_j}{4}=\sigma_{s,i,j,}\frac{\Delta x_i \Delta y_j}{4}\left(\phi_{i,j,1}^{\left(l+\frac{1}{2}\right)}-\phi_{i,j,1}^{(l)}\right)\,, \qquad (354)$$

$$\frac{\Delta y_j}{2}\left[g_{i,j,2+}^{x,(l+1)} - \left(\frac{g_{i,j,1}^{x,(l+1)} - g_{i,j,2}^{x,(l+1)}}{2}\right)\right]$$

$$+\frac{\Delta x_i}{2}\left[\left(\frac{g_{i,j,3}^{y,(l+1)} - g_{i,j,2}^{y,(l+1)}}{2}\right) - g_{i,j,2-}^{y,(l+1)}\right]$$

$$+\sigma_{a,i,j}f_{i,j,2}^{(l+1)}\frac{\Delta x_i \Delta y_j}{4} = \sigma_{s,i,j}\frac{\Delta x_i \Delta y_j}{4}\left(\phi_{i,j,2}^{\left(l+\frac{1}{2}\right)} - \phi_{i,j,2}^{(l)}\right), \qquad (355)$$

$$\frac{\Delta y_j}{2}\left[g_{i,j,3-}^{x,(l+1)} - \left(\frac{g_{i,j,3}^{x,(l+1)} - g_{i,j,4}^{x,(l+1)}}{2}\right)\right]$$

$$+\frac{\Delta x_i}{2}\left[g_{i,j,3+}^{y,(l+1)} - \left(\frac{g_{i,j,3}^{y,(l+1)} - g_{i,j,2}^{y,(l+1)}}{2}\right)\right]$$

$$+\sigma_{a,i,j}f_{i,j,3}^{(l+1)}\frac{\Delta x_i \Delta y_j}{4} = \sigma_{s,i,j}\frac{\Delta x_i \Delta y_j}{4}\left(\phi_{i,j,3}^{\left(l+\frac{1}{2}\right)} - \phi_{i,j,3}^{(l)}\right), \qquad (356)$$

$$\frac{\Delta y_j}{2}\left[\left(\frac{g_{i,j,3}^{x,(l+1)} - g_{i,j,4}^{x,(l+1)}}{2}\right) - g_{i,j,4+}^{x,(l+1)}\right]$$

$$+\frac{\Delta x_i}{2}\left[g_{i,j,4-}^{y,(l+1)} \left(\frac{g_{i,j,1}^{y,(l+1)} - g_{i,j,4}^{y,(l+1)}}{2}\right)\right]$$

$$+\sigma_{a,i,j}f_{i,j,4}^{(l+1)}\frac{\Delta x_i \Delta y_j}{4} = \sigma_{s,i,j}\frac{\Delta x_i \Delta y_j}{4}\left(\phi_{i,j,4}^{\left(l+\frac{1}{2}\right)} - \phi_{i,j,4}^{(l)}\right). \qquad (357)$$

We define the following corrections:

$$f_{i,N}^{(l+1)} = \phi_{i,N}^{(l+1)} - \phi_{i,N}^{\left(l+\frac{1}{2}\right)}, N = 1,2,3,4, \qquad (358)$$

$$g_{i,N}^{(l+1)} = J_{i,N}^{(l+1)} - J_{i,N}^{\left(l+\frac{1}{2}\right)}, N = 1,2,3,4. \qquad (359)$$

We next remove the dependencies on the edges, $1-, 1+, 2-, 2+, 3-, 3+, 4-, 4+,$ by first obtaining,

$$g_{i,j,1-}^{x,(l+1)} = \sum_{\mu>0} w_m \mu_m \left[\psi_{i-1,j,2}^{(l+1)} - \psi_{i-1,j,2}^{(l+\frac{1}{2})} \right] + \sum_{\mu<0} w_m \mu_m \left[\psi_{i,j,1}^{(l+1)} - \psi_{i,j,1}^{(l+\frac{1}{2})} \right] , \qquad (360)$$

which, if we use a P_1 expansion of the angular intensity becomes,

$$g_{i,j,1-}^{x,(l+1)} =$$

$$\sum_{\mu>0} w_m \mu_m \left[\left(\frac{\phi_{i-1,j,2}}{4} + \frac{3\mu_m J_{i-1,j,2}^x}{4} \right)^{(l+1)} - \left(\frac{\phi_{i-1,j,2}}{4} + \frac{3\mu_m J_{i-1,j,2}^x}{4} \right)^{(l+\frac{1}{2})} \right]$$

$$+ \sum_{\mu<0} w_m \mu_m \left[\left(\frac{\phi_{i,j,1}}{4} + \frac{3\mu_m J_{i,j,1}^x}{4} \right)^{(l+1)} - \left(\frac{\phi_{i,j,1}}{4} + \frac{3\mu_m J_{i,j,1}^x}{2} \right)^{(l+\frac{1}{2})} \right] . \qquad (361)$$

This reduces to,

$$g_{i,j,1-}^{x,(l+1)} = \frac{\gamma}{4} \left(f_{i-1,j,2}^{(l+1)} - f_{i,j,1}^{(l+1)} \right) + \frac{1}{2} \left(g_{i-1,j,2}^{x,(l+1)} + g_{i,j,1}^{x,(l+1)} \right) . \qquad (362)$$

Similarly, we find,

$$g_{i,j,1+}^{y,(l+1)} = \frac{\gamma}{4} \left(f_{i,j-1,4}^{(l+1)} - f_{i,j,1}^{(l+1)} \right) + \frac{1}{2} \left(g_{i,j-1,4}^{y,(l+1)} + g_{i,j,1}^{y,(l+1)} \right) , \qquad (363)$$

$$g_{i,j,2-}^{y,(l+1)} = \frac{\gamma}{4} \left(f_{i,j-1,3}^{(l+1)} - f_{i,j,2}^{(l+1)} \right) + \frac{1}{2} \left(g_{i,j-1,3}^{y,(l+1)} + g_{i,j,2}^{y,(l+1)} \right) , \qquad (364)$$

$$g_{i,j,2+}^{x,(l+1)} = \frac{\gamma}{4} \left(f_{i,j,2}^{(l+1)} - f_{i+1,j,1}^{(l+1)} \right) + \frac{1}{2} \left(g_{i,j,2}^{x,(l+1)} + g_{i+1,j,1}^{x,(l+1)} \right) , \qquad (365)$$

$$g_{i,j,3-}^{x,(l+1)} = \frac{\gamma}{4} \left(f_{i,j,3}^{(l+1)} - f_{i+1,j,4}^{(l+1)} \right) + \frac{1}{2} \left(g_{i,j,3}^{x,(l+1)} + g_{i+1,j,4}^{x,(l+1)} \right) , \qquad (366)$$

$$g_{i,j,3+}^{y,(l+1)} = \frac{\gamma}{4} \left(f_{i,j,3}^{(l+1)} - f_{i,j+1,2}^{(l+1)} \right) + \frac{1}{2} \left(g_{i,j,3}^{y,(l+1)} + g_{i,j+1,2}^{y,(l+1)} \right) , \qquad (367)$$

$$g_{i,j,4-}^{y,(l+1)} = \frac{\gamma}{4} \left(f_{i,j,4}^{(l+1)} - f_{i,j+1,1}^{(l+1)} \right) + \frac{1}{2} \left(g_{i,j,4}^{y,(l+1)} + g_{i,j+1,1}^{y,(l+1)} \right) , \qquad (368)$$

$$g_{i,j,4+}^{x,(l+1)} = \frac{\gamma}{4}\left(f_{i-1,j,3}^{(l+1)} - f_{i,j,4}^{(l+1)}\right) + \frac{1}{2}\left(g_{i-1,j,3}^{x,(l+1)} + g_{i,j,4}^{x,(l+1)}\right) , \qquad (369)$$

where γ is the quadrature normalization defined as the sum of the quadrature weights,

$$\gamma = \sum_{n=1}^{N/2} w_n . \qquad (370)$$

We substitute Eqs. (362) - (369) into Eqs. (354) - (357) which yields,

$$\frac{\Delta y_j}{2}\left[\left(\frac{g_{i,j,1}^{x,(l+1)} - g_{i,j,2}^{x,(l+1)}}{2}\right) - \frac{\gamma}{4}\left(f_{i-1,j,2}^{(l+1)} - f_{i,j,1}^{(l+1)}\right) - \frac{1}{2}\left(g_{i-1,j,2}^{x,(l+1)} + g_{i,j,1}^{x,(l+1)}\right)\right]$$

$$+\frac{\Delta x_i}{2}\left[\left(\frac{g_{i,j,1}^{y,(l+1)} - g_{i,j,4}^{y,(l+1)}}{2}\right) - \frac{\gamma}{4}\left(f_{i,j-1,4}^{(l+1)} - f_{i,j,1}^{(l+1)}\right) - \frac{1}{2}\left(g_{i,j-1,4}^{y,(l+1)} + g_{i,j,1}^{y,(l+1)}\right)\right]$$

$$+\sigma_{a,i,j}f_{i,j,1}^{(l+1)}\frac{\Delta x_i \Delta y_j}{4} = \sigma_{s,i,j,}\frac{\Delta x_i \Delta y_j}{4}\left(\phi_{i,j,1}^{\left(l+\frac{1}{2}\right)} - \phi_{i,j,1}^{(l)}\right) , \qquad (371)$$

$$\frac{\Delta y_j}{2}\left[\frac{\gamma}{4}\left(f_{i,j,2}^{(l+1)} - f_{i+1,j,1}^{(l+1)}\right) + \frac{1}{2}\left(g_{i,j,2}^{x,(l+1)} + g_{i+1,j,1}^{x,(l+1)}\right) - \left(\frac{g_{i,j,1}^{x,(l+1)} - g_{i,j,2}^{x,(l+1)}}{2}\right)\right]$$

$$+\frac{\Delta x_i}{2}\left[\left(\frac{g_{i,j,3}^{y,(l+1)} - g_{i,j,2}^{y,(l+1)}}{2}\right) - \frac{\gamma}{4}\left(f_{i,j-1,3}^{(l+1)} - f_{i,j,2}^{(l+1)}\right) - \frac{1}{2}\left(g_{i,j-1,3}^{y,(l+1)} + g_{i,j,2}^{y,(l+1)}\right)\right]$$

$$+\sigma_{a,i,j}f_{i,j,2}^{(l+1)}\frac{\Delta x_i \Delta y_j}{4} = \sigma_{s,i,j,}\frac{\Delta x_i \Delta y_j}{4}\left(\phi_{i,j,2}^{\left(l+\frac{1}{2}\right)} - \phi_{i,j,2}^{(l)}\right) , \qquad (372)$$

$$\frac{\Delta y_j}{2}\left[\frac{\gamma}{4}\left(f_{i,j,3}^{(l+1)} - f_{i+1,j,4}^{(l+1)}\right) + \frac{1}{2}\left(g_{i,j,3}^{x,(l+1)} + g_{i+1,j,4}^{x,(l+1)}\right) - \left(\frac{g_{i,j,3}^{x,(l+1)} - g_{i,j,4}^{x,(l+1)}}{2}\right)\right]$$

$$+\frac{\Delta x_i}{2}\left[\frac{\gamma}{4}\left(f_{i,j,3}^{(l+1)} - f_{i,j+1,2}^{(l+1)}\right) + \frac{1}{2}\left(g_{i,j,3}^{y,(l+1)} + g_{i,j+1,2}^{y,(l+1)}\right) - \left(\frac{g_{i,j,3}^{y,(l+1)} - g_{i,j,2}^{y,(l+1)}}{2}\right)\right]$$

$$+\sigma_{a,i,j}f_{i,j,3}^{(l+1)}\frac{\Delta x_i \Delta y_j}{4} = \sigma_{s,i,j,}\frac{\Delta x_i \Delta y_j}{4}\left(\phi_{i,j,3}^{\left(l+\frac{1}{2}\right)} - \phi_{i,j,3}^{(l)}\right) , \qquad (373)$$

$$\frac{\Delta y_j}{2} \left[\left(\frac{g_{i,j,3}^{x,(l+1)} - g_{i,j,4}^{x,(l+1)}}{2} \right) - \frac{\gamma}{4} \left(f_{i-1,j,3}^{(l+1)} - f_{i,j,4}^{(l+1)} \right) - \frac{1}{2} \left(g_{i-1,j,3}^{x,(l+1)} + g_{i,j,4}^{x,(l+1)} \right) \right]$$

$$+ \frac{\Delta x_i}{2} \left[\frac{\gamma}{4} \left(f_{i,j,4}^{(l+1)} - f_{i,j+1,1}^{(l+1)} \right) + \frac{1}{2} \left(g_{i,j,4}^{y,(l+1)} + g_{i,j+1,1}^{y,(l+1)} \right) \left(\frac{g_{i,j,1}^{y,(l+1)} - g_{i,j,4}^{y,(l+1)}}{2} \right) \right]$$

$$+ \sigma_{a,i,j} f_{i,j,4}^{(l+1)} \frac{\Delta x_i \Delta y_j}{4} = \sigma_{s,i,j} \frac{\Delta x_i \Delta y_j}{4} \left(\phi_{i,j,4}^{(l+\frac{1}{2})} - \phi_{i,j,4}^{(l)} \right) . \quad (374)$$

We use very simple "within-cell" approximations to eliminate the edge scalar intensity corrections:

$$f_{i,j,1-} = f_{i,j,1} \quad , \quad f_{i,j,1+} = f_{i,j,1} ,$$

$$f_{i,j,2-} = f_{i,j,2} \quad , \quad f_{i,j,2+} = f_{i,j,2} ,$$

$$f_{i,j,3-} = f_{i,j,3} \quad , \quad f_{i,j,3+} = f_{i,j,3} ,$$

$$f_{i,j,4-} = f_{i,j,4} \quad , \quad f_{i,j,4+} = f_{i,j,4} . \quad (375)$$

These allow us to reduce Eqs. (345) - (348) and Eqs. (349) - (352) to:

$$g_{i,j,1}^{x,(l+1)} = g_{i,j,2}^{x,(l+1)} = - \left(\frac{1}{3\sigma_{t,i,j}} \right) \left(\frac{f_{i,j,2}^{(l+1)} - f_{i,j,1}^{(l+1)}}{\Delta x_i} \right) , \quad (376)$$

$$g_{i,j,3}^{x,(l+1)} = g_{i,j,4}^{x,(l+1)} = - \left(\frac{1}{3\sigma_{t,i,j}} \right) \left(\frac{f_{i,j,3}^{(l+1)} - f_{i,j,4}^{(l+1)}}{\Delta x_i} \right) , \quad (377)$$

$$g_{i,j,1}^{y,(l+1)} = g_{i,j,4}^{y,(l+1)} = - \left(\frac{1}{3\sigma_{t,i,j}} \right) \left(\frac{f_{i,j,4}^{(l+1)} - f_{i,j,1}^{(l+1)}}{\Delta y_j} \right) , \quad (378)$$

$$g_{i,j,2}^{y,(l+1)} = g_{i,j,3}^{y,(l+1)} = - \left(\frac{1}{3\sigma_{t,i,j}} \right) \left(\frac{f_{i,j,3}^{(l+1)} - f_{i,j,4}^{(l+1)}}{\Delta y_j} \right) . \quad (379)$$

By using Eqs. (376) - (379) with Eqs. (371) - (374) we arrive at four equations containing only the corner direction-integrated intensity corrections, $f_{1,2,3,4}$:

$$\left[\frac{D_{i,j}}{\Delta x_i^2} + \frac{\gamma}{2\Delta x_i} + \frac{D_{i,j}}{\Delta y_j^2} + \frac{\gamma}{2\Delta y_j} + \sigma_{a,i,j}\right] f_{i,j,1}^{(l+1)}$$

$$+ \left[\frac{-D_{i,j}}{\Delta x_i^2}\right] f_{i,j,2}^{(l+1)} + \left[\frac{D_{i-1,j}}{\Delta x_i \Delta x_{i-1}} - \frac{\gamma}{2\Delta x_i}\right] f_{i-1,j,2}^{(l+1)} + \left[\frac{-D_{i-1,j}}{\Delta x_i \Delta x_{i-1}}\right] f_{i-1,j,1}^{(l+1)}$$

$$+ \left[\frac{-D_{i,j}}{\Delta y_j^2}\right] f_{i,j,4}^{(l+1)} + \left[\frac{D_{i,j-1}}{\Delta y_j \Delta y_{j-1}} - \frac{\gamma}{2\Delta y_j}\right] f_{i,j-1,4}^{(l+1)} + \left[\frac{-D_{i,j-1}}{\Delta y_j \Delta y_{j-1}}\right] f_{i,j-1,1}^{(l+1)}$$

$$= \sigma_{s,i,j}\left(\phi_{i,j,1}^{\left(l+\frac{1}{2}\right)} - \phi_{i,j,1}^{(l)}\right), \tag{380}$$

$$\left[\frac{D_{i,j}}{\Delta x_i^2} + \frac{\gamma}{2\Delta x_i} + \frac{D_{i,j}}{\Delta y_j^2} + \frac{\gamma}{2\Delta y_j} + \sigma_{a,i,j}\right] f_{i,j,2}^{(l+1)}$$

$$+ \left[\frac{-D_{i,j}}{\Delta x_i^2}\right] f_{i,j,1}^{(l+1)} + \left[\frac{D_{i+1,j}}{\Delta x_i \Delta x_{i+1}} - \frac{\gamma}{2\Delta x_i}\right] f_{i+1,j,1}^{(l+1)} + \left[\frac{-D_{i+1,j}}{\Delta x_i \Delta x_{i+1}}\right] f_{i+1,j,2}^{(l+1)}$$

$$+ \left[\frac{-D_{i,j}}{\Delta y_j^2}\right] f_{i,j,3}^{(l+1)} + \left[\frac{D_{i,j-1}}{\Delta y_j \Delta y_{j-1}} - \frac{\gamma}{2\Delta y_j}\right] f_{i,j-1,3}^{(l+1)} + \left[\frac{-D_{i,j-1}}{\Delta y_j \Delta y_{j-1}}\right] f_{i,j-1,2}^{(l+1)}$$

$$= \sigma_{s,i,j}\left(\phi_{i,j,2}^{\left(l+\frac{1}{2}\right)} - \phi_{i,j,2}^{(l)}\right), \tag{381}$$

$$\left[\frac{D_{i,j}}{\Delta x_i^2} + \frac{\gamma}{2\Delta x_i} + \frac{D_{i,j}}{\Delta y_j^2} + \frac{\gamma}{2\Delta y_j} + \sigma_{a,i,j}\right] f_{i,j,3}^{(l+1)}$$

$$+ \left[\frac{-D_{i,j}}{\Delta x_i^2}\right] f_{i,j,4}^{(l+1)} + \left[\frac{D_{i+1,j}}{\Delta x_i \Delta x_{i+1}} - \frac{\gamma}{2\Delta x_i}\right] f_{i+1,j,4}^{(l+1)} + \left[\frac{-D_{i+1,j}}{\Delta x_i \Delta x_{i+1}}\right] f_{i+1,j,3}^{(l+1)}$$

$$+ \left[\frac{-D_{i,j}}{\Delta y_j^2}\right] f_{i,j,2}^{(l+1)} + \left[\frac{D_{i,j+1}}{\Delta y_j \Delta y_{j+1}} - \frac{\gamma}{2\Delta y_j}\right] f_{i,j+1,2}^{(l+1)} + \left[\frac{-D_{i,j+1}}{\Delta y_j \Delta y_{j+1}}\right] f_{i,j+1,3}^{(l+1)}$$

$$= \sigma_{s,i,j}\left(\phi_{i,j,3}^{\left(l+\frac{1}{2}\right)} - \phi_{i,j,3}^{(l)}\right), \tag{382}$$

$$\left[\frac{D_{i,j}}{\Delta x_i^2} + \frac{\gamma}{2\Delta x_i} + \frac{D_{i,j}}{\Delta y_j^2} + \frac{\gamma}{2\Delta y_j} + \sigma_{a,i,j}\right] f_{i,j,4}^{(l+1)}$$

$$+ \left[\frac{-D_{i,j}}{\Delta x_i^2}\right] f_{i,j,3}^{(l+1)} + \left[\frac{D_{i-1,j}}{\Delta x_i \Delta x_{i-1}} - \frac{\gamma}{2\Delta x_i}\right] f_{i-1,j,3}^{(l+1)} + \left[\frac{-D_{i-1,j}}{\Delta x_i \Delta x_{i-1}}\right] f_{i-1,j,4}^{(l+1)}$$

$$+ \left[\frac{-D_{i,j}}{\Delta y_j^2}\right] f_{i,j,1}^{(l+1)} + \left[\frac{D_{i,j+1}}{\Delta y_j \Delta y_{j+1}} - \frac{\gamma}{2\Delta y_j}\right] f_{i,j+1,1}^{(l+1)} + \left[\frac{-D_{i,j+1}}{\Delta y_j \Delta y_{j+1}}\right] f_{i,j+1,4}^{(l+1)}$$

$$= \sigma_{s,i,j}\left(\phi_{i,j,4}^{\left(l+\frac{1}{2}\right)} - \phi_{i,j,4}^{(l)}\right), \tag{383}$$

where we have defined,

$$D_{i,j} = -\frac{1}{3\sigma_{t,i,j}}. \tag{384}$$

These equations, valid only in the interior of the domain, can be written in matrix form as,

$$\mathbf{D}F = \mathbf{P}\Phi, \tag{385}$$

where,

$$\mathbf{D} = \begin{bmatrix} d & c & 0 & 0 & g & 0 & 0 & f & a & b & 0 & e & 0 & 0 & 0 & 0 & 0 & 0 & 0 \\ 0 & 0 & 0 & 0 & 0 & g & f & 0 & b & a & e & 0 & h & i & 0 & 0 & 0 & 0 & 0 \\ 0 & 0 & 0 & 0 & 0 & 0 & 0 & 0 & 0 & e & a & b & 0 & 0 & i & h & 0 & j & k & 0 \\ 0 & 0 & c & d & 0 & 0 & 0 & 0 & e & 0 & b & a & 0 & 0 & 0 & 0 & j & 0 & 0 & k \end{bmatrix}, \tag{386}$$

$$a = \left[\frac{D_{i,j}}{\Delta x_i^2} + \frac{\gamma}{2\Delta x_i} + \frac{D_{i,j}}{\Delta y_j^2} + \frac{\gamma}{2\Delta y_j} + \sigma_{a,i,j}\right], \tag{387}$$

$$b = \left[\frac{-D_{i,j}}{\Delta x_i^2}\right], \tag{388}$$

$$c = \left[\frac{D_{i-1,j}}{\Delta x_i \Delta x_{i-1}} - \frac{\gamma}{2\Delta x_i}\right], \tag{389}$$

$$d = \left[\frac{-D_{i-1,j}}{\Delta x_i \Delta x_{i-1}}\right], \tag{390}$$

$$e = \left[\frac{-D_{i,j}}{\Delta y_j^2} \right] , \qquad (391)$$

$$f = \left[\frac{D_{i,j-1}}{\Delta y_j \Delta y_{j-1}} - \frac{\gamma}{2\Delta y_j} \right] , \qquad (392)$$

$$g = \left[\frac{-D_{i,j-1}}{\Delta y_j \Delta y_{j-1}} \right] , \qquad (393)$$

$$h = \left[\frac{D_{i+1,j}}{\Delta x_i \Delta x_{i+1}} - \frac{\gamma}{2\Delta x_i} \right] , \qquad (394)$$

$$i = \left[\frac{-D_{i+1,j}}{\Delta x_i \Delta x_{i+1}} \right] , \qquad (395)$$

$$j = \left[\frac{D_{i,j+1}}{\Delta y_j \Delta y_{j+1}} - \frac{\gamma}{2\Delta y_j} \right] , \qquad (396)$$

$$k = \left[\frac{-D_{i,j+1}}{\Delta y_j \Delta y_{j+1}} \right] , \qquad (397)$$

$$\mathbf{P} = \frac{\sigma_{s,i} \Delta x_i}{2} . \qquad (398)$$

$$F = \begin{bmatrix} f_{i-1,j,1} \\ f_{i-1,j,2} \\ f_{i-1,j,3} \\ f_{i-1,j,4} \\ f_{i,j-1,1} \\ f_{i,j-1,2} \\ f_{i,j-1,3} \\ f_{i,j-1,4} \\ f_{i,j,1} \\ f_{i,j,2} \\ f_{i,j,3} \\ f_{i,j,4} \\ f_{i+1,j,1} \\ f_{i+1,j,2} \\ f_{i+1,j,3} \\ f_{i+1,j,4} \\ f_{i,j+1,1} \\ f_{i,j+1,2} \\ f_{i,j+1,3} \\ f_{i,j+1,4} \end{bmatrix}^{(l+\frac{1}{2})}, \tag{399}$$

$$\mathbf{P} = \sigma_{s,i,j} , \tag{400}$$

$$\Phi = \begin{bmatrix} \phi_{i,j,1}^{(l+\frac{1}{2})} & - & \phi_{i,j,1}^{(l)} \\ \phi_{i,j,2}^{(l+\frac{1}{2})} & - & \phi_{i,j,2}^{(l)} \\ \phi_{i,j,3}^{(l+\frac{1}{2})} & - & \phi_{i,j,3}^{(l)} \\ \phi_{i,j,4}^{(l+\frac{1}{2})} & - & \phi_{i,j,4}^{(l)} \end{bmatrix} \tag{401}$$

In the next section, we will perform a Fourier analysis of this acceleration scheme applied to the SCB and UCB transport equations.

4.7   X-Y Geometry Fourier Analysis

To determine the effectiveness of accelerating UCB with SCB derived M4S acceleration equations we perform a Fourier analysis.

4.7.1 Fourier Analysis of Source Iterations: SCB

The Fourier analysis of source iteration applied to SCB begins with Eqs. (310) written in terms of the iteration errors. We assume an infinite medium with zero source which results in,

$$
\mathbf{H}_m
\begin{bmatrix}
\hat{\psi}_{m,i-1,j,2}^{(l+1)} \\
\hat{\psi}_{m,i,j-1,4}^{(l+1)} \\
\hat{\psi}_{m,i+1,j-1,3}^{(l+1)} \\
\hat{\psi}_{m,i+1,j,1}^{(l+1)} \\
\hat{\psi}_{m,i+1,j,4}^{(l+1)} \\
\hat{\psi}_{m,i,j+1,2}^{(l+1)} \\
\hat{\psi}_{m,i,j+1,1}^{(l+1)} \\
\hat{\psi}_{m,i-1,j,3}^{(l+1)}
\end{bmatrix}
+ \mathbf{T}_m
\begin{bmatrix}
\hat{\psi}_{m,i,j,1}^{(l+1)} \\
\hat{\psi}_{m,i,j,2}^{(l+1)} \\
\hat{\psi}_{m,i,j,3}^{(l+1)} \\
\hat{\psi}_{m,i,j,4}^{(l+1)}
\end{bmatrix}
= \frac{\sigma_{s,i,j}}{16}\mathbf{I}
\begin{bmatrix}
\hat{\phi}_{i,j,1}^{(l)} \\
\hat{\phi}_{i,j,2}^{(l)} \\
\hat{\phi}_{i,j,3}^{(l)} \\
\hat{\phi}_{i,j,4}^{(l)}
\end{bmatrix},
\tag{402}
$$

where l is the iteration index.

The discrete Fourier mode ansatz in x-y geometry are,

$$
\begin{bmatrix}
\hat{\psi}_{m,i,j,1} \\
\hat{\psi}_{m,i,j,2} \\
\hat{\psi}_{m,i,j,3} \\
\hat{\psi}_{m,i,j,4}
\end{bmatrix}^{(l)}
= \omega^l e^{i(\lambda+\nu)}
\begin{bmatrix}
a_{m,i,j,1} \\
a_{m,i,j,2} \\
a_{m,i,j,3} \\
a_{m,i,j,4}
\end{bmatrix},
\tag{403}
$$

$$
\begin{bmatrix}
\hat{\phi}_{m,i,j,1} \\
\hat{\phi}_{m,i,j,2} \\
\hat{\phi}_{m,i,j,3} \\
\hat{\phi}_{m,i,j,4}
\end{bmatrix}^{(l)}
= \omega^l e^{i(\lambda+\nu)}
\begin{bmatrix}
A_{m,i,j,1} \\
A_{m,i,j,2} \\
A_{m,i,j,3} \\
A_{m,i,j,4}
\end{bmatrix}.
\tag{404}
$$

Substituting the Fourier ansatz into our system Eq. (402) yields the following equations,

$$
\omega \mathbf{L}_m^{+,+}
\begin{bmatrix}
a_{m,i,j,1} \\
a_{m,i,j,2} \\
a_{m,i,j,3} \\
a_{m,i,j,4}
\end{bmatrix}
= \mathbf{P_s}
\begin{bmatrix}
A_{i,j,1} \\
A_{i,j,2} \\
A_{i,j,3} \\
A_{i,j,4}
\end{bmatrix}
, \mu > 0, \eta > 0,
\tag{405}
$$

$$
\omega \mathbf{L}_m^{-,+}
\begin{bmatrix}
a_{m,i,j,1} \\
a_{m,i,j,2} \\
a_{m,i,j,3} \\
a_{m,i,j,4}
\end{bmatrix}
= \mathbf{P_s}
\begin{bmatrix}
A_{i,j,1} \\
A_{i,j,2} \\
A_{i,j,3} \\
A_{i,j,4}
\end{bmatrix}
, \mu < 0, \eta > 0,
\tag{406}
$$

$$\omega \mathbf{L}_m^{+,-} \begin{bmatrix} a_{m,i,j,1} \\ a_{m,i,j,2} \\ a_{m,i,j,3} \\ a_{m,i,j,4} \end{bmatrix} = \mathbf{Ps} \begin{bmatrix} A_{i,j,1} \\ A_{i,j,2} \\ A_{i,j,3} \\ A_{i,j,4} \end{bmatrix} , \mu > 0 , \eta < 0 , \tag{407}$$

$$\omega \mathbf{L}_m^{-,-} \begin{bmatrix} a_{m,i,j,1} \\ a_{m,i,j,2} \\ a_{m,i,j,3} \\ a_{m,i,j,4} \end{bmatrix} = \mathbf{Ps} \begin{bmatrix} A_{i,j,1} \\ A_{i,j,2} \\ A_{i,j,3} \\ A_{i,j,4} \end{bmatrix} , \mu < 0 , \eta < 0 , \tag{408}$$

where $\mathbf{L}_m^{+,+}$, $\mathbf{L}_m^{-,+}$, $\mathbf{L}_m^{+,-}$ and $\mathbf{L}_m^{-,-}$ are equal to,

$$\mathbf{L}_m^{+,+} = \begin{bmatrix} a+b+c & a - de^{-i\lambda \Delta x_i} & 0 & b - fe^{-i\nu \Delta y_j} \\ -a & a+b+c & b - fe^{-i\nu \Delta y_j} & 0 \\ 0 & -b & a+b+c & -a \\ -b & 0 & a - de^{-i\lambda \Delta x_i} & a+b+c \end{bmatrix} , \tag{409}$$

$$\mathbf{L}_m^{-,+} = \begin{bmatrix} -a+b+c & a & 0b - fe^{-i\nu \Delta y_j} \\ -a + de^{-i\lambda \Delta x_i} & -a+b+c & b - fe^{-i\nu \Delta y_j} & 0 \\ 0 & -b & -a+b+c & -a + de^{-i\lambda \Delta x_i} \\ -b & 0 & a & -a+b+c \end{bmatrix} , \tag{410}$$

$$\mathbf{L}_m^{+,-} = \begin{bmatrix} a-b+c & a - de^{-i\lambda \Delta x_i} & 0 & b \\ -a & a-b+c & b & 0 \\ 0 & -b + fe^{-i\nu \Delta y_j} & a-b+c & -a \\ -b + fe^{-i\nu \Delta y_j} & 0 & a - de^{-i\lambda \Delta x_i} & a-b+c \end{bmatrix} , \tag{411}$$

$$\mathbf{L}_m^{-,-} = \begin{bmatrix} -a-b+c & a & 0 & b \\ -a + de^{-i\lambda \Delta x_i} & -a-b+c & b & 0 \\ 0 & -b + fe^{-i\nu \Delta y_j} & -a-b+c & -a + de^{-i\lambda \Delta x_i} \\ -b + fe^{-i\nu \Delta y_j} & 0 & a & -a-b+c \end{bmatrix} , \tag{412}$$

$$\mathbf{Ps} = \frac{\sigma_{s,i,j} \Delta x_i \Delta y_j}{16} \begin{bmatrix} \mathbf{I} \end{bmatrix} , \tag{413}$$

where,

$$a = \frac{\mu_m \Delta y_j}{4} , \tag{414}$$

$$b = \frac{\eta_m \Delta x_i}{4} , \tag{415}$$

$$c = \frac{\sigma_{t,i,j}\Delta y_j \Delta x_i}{4} , \tag{416}$$

$$d = \frac{\mu_m \Delta y_j}{2} , \tag{417}$$

$$f = \frac{\eta_m \Delta x_i}{2} . \tag{418}$$

Rearranging Eqs. (405) - (408) we arrive at,

$$\omega \begin{bmatrix} a_{m,1} \\ a_{m,2} \\ a_{m,3} \\ a_{m,4} \end{bmatrix} = \sum_m w_m \left[\left(\mathbf{L}_m^{+,+}\right)^{-1} + \left(\mathbf{L}_m^{-,+}\right)^{-1} + \left(\mathbf{L}_m^{+,-}\right)^{-1} + \left(\mathbf{L}_m^{-,-}\right)^{-1} \right] \mathbf{P_s} \begin{bmatrix} A_1 \\ A_2 \\ A_3 \\ A_4 \end{bmatrix} \tag{419}$$

which is equivalent to,

$$\omega \begin{bmatrix} a_{m,1} \\ a_{m,2} \\ a_{m,3} \\ a_{m,4} \end{bmatrix} = \Lambda_{SCB} \begin{bmatrix} A_1 \\ A_2 \\ A_3 \\ A_4 \end{bmatrix} . \tag{420}$$

4.7.2 Fourier Analysis of Source Iterations: UCB

The same methodology that we applied to SCB is used to Fourier analyze UCB. We write Eq. (310) in terms of the iteration errors. We assume an infinite medium with zero source which results in the following system,

$$\mathbf{H}_m \begin{bmatrix} \hat{\psi}^{(l+1)}_{m,i-1,j,2} \\ \hat{\psi}^{(l+1)}_{m,i,j-1,4} \\ \hat{\psi}^{(l+1)}_{m,i+1,j-1,3} \\ \hat{\psi}^{(l+1)}_{m,i+1,j,1} \\ \hat{\psi}^{(l+1)}_{m,i+1,j,4} \\ \hat{\psi}^{(l+1)}_{m,i,j+1,2} \\ \hat{\psi}^{(l+1)}_{m,i,j+1,1} \\ \hat{\psi}^{(l+1)}_{m,i-1,j,3} \end{bmatrix} + \mathbf{T}_m \begin{bmatrix} \hat{\psi}^{(l+1)}_{m,i,j,1} \\ \hat{\psi}^{(l+1)}_{m,i,j,2} \\ \hat{\psi}^{(l+1)}_{m,i,j,3} \\ \hat{\psi}^{(l+1)}_{m,i,j,4} \end{bmatrix} = \frac{\sigma_{s,i,j}}{16}\mathbf{I} \begin{bmatrix} \hat{\phi}^{(l)}_{i,j,1} \\ \hat{\phi}^{(l)}_{i,j,2} \\ \hat{\phi}^{(l)}_{i,j,3} \\ \hat{\phi}^{(l)}_{i,j,4} \end{bmatrix} , \tag{421}$$

where the coefficients were defined in Section 4.5 and l is the iteration index.

The discrete Fourier mode ansatz in x-y geometry are,

$$
\begin{bmatrix} \hat{\psi}_{m,i,j,1} \\ \hat{\psi}_{m,i,j,2} \\ \hat{\psi}_{m,i,j,3} \\ \hat{\psi}_{m,i,j,4} \end{bmatrix}^{(l)} = \omega^l e^{i(\lambda x_i + \nu y_j)} \begin{bmatrix} a_{m,i,j,1} \\ a_{m,i,j,2} \\ a_{m,i,j,3} \\ a_{m,i,j,4} \end{bmatrix} ,
\tag{422}
$$

$$
\begin{bmatrix} \hat{\phi}_{m,i,j,1} \\ \hat{\phi}_{m,i,j,2} \\ \hat{\phi}_{m,i,j,3} \\ \hat{\phi}_{m,i,j,4} \end{bmatrix}^{(l)} = \omega^l e^{i(\lambda x_i + \nu y_j)} \begin{bmatrix} A_{m,i,j,1} \\ A_{m,i,j,2} \\ A_{m,i,j,3} \\ A_{m,i,j,4} \end{bmatrix} .
\tag{423}
$$

Substituting the Fourier ansatz into our system Eq. (421) yields the following equations,

$$
\omega \mathbf{L}_m^{+,+} \begin{bmatrix} a_{m,i,j,1} \\ a_{m,i,j,2} \\ a_{m,i,j,3} \\ a_{m,i,j,4} \end{bmatrix} = \mathbf{P}_{m,s} \begin{bmatrix} A_{i,j,1} \\ A_{i,j,2} \\ A_{i,j,3} \\ A_{i,j,4} \end{bmatrix} , \mu > 0 , \eta > 0 ,
\tag{424}
$$

$$
\omega \mathbf{L}_m^{-,+} \begin{bmatrix} a_{m,i,j,1} \\ a_{m,i,j,2} \\ a_{m,i,j,3} \\ a_{m,i,j,4} \end{bmatrix} = \mathbf{P}_{m,s} \begin{bmatrix} A_{i,j,1} \\ A_{i,j,2} \\ A_{i,j,3} \\ A_{i,j,4} \end{bmatrix} , \mu < 0 , \eta > 0 ,
\tag{425}
$$

$$
\omega \mathbf{L}_m^{+,-} \begin{bmatrix} a_{m,1,i,j} \\ a_{m,2,i,j} \\ a_{m,3,i,j} \\ a_{m,4,i,j} \end{bmatrix} = \mathbf{P}_{m,s} \begin{bmatrix} A_{i,j,1} \\ A_{i,j,2} \\ A_{i,j,3} \\ A_{i,j,4} \end{bmatrix} , \mu > 0 , \eta < 0 ,
\tag{426}
$$

$$
\omega \mathbf{L}_m^{-,-} \begin{bmatrix} a_{m,i,j,1} \\ a_{m,i,j,2} \\ a_{m,i,j,3} \\ a_{m,i,j,4} \end{bmatrix} = \mathbf{P}_{m,s} \begin{bmatrix} A_{i,j,1} \\ A_{i,j,2} \\ A_{i,j,3} \\ A_{i,j,4} \end{bmatrix} , \mu < 0 , \eta < 0 ,
\tag{427}
$$

where $\mathbf{L}_m^{+,+}$, $\mathbf{L}_m^{-,+}$, $\mathbf{L}_m^{+,-}$ and $\mathbf{L}_m^{-,-}$ are equal to,

$$
\mathbf{L}_m^{+,+} = \begin{bmatrix} ac + bd + 1 & -ach & -bdl & 0 \\ -ac & a + bd + 1 + afh & 0 & -bdl \\ 0 & -bd & -ac & a + b + 1 + afh + bgl \\ -bd & 0 & ac + b + 1 + bgl & -ach \end{bmatrix} ,
\tag{428}
$$

$$\mathbf{L}_m^{-,+} = \begin{bmatrix} ac+b+1+bgk & -ach & -bd & 0 \\ -ac & a+b+1+afh+bgk & 0 & -bd \\ 0 & -bdk & -ac & a+bd+1+afh \\ -bdk & 0 & ac+bd+1 & -ach \end{bmatrix},$$

$$(429)$$

$$\mathbf{L}_m^{+,-} = \begin{bmatrix} a+bd+1+afj & -ac & -bdl & 0 \\ -acj & ac+bd+1 & 0 & -bdl \\ 0 & -bd & -acj & ac+b+1+bgl \\ -bd & 0 & a+b+1+afj+bgl & -ac \end{bmatrix},$$

$$(430)$$

$$\mathbf{L}_m^{-,-} = \begin{bmatrix} a+b+1+afj+bgj & -ac & -bd & 0 \\ -acj & ac+b+1+bgk & 0 & -bd \\ 0 & -bdk & -acj & ac+bd+1 \\ -bdk & 0 & a+bd+1+afj & -ac \end{bmatrix},$$

$$(431)$$

$$\mathbf{P_{m,s}} = \frac{1}{4}\left[\mathbf{G}\right], \tag{432}$$

where,

$$a = \frac{2\mu_m}{\Delta x_i \sigma_{t,i,j}}, \tag{433}$$

$$b = \frac{2\eta_m}{\Delta y_j \sigma_{t,i,j}}, \tag{434}$$

$$c = (1+\beta^x), \tag{435}$$

$$d = (1+\beta^y), \tag{436}$$

$$f = \beta^x, \tag{437}$$

$$g = \beta^y, \tag{438}$$

$$h = e^{-i\lambda\Delta x_i}, \tag{439}$$

$$l = e^{-i\nu\Delta y_j} \,, \tag{440}$$

$$j = e^{i\lambda\Delta x_i} \,, \tag{441}$$

$$k = e^{i\nu\Delta y_j} \,, \tag{442}$$

where $\beta^{x,y}$ and $\mathbf{G}$ were defined in Section 4.5.   Rearranging Eqs. (405) - (408) we arrive at,

$$\omega \begin{bmatrix} a_{m,1} \\ a_{m,2} \\ a_{m,3} \\ a_{m,4} \end{bmatrix} = \sum_m w_m \left[\left(\left(\mathbf{L}_m^{+,+}\right)^{-1} + \left(\mathbf{L}_m^{-,+}\right)^{-1} + \left(\mathbf{L}_m^{+,-}\right)^{-1} + \left(\mathbf{L}_m^{-,-}\right)^{-1} \right) \mathbf{P}_{m,s} \right] \begin{bmatrix} A_1 \\ A_2 \\ A_3 \\ A_4 \end{bmatrix} \tag{443}$$

which is equivalent to,

$$\begin{bmatrix} a_{m,1} \\ a_{m,2} \\ a_{m,3} \\ a_{m,4} \end{bmatrix} = \Lambda_{SCB} \begin{bmatrix} A_1 \\ A_2 \\ A_3 \\ A_4 \end{bmatrix} \,. \tag{444}$$

4.7.3 Fourier Analysis of Modified 4-Step Diffusion Equations

The Fourier analysis of the x-y geometry SCB derived M4S DSA equations begins with Eq. (399). The discrete Fourier mode ansatz are,

$$\begin{bmatrix} f_{i,j,1} \\ f_{i,j,2} \\ f_{i,j,3} \\ f_{i,j,4} \end{bmatrix}^{(l+1)} = \omega^l e^{i(\lambda+\nu)} \begin{bmatrix} a_1 \\ a_2 \\ a_3 \\ a_4 \end{bmatrix} \,, \tag{445}$$

$$\begin{bmatrix} \hat{\phi}_{i,j,1} \\ \hat{\phi}_{i,j,2} \\ \hat{\phi}_{i,j,3} \\ \hat{\phi}_{i,j,4} \end{bmatrix}^{(l)} = \omega^l e^{i(\lambda+\nu)} \begin{bmatrix} A_1 \\ A_2 \\ A_3 \\ A_4 \end{bmatrix} \,. \tag{446}$$

Substituting the Fourier ansatz into Eq. (399) yields the following matrix eigenvalue/eigenvector system:

$$\omega \mathbf{D} \begin{bmatrix} a_1 \\ a_2 \\ a_3 \\ a_4 \end{bmatrix} = \mathbf{P_D} \begin{bmatrix} A_1 \\ A_2 \\ A_3 \\ A_4 \end{bmatrix} , \tag{447}$$

where $\mathbf{D}$ is equal to,

$$\begin{bmatrix} A & B & C & D \\ E & F & G & H \\ I & J & K & L \\ M & N & O & P \end{bmatrix} , \tag{448}$$

where

$$A = \left[\frac{D_{i,j}}{\Delta x_i^2} + \frac{\gamma}{2\Delta x_i} + \frac{D_{i,j}}{\Delta y_j^2} + \frac{\gamma}{2\Delta y_j} + \sigma_{a,i,j} \right]$$

$$+ \left[\frac{-D_{i,j}}{\Delta x_i^2} e^{-i\lambda\Delta x_i} \right] + \left[\frac{-D_{i,j}}{\Delta y_j^2} e^{-i\nu\Delta y_j} \right] , \tag{449}$$

$$B = \left[\frac{-D_{i,j}}{\Delta x_i^2} \right] + \left[\frac{-\gamma}{2\Delta x_i} + \frac{D_{i,j}}{\Delta x_i^2} \right] e^{-i\lambda\Delta x_i} , \tag{450}$$

$$C = 0 , \tag{451}$$

$$D = \left[\frac{-D_{i,j}}{\Delta y_j^2} \right] + \left[\frac{-\gamma}{2\Delta y_j} + \frac{D_{i,j}}{\Delta y_j^2} \right] e^{-i\nu\Delta y_j} , \tag{452}$$

$$E = \left[\frac{-D_{i,j}}{\Delta x_i^2} \right] + \left[\frac{-\gamma}{2\Delta x_i} + \frac{D_{i,j}}{\Delta x_i^2} \right] e^{i\lambda\Delta x_i} , \tag{453}$$

$$F = \left[\frac{D_{i,j}}{\Delta x_i^2} + \frac{\gamma}{2\Delta x_i} + \frac{D_{i,j}}{\Delta y_j^2} + \frac{\gamma}{2\Delta y_j} + \sigma_{a,i,j} \right]$$

$$+ \left[\frac{-D_{i,j}}{\Delta x_i^2} e^{i\lambda\Delta x_i} \right] + \left[\frac{-D_{i,j}}{\Delta y_j^2} e^{-i\nu\Delta y_j} \right] , \tag{454}$$

$$G = \left[\frac{-D_{i,j}}{\Delta y_j^2} \right] + \left[\frac{-\gamma}{2\Delta y_j} + \frac{D_{i,j}}{\Delta y_j^2} \right] e^{-i\nu\Delta y_j} , \tag{455}$$

$$H = 0 \,, \tag{456}$$

$$I = 0 \,, \tag{457}$$

$$J = \left[\frac{-D_{i,j}}{\Delta y_j^2} \right] + \left[\frac{-\gamma}{2\Delta y_j} + \frac{D_{i,j}}{\Delta y_j^2} \right] e^{i\nu \Delta y_j} \,, \tag{458}$$

$$K = \left[\frac{D_{i,j}}{\Delta x_i^2} + \frac{\gamma}{2\Delta x_i} + \frac{D_{i,j}}{\Delta y_j^2} + \frac{\gamma}{2\Delta y_j} + \sigma_{a,i,j} \right]$$
$$+ \left[\frac{-D_{i,j}}{\Delta x_i^2} e^{i\lambda \Delta x_i} \right] + \left[\frac{-D_{i,j}}{\Delta y_j^2} e^{i\nu \Delta y_j} \right] \,, \tag{459}$$

$$L = \left[\frac{-D_{i,j}}{\Delta x_i^2} \right] + \left[\frac{-\gamma}{2\Delta x_i} + \frac{D_{i,j}}{\Delta x_i^2} \right] e^{i\lambda \Delta x_i} \,, \tag{460}$$

$$M = \left[\frac{-D_{i,j}}{\Delta y_j^2} \right] + \left[\frac{-\gamma}{2\Delta y_j} + \frac{D_{i,j}}{\Delta y_j^2} \right] e^{i\nu \Delta y_j} \,, \tag{461}$$

$$N = 0 \,, \tag{462}$$

$$O = \left[\frac{-D_{i,j}}{\Delta x_i^2} \right] + \left[\frac{-\gamma}{2\Delta x_i} + \frac{D_{i,j}}{\Delta x_i^2} \right] e^{-i\lambda \Delta x_i} \,, \tag{463}$$

$$P = \left[\frac{D_{i,j}}{\Delta x_i^2} + \frac{\gamma}{2\Delta x_i} + \frac{D_{i,j}}{\Delta y_j^2} + \frac{\gamma}{2\Delta y_j} + \sigma_{a,i,j} \right]$$
$$+ \left[\frac{-D_{i,j}}{\Delta x_i^2} e^{-i\lambda \Delta x_i} \right] + \left[\frac{-D_{i,j}}{\Delta y_j^2} e^{i\nu \Delta y_j} \right] \,, \tag{464}$$

and $\mathbf{P_D}$ is equal to,

$$\mathbf{P_D} = \sigma_{s,i,j} \left[\mathbf{I} \right] \,. \tag{465}$$

The Fourier analysis of the SCB system accelerated with the SCB derived modified 4-step equations and the UCB system accelerated with SCB derived modified 4-step equations can be represented in the following matrix notation,

$$\omega \begin{bmatrix} A_1 \\ A_2 \\ A_3 \\ A_4 \end{bmatrix} = [\Lambda_{SCB,UCB} + \mathbf{E}(\Lambda_{SCB,UCB} - \mathbf{I})] \begin{bmatrix} A_1 \\ A_2 \\ A_3 \\ A_4 \end{bmatrix} , \tag{466}$$

where,

$$\mathbf{E} = \mathbf{D}^{-1} \mathbf{P_D} , \tag{467}$$

where ω is an eigenvalue, $A_{1,2,3,4}$ is an eigenfunction and $\mathbf{I}$ is the identity matrix.

4.8 Numerical Results

4.8.1 Fourier Analysis Results

Following the same methodology performed in slab geometry, we have Fourier analyzed SCB and UCB accelerated with SCB derived modified 4-step equations using a S_8 level-symmetric angular quadrature set for our x-y geometry results. The iterative scheme was also implemented to verify the results of the analysis. Figures 14 and 15 show the results of this Fourier analysis. These figures represent the spectral radii as a function of mesh spacing in the x and y directions. The accelerated SCB plot shows a maximum spectral radius of 0.4567 for $c = 1.0$ and an optical thickness of approximately 1.0 mean-free-paths (mfp). The SCB-accelerated UCB plot shows a maximum spectral radius of 0.370 for $c = 1.0$ and an optical thickness of approximately 1.0 mean-free-paths (mfp).

Numerical results were generated for a 20×20 plane, an S_8 quadrature set, vacuum boundary conditions, zero sources and a convergence to $\phi = 0$ for a range of optical thicknesses. To get the most accurate results all of the Fourier modes were excited
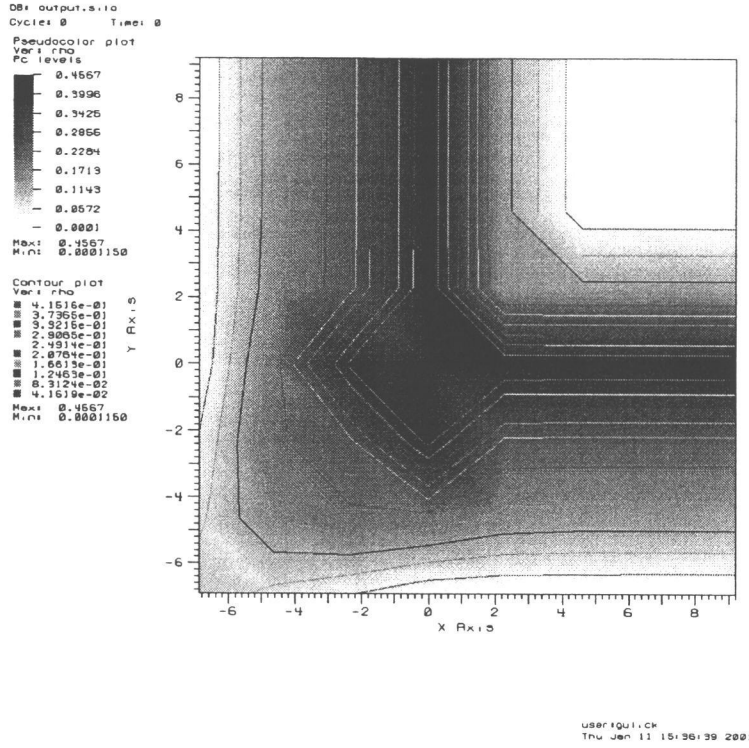
Fig. 14: Maximum eigenvalues $\omega(\lambda, \nu)$ as a function of Δx and Δy for SCB in x-y geometry with SCB derived "Modified 4-Step" diffusion synthetic acceleration (DSA).

by picking a random initial guess for the angular intensity. The problem was then allowed to run until a stable spectral radius was achieved. In Figures 16 and 17 the spectral radius ρ is plotted as a function of Δx and Δy.

The spectral radii, ρ, for several specific mesh sizes $(\Delta x, \Delta y)$ are shown in Tables 4, 5, 4, and 5.

The data in tabular form allows us to easily compare the SCB and UCB Fourier analysis results, Figures 14 and 15, with the implementation results, Figures 16 and 17. The implementation results match quite well with the Fourier analysis re-
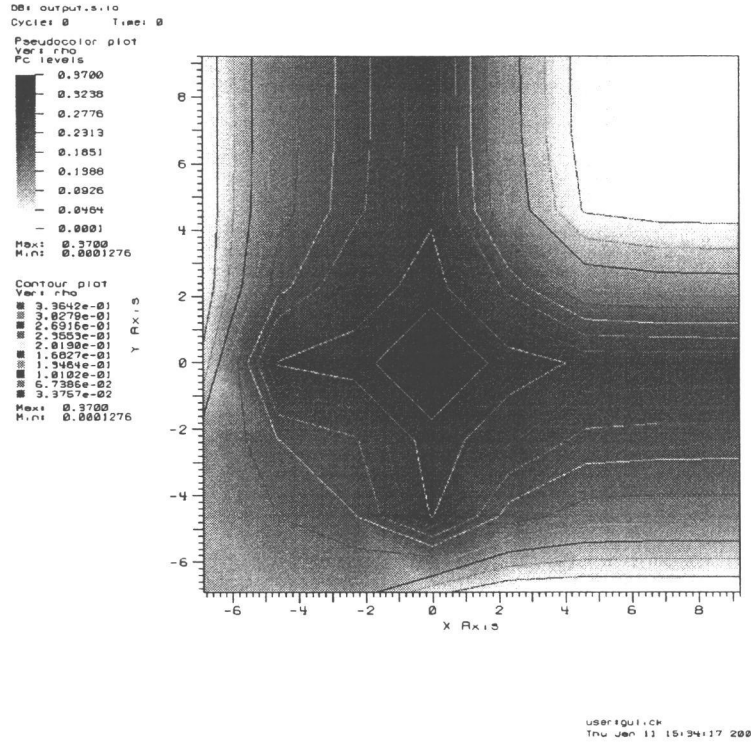
Fig. 15: Maximum eigenvalues $\omega(\lambda, \nu)$ as a function of Δx and Δy for UCB in x-y geometry with SCB derived "Modified 4-Step" diffusion synthetic acceleration (DSA).

sults. Since the problem is fairly small, 20×20, the thin implementation results should be and are significantly less than the Fourier analysis. This is because the Fourier analysis assumes the system is infinite while the test problems are finite. This also means that the implementation results, when the problem is optically thick, should match very closely with the Fourier analysis. Our figures and tables confirm that the implementation code's spectral radii are nearly identical to those of the Fourier analysis. We also note that the spectral radii for the SCB and UCB discretizations
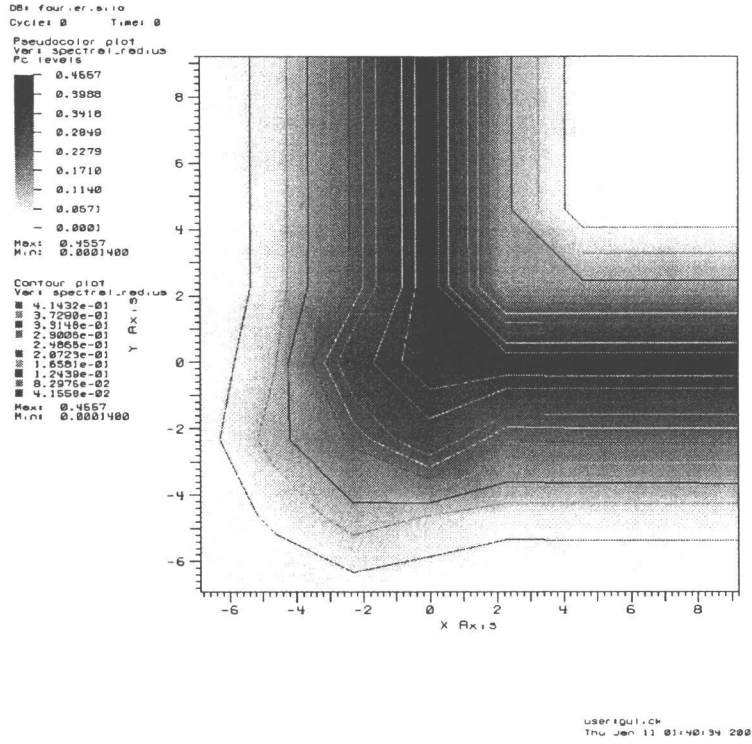
Fig. 16: Maximum spectral radii as a function of Δx and Δy for SCB in x-y geometry with SCB derived "Modified 4-Step" diffusion synthetic acceleration (DSA).

accelerated with M4S DSA are extremely small in thick limit; This indicates that, in such problems, the iterative method will be rapidly convergent.

4.8.2 Implementation Code Model Problem

We present a representative x-y geometry problem to verify the operation of the discretizations and acceleration scheme. These results show that the DSA is properly accelerating our iterative system. Figure (18) illustrates the x-y geometry model
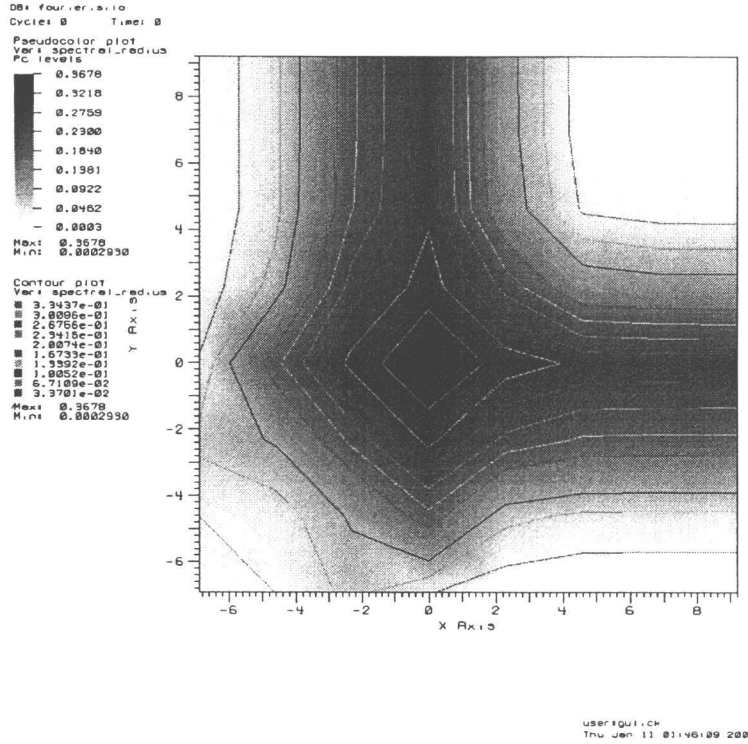
Fig. 17: Maximum spectral radii as a function of Δx and Δy for UCB in x-y geometry with SCB derived "Modified 4-Step" diffusion synthetic acceleration (DSA).

problem.

Figures (19), and (20) show that the SCB solutions with and without acceleration are identical. Figures (21) and (22) illustrate the same result for the UCB discretization. This means that the acceleration method is not changing the solution, just the rate at which the scheme is converging to the solution.

Table 6 shows the convergence results for the x-y geometry model problem. It is obvious that the DSA is *effective* at increasing the iterative convergence rate. It is very important to note that the model problem, like any finite problem must have a

Table 2: X-Y UCB Fourier Analysis Results

$\sigma_t \Delta x$	$\sigma_t \Delta y$					
	0.1	1.0	10.0	100.0	1000.0	10000.0
0.1	0.231	0.324	0.275	0.225	0.220	0.220
1.0	0.324	0.370	0.323	0.296	0.293	0.293
10.0	0.275	0.323	0.226	0.130	0.119	0.118
100.0	0.225	0.296	0.130	0.031	0.017	0.016
1000.0	0.220	0.293	0.119	0.017	0.002	0.001
10000.0	0.220	0.293	0.118	0.016	0.001	< 0.001

Table 3: X-Y UCB Implementation Results

$\sigma_t \Delta x$	$\sigma_t \Delta y$					
	0.1	1.0	10.0	100.0	1000.0	10000.0
0.1	0.209	0.312	0.249	0.199	0.194	0.194
1.0	0.312	0.368	0.321	0.293	0.290	0.289
10.0	0.227	0.321	0.223	0.128	0.118	0.117
100.0	0.196	0.293	0.129	0.030	0.017	0.015
1000.0	0.194	0.291	0.118	0.017	0.002	0.001
10000.0	0.194	0.288	0.117	0.015	0.001	< 0.001

spectral radius less than that of the Fourier analysis, which it does.

4.9 Summary

In this chapter we described discretization techniques for the equation of transfer in x-y geometry, including techniques for treating frequency, time, and angle. We then introduced the corner balance family of spatial discretizations in x-y geometry. We reviewed the simple corner balance and upstream corner balance closures and the associated scheme for source iteration. We then derived the M4S DSA equations in x-y geometry.

Table 4: X-Y SCB Fourier Analysis Results

$\sigma_t \Delta x$	$\sigma_t \Delta y$					
	0.1	1.0	10.0	100.0	1000.0	10000.0
0.1	0.242	0.426	0.237	0.236	0.236	0.236
1.0	0.426	0.456	0.457	0.457	0.457	0.457
10.0	0.237	0.457	0.140	0.135	0.135	0.135
100.0	0.236	0.457	0.135	0.015	0.015	0.015
1000.0	0.236	0.457	0.135	0.015	0.001	0.001
10000.0	0.236	0.457	0.135	0.015	0.001	< 0.001

Table 5: X-Y SCB Implementation Results

$\sigma_t \Delta x$	$\sigma_t \Delta y$					
	0.1	1.0	10.0	100.0	1000.0	10000.0
0.1	0.220	0.343	0.215	0.214	0.215	0.215
1.0	0.344	0.452	0.455	0.456	0.455	0.456
10.0	0.210	0.455	0.137	0.134	0.134	0.134
100.0	0.214	0.456	0.133	0.014	0.015	0.015
1000.0	0.214	0.455	0.134	0.014	0.001	0.001
10000.0	0.215	0.455	0.134	0.015	0.001	< 0.001

A Fourier analysis of UCB accelerated with SCB-derived modified 4-step DSA equations was performed. We demonstrated that the implemented algorithm verifies our Fourier analysis. The results clearly show that SCB derived diffusion acceleration equations are very effective at increasing the rate of iterative convergence of UCB in x-y geometry.
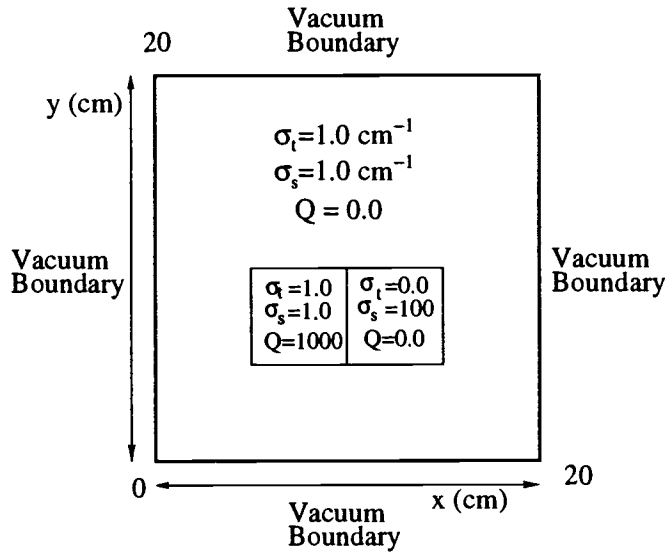
Fig. 18: SCB and UCB x-y model stencil.

Table 6: X-Y Model Problem Results

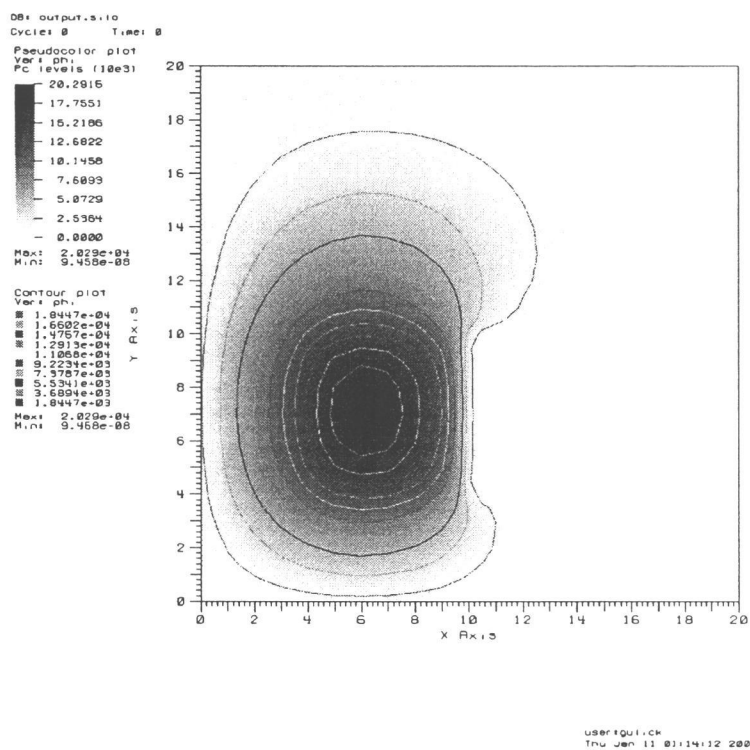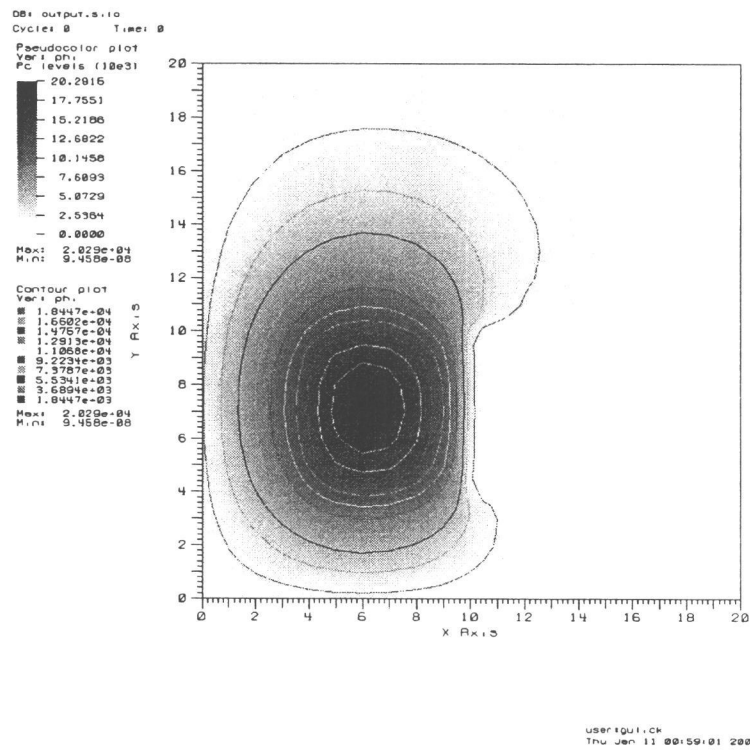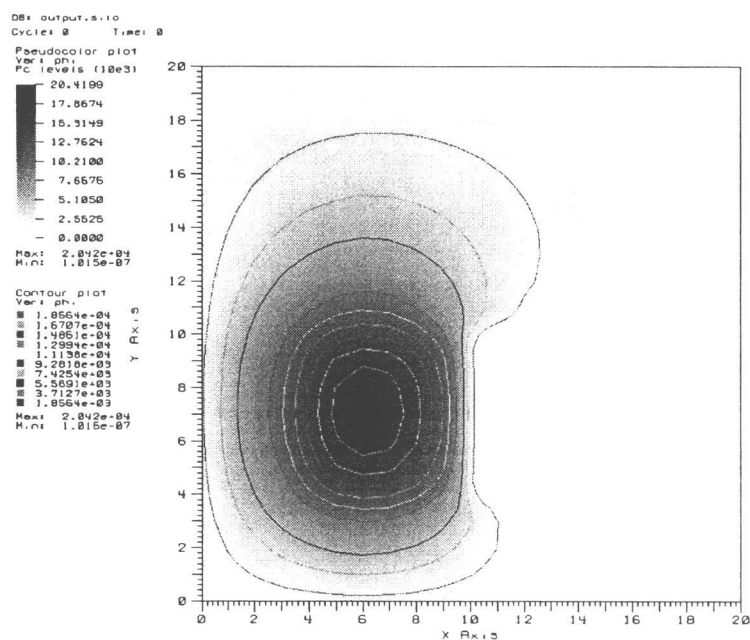| Discretization:	$Iterations_{SI}$:	$Iterations_{DSA}$:	ρ_{SI}:	ρ_{DSA}:	ϵ:
SCB	791	23	0.976	0.419	$1.0e^{-6}$
UCB	787	18	0.976	0.336	$1.0e^{-6}$

Fig. 19: X-Y SCB model problem results without acceleration.

Fig. 20: X-Y SCB model problem results with acceleration.

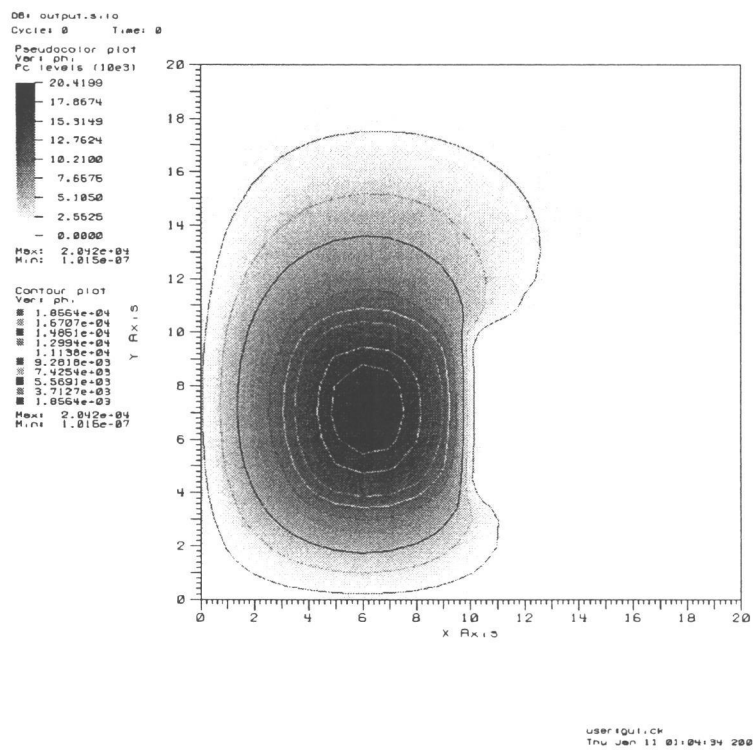Fig. 21: X-Y UCB model problem results without acceleration.

Fig. 22: X-Y UCB model problem results with acceleration.

5 CONCLUSION

5.1 Summary of Results

We had four primary objectives for this thesis; slab geometry Fourier analysis of SCB and UCB discretizations accelerated with M4S DSA, slab geometry implementation analysis of the same system, x-y geometry Fourier analysis of the SCB and UCB discretization accelerated with M4S DSA, and x-y geometry implementation analysis of the same system. In this chapter summarize our work, discuss the significance of our results and consider areas for future work.

We introduced a new *mildly* inconsistent application of the M4S equations. We proposed applying M4S acceleration equations derived from SCB to the UCB source iteration equations. The success of this *mildly* inconsistent application was judged with two primary metrics; convergence rate and "correctness". We defined convergence rate to be the error reduction rate on each successive iteration. "Correctness" here means the accelerated solution is equal to the solution achieved using only source iteration. Fourier analysis results show that in slab geometry and x-y geometry the scheme should be highly *effective* and our implementation of the method supports this assertion; M4S DSA equations derived from SCB substantially increase the iterative convergence rate of otherwise slowly converging UCB source iteration problems. Our results also show this scheme to be *"correct"*; implementing the technique results in identical solutions between unaccelerated UCB and accelerated UCB.

Our analytic and implementation results support the initial observations of Palmer [Pal93]. Our work verifies that on orthogonal meshes it is possible to rapidly accelerate UCB with SCB derived DSA equations. We conclude that if modified 4-Step DSA equations can be derived from SCB transport equations [Pal93], and, provided that the fore-mentioned acceleration equations can be efficiently solved, we can greatly increase

the convergence rate and therefore the rate at which solutions can be attained.

5.2 Scientific Computing

The computational analysis software developed in this thesis was written in C++. The motivation for using C++ was based on several different influences. Scientific computing has predominantly used high performance procedural languages. Procedural programming techniques were used primarily because emerging software engineering techniques degraded performance too severely to be cost effective. Modern software engineering techniques, primarily the C++ language and compilers, have matured to the point where performance is no longer a problem. The fundamentally different programming ideologies can now be applied to scientific computing problems without degrading performance. These new forms of abstraction, such as object-oriented programming, can actually simplify the creation of cutting edge numerical computation packages. One very beneficial result of C++ and object-oriented programming is the concept of software reuse. Software reuse allows programmers to use objects and abstractions created by others in their own projects. Instead of having to fully understand the programming of how the object works and behaves, a programmer can simply use behavior and state provided by the object. This capability is just recently stating to gain momentum and acceptance in scientific computing communities.

For this thesis modern software engineering techniques were employed in the creation of the Fourier analysis and implementation codes. The Matrix Template Library (MTL) [Sie99] was extensively employed along with object-oriented programming techniques. The use of C++ greatly increased the ease by which changes and modifications could be made to the analysis packages. The ability to use behavior offered by the MTL also greatly eased implementation of new high-performance numerical

algebra routines.

There were also drawbacks to using a fundamentally different means of programming. There is a very intense learning curve associated with object-oriented programming. The author found that several revisions were necessary as new and far superior methods of programming were discovered. Another concern was the lack of control over the numerical linear algebra packages. Numerical issues were noticed in some limits which indicated some problems with the linear algebra coding. This will be discussed in the next section. Our results were obtained using a Sun Ultra 10 workstation running the KAI KCC compiler.

5.3 Discussion

The modifications that Adams [Ada97] made to SCB in designing UCB resulted in a discretization with several very appealing characteristics. However, source iteration suffers from the problematic decrease in iterative convergence rate when the system of interest becomes highly diffusive. One solution to this convergence problem is to use a form of acceleration to increase the rate of iterative convergence while still preserving the unaccelerated result. The non-conventional form of the UCB closure makes deriving a consistent set of acceleration equations a difficult task. What we have found is that deriving M4S DSA equations from a similar discretization, SCB, yields acceleration equations that effectively accelerate slab and x-y geometry UCB.

Our results indicate that our scheme is highly successful. However, we had numerical difficulties with the diffusion solvers in high aspect ratio problems. Our diffusion solvers became unstable and failed to converge for certain high aspect ratio problems. This points out the fact that although the rate of convergence of the scheme can be greatly increased, effective diffusion solvers must be available to rapidly solve the DSA equations. If too much time is spent solving the diffusion acceleration equations, the

overall cpu time needed for convergence may actually be greater than that of source iteration.

5.4 Future Work

Several aspects of this research require further investigation.

The derivation and implementation of the acceleration equations needs to be extended from orthogonal meshes in x-y geometry to unstructured polygonal meshes. The motivation for using UCB is that it is a discretization that rapidly sweeps through polygonal cells. This is not a serious issue for regular orthogonal geometries. By extending the implementation to arbitrarily connected polygons we can determine whether the method is as effective as it is for orthogonal mesh schemes.

A method needs to be determined for performing Fourier analysis of the scheme on polygons. Warsa and Wareing have discussed a technique to Fourier analyze triangular meshes and they indicate it is highly effective at predicting convergence characteristics for unstructured meshes [War00a] [War00b]. Performing this type of analysis would provide insight into how the scheme behaves on non-orthogonal meshes.

Finally, research needs to be performed investigating new ways of reducing the time required to solve the diffusion acceleration equations. Currently M4S requires the solution of an asymmetric matrix. This adds a great deal of computational expense to the transport/DSA sweeps. One possibility is to use other types of *mildly* inconsistent acceleration schemes to accelerate UCB. One of particular interest is simplified P1 DSA [Pal93]. Simplified P1 DSA yields symmetric matrices which are easy to solve compared to the non-symmetric matrices resulting from M4S DSA. This could potentially yield a highly convergent rapid scheme for polygonal mesh UCB transport.

BIBLIOGRAPHY

[ABDP81] R.E. Alcouffe, A. Brandt, J.E. Dendy, and J. Painter. The multi-grid method for the diffusion equation with strongly discontinous coefficients. *SIAM J. Sci. Comput.*, 2:430–454, 1981.

[Ada91] M.L. Adams. A new transport discretization scheme for arbitrary spatial meshes in xy geometry. In *Proceedings ANS Topical Meeting, Advances in Mathematics, Computations, and Reactor Physics*, volume 3, pages 2-1 through 2-9. The American Nuclear Society, 1991.

[Ada97] M. L. Adams. Subcell balance methods for radiative transfer on abritrary grids. *Transp. Theory Stat. Phys.*, 26(4–5):385–431, 1997.

[Alc77] R. E. Alcouffe. Diffusion synthetic acceleration methods for the diamond-differenced discrete-ordinates equations. *Nucl. Sci. Eng.*, 64:344–355, 1977.

[AM92] M. L. Adams and W. R. Martin. Diffusion synthetic acceleration of discontinuous finite element transport iterations. *Nucl. Sci. Eng.*, 111:145–167, 1992.

[Bur91] D.E. Burton. Conservation of energy, momentum and angular momentum in lagrangian staggered-grid hydrodynamics. Technical Report UCRL-JC-105926, Lawrence Livermore National Laboratory, 1991.

[GO99] M.L. Hall G.L. Olson, L.H. Auer. Diffusion, p1, and other approximate forms of radiation transport. Technical Report LA-UR-99-471, Los Alamos National Laboratory, 1999.

[Gol64]   V. Y. Gol'din. A quasi-diffusion method of solving the kinetic equation. *U.S.S.R. Computational Mathematics and Mathematical Physics*, 4(6):136–149, 1964.

[Kha85]   H. Khalil. A nodal diffusion technique for synthetic acceleration of nodal S_n calculations. *Nucl. Sci. Eng.*, 90:263–280, 1985.

[Kim00]   Kang-Seog Kim. *Coarse-Mesh and One-Cell Block Inversion Based Diffusion Synthetic Acceleration*. PhD thesis, Oregon State University, 2000.

[Kop63]   H. J. Kopp. Synthetic method solution of the transport equation. *Nucl. Sci. Eng.*, 17:65–74, 1963.

[Lar82a]   E. W. Larsen. Spatial convergence properties of the diamond difference method in x,y geometry. *Nucl. Sci. Eng.*, 80:710–713, 1982.

[Lar82b]   E. W. Larsen. Unconditionally stable diffusion-synthetic acceleration methods for the slab geometry discrete ordinates equations. part I: Theory. *Nucl. Sci. Eng.*, 82:47–63, 1982.

[Lar84]   E. W. Larsen. Diffusion-synthetic acceleration methods for discrete ordinates problems. *Transp. Theory Stat. Phys.*, 13(1–2):107–126, 1984.

[Lar99]   E.W. Larsen. Computation transport theory: Research issues and emerging applications. In *Proceedings International Topical Meeting, Mathematics and Computation, Reactor Physics and Environmental Analysis in Nuclear Applications*, Madrid, Spain, September 1999.

[LM82]   E. W. Larsen and D. R. McCoy. Unconditionally stable diffusion-synthetic acceleration methods for the slab geometry discrete ordinates equations. part II: Numerical results. *Nucl. Sci. Eng.*, 82:64–70, 1982.

[LM84]   E. E. Lewis and W. F. Miller, Jr. *Computational Methods of Neutron Transport*. Wiley, New York, 1984.

[LMM89] E. W. Larsen, J. E. Morel, and J. M. McGhee. Asymptotic solutions of numerical transport problems in optically thick, diffusive regimes ii. *J. Comput. Phys.*, 83:212–236, 1989.

[LP97]   Rubin H. Landau and Manuel J. Paez. *Computational Physics, Problem Solving with Computers*. John Wiley and Sons, Inc., New York, New York, 1997.

[MDW93] J. E. Morel, J. E. Dendy, Jr., and T. A. Wareing. Diffusion-accelerated solution of the two-dimensional S_n equations with bilinear-discontinous differencing. *Nucl. Sci. Eng.*, 115:304–319, 1993.

[MLA98] W.F. Walters M. L. Adams, T.A. Wareing. Characteristic methods in thick diffusive problems. *Nucl. Sci. Eng.*, 130:18–46, 1998.

[Mor82] J. E. Morel. A synthetic acceleration method for discrete ordinates calculations with highly anisotropic scattering. *Nucl. Sci. Eng.*, 82:34–46, 1982.

[MWS96] J. E. Morel, T. A. Wareing, and K. Smith. A linear-discontinous spatial differencing scheme for S_n radiative transfer calculations. *J. Comput. Phys.*, 128:445–462, 1996.

[Pal93] Todd S. Palmer. Curvilinear geometry transport discretizations in thick diffusive regions. Master's thesis, University of Michigan, 1993.

[Pal01] T.S. Palmer. Differencing the diffusion equation on unstructured polygonal meshes in two dimensions. *To appear in Ann. Nucl. Ener.*, 2001.

[Pau98]   S. D. Pautz. Discrete ordinates transport methods for problems with highly forward-peaked scattering. Technical Report LA-133444-T, Los Alamos National Laboratory, 1998.

[Pom73]   G. C. Pomraning. *The Equations of Radiation Hydrodynamics*. Pergamon Press, New York, New York, 1973.

[RAN97]   G. L. Ramone, M. L. Adams, and P. F. Nowak. A transport synthetic acceleration method for transport iterations. *Nucl. Sci. Eng.*, 125:257–283, 1997.

[Sie99]   Jeremy G Siek. *Framework for Portable High Performance Numerical Linear Algebra*. PhD thesis, University of Notre Dame, 1999.

[TWM94]   W.F. Walters T.A. Wareing and J.E. Morel. Diffusion-accelerated solution of the two-dimensional x-y s_n equations with linear-bilinear nodal differencing. *Nucl. Sci. Eng.*, 118:122, 1994.

[War93]   T.A. Wareing. New diffusion synthetic acceleration methods for the s_N equations with corner balance spatial differencing. In *Proceedings Joint International Conference on Mathematical Methods and Supercomputing in Nuclear Applications*, volume 2, pages 500–511, Karlsruhe, Germany, April 19-23 1993.

[War00a]   T.A. Wareing, May 2000. Personal communication.

[War00b]   J. Warsa, August 2000. Personal communication.